AD-A043 921 ARMY MISSILE RESEARCH AND DEVELOPMENT COMMAND REDSTO--ETC F/G 17/7
PERSHING PII INERTIAL MEASUREMENT UNIT FIELD GYROCOMPASS TEST. (U)
JUN 77 H V WHITE

UNCLASSIFIED DRDMI-TG-77-16 NL

1 OF 2
AD
A043921

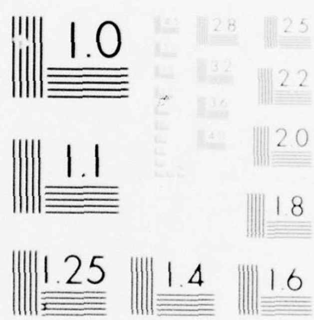

MICROCOPY RESOLUTION TEST CHART
NATIONAL BUREAU OF STANDARDS-1963-A

AD A043921

12

TECHNICAL REPORT TG-77-16

PERSHING PII INERTIAL MEASUREMENT UNIT FIELD GYROCOMPASS TEST

U.S. ARMY
MISSILE
RESEARCH
AND
DEVELOPMENT
COMMAND

Guidance and Control Directorate
Technology Laboratory

June 1977

Approved for public release; distribution unlimited.

Redstone Arsenal, Alabama 35809

DMI FORM 1000, 1 APR 77

DISPOSITION INSTRUCTIONS

DESTROY THIS REPORT WHEN IT IS NO LONGER NEEDED. DO NOT RETURN IT TO THE ORIGINATOR.

DISCLAIMER

THE FINDINGS IN THIS REPORT ARE NOT TO BE CONSTRUED AS AN OFFICIAL DEPARTMENT OF THE ARMY POSITION UNLESS SO DESIGNATED BY OTHER AUTHORIZED DOCUMENTS.

TRADE NAMES

USE OF TRADE NAMES OR MANUFACTURERS IN THIS REPORT DOES NOT CONSTITUTE AN OFFICIAL INDORSEMENT OR APPROVAL OF THE USE OF SUCH COMMERCIAL HARDWARE OR SOFTWARE.

UNCLASSIFIED

SECURITY CLASSIFICATION OF THIS PAGE (When Data Entered)

REPORT DOCUMENTATION PAGE		READ INSTRUCTIONS BEFORE COMPLETING FORM
1. REPORT NUMBER TG-77-16	2. GOVT ACCESSION NO. (14) DRDMI-TG-77-16	3. RECIPIENT'S CATALOG NUMBER
4. TITLE (and Subtitle) (6) PERSHING PII INERTIAL MEASUREMENT UNIT FIELD GYROCOMPASS TEST		5. TYPE OF REPORT & PERIOD COVERED (9) Technical Report
		6. PERFORMING ORG. REPORT NUMBER
7. AUTHOR(s) (10) H. V. White		8. CONTRACT OR GRANT NUMBER(s)
9. PERFORMING ORGANIZATION NAME AND ADDRESS Commander US Army Missile Research and Development Command Attn: DRDMI-TG Redstone Arsenal, Alabama 35809		10. PROGRAM ELEMENT, PROJECT, TASK AREA & WORK UNIT NUMBERS AMCMS 633311.5990012
11. CONTROLLING OFFICE NAME AND ADDRESS Commander US Army Missile Research and Development Command Attn: DRDMI-TI Redstone Arsenal, Alabama 35809		12. REPORT DATE (11) June 1977
		13. NUMBER OF PAGES 101 (12) 104p.
14. MONITORING AGENCY NAME & ADDRESS (if different from Controlling Office)		15. SECURITY CLASS. (of this report) Unclassified
		15a. DECLASSIFICATION/DOWNGRADING SCHEDULE

16. DISTRIBUTION STATEMENT (of this Report)

Approved for public release; distribution unlimited.

17. DISTRIBUTION STATEMENT (of the abstract entered in Block 20, if different from Report)

18. SUPPLEMENTARY NOTES

410 138

19. KEY WORDS (Continue on reverse side if necessary and identify by block number)

20. ABSTRACT (Continue on reverse side if necessary and identify by block number)

This report presents a description of the PERSHING PII Inertial Measurement Unit field gyrocompass test which provided the first accuracy data outside a benign laboratory environment. Results are presented and discussed.

It was determined that RMS and average errors increased under field conditions but the standard deviation, about the average at each azimuth heading for which data were taken, was essentially the same as laboratory results. A temperature related anomaly was identified which will be an item for close scrutiny during future tests.

ABSTRACT (Continued)

bpg

Block 20 (Concluded)

No catastrophic performance breakdown occurred; however, since errors tend to grow when the equipment is operated outside a benign laboratory environment, no relaxation of the current gyrocompass accuracy specification is recommended.

CONTENTS

ACKNOWLEDGMENTS

The author wishes to thank the following personnel for jobs well done:

Messrs. Thomas J. Snowden, William G. Robertson, and Newman L. Oldham of the Guidance and Control Directorate, Technology Laboratory performed key tasks in the setup and performance of this test.

Mr. E. Lynwood Bailey, also of the Guidance and Control Directorate, implemented accelerometer average power spectrum analysis.

Mr. George E. Knipe of the Technical Assistance and New Equipment Training Division, MIRCOM, provided equipment, facilities, and other assistance.

SP5 Peter Laracuente of the Equipment Management Division, RASA, provided operating procedures and equipment handling assistance.

SP5 Douglas Isaacson of the Atmospheric Sciences Laboratory, US Army Electronics Command, acquired, reduced, and provided meteorological data.

I. INTRODUCTION

The PERSHING PII Inertial Measurement Unit (IMU) features the capability of azimuth self-alignment. This operational mode, often referred to as gyrocompassing, allows determination of the azimuth heading of the X (downrange) accelerometer input axis for targeting purposes without using external reference equipment and operating personnel.

Internal instrument and electronic anomalies and base motions coupled from the outside world through the launcher and missile body to the IMU are among the error sources which degrade gyrocompass performance. The latter error source comes into play in a field environment situation and it is this source which the field test was designed to address.

Two Engineering Models (EM) IMU's have been subjected to extensive gyrocompass tests to determine self-alignment performance within a benign laboratory environment. These tests have provided a good indication of gyrocompass performance in the absence of base motions.

II. TEST OBJECTIVE

The objective of this test was to determine if gyrocompass accuracy degrades by a significant amount when the IMU is exposed to base motions and other environmental stimuli such as may be experienced outdoors with the unit installed in a missile which is mounted on an Erector-Launcher (EL).

The test was designed to provide initial data when operating under essentially ambient, outdoor environmental stimuli and should not be construed to be an all-inclusive, finely controlled test operation. Such a full-scale test will be performed by the prime contractor during the second quarter of CY77 in which actual PII missile body hardware will be utilized.

The early test was designed to provide 3 to 6 months lead time for addressing any problems that may surface while the full-scale test is under preparation by the prime contractor.

III. DISCUSSION OF TEST SETUP

The test was performed using a PERSHING P1a missile system. The Guidance and Control (G&C) section shroud was modified to provide access for interconnecting cables, a cooling air hose, and manual rotation of the IMU case. The ST-120 platform and mount were removed and a specially designed test fixture was installed which housed the PII IMU. Figure 1 shows the modified G&C section with test fixture and IMU installed in the normal operating position.

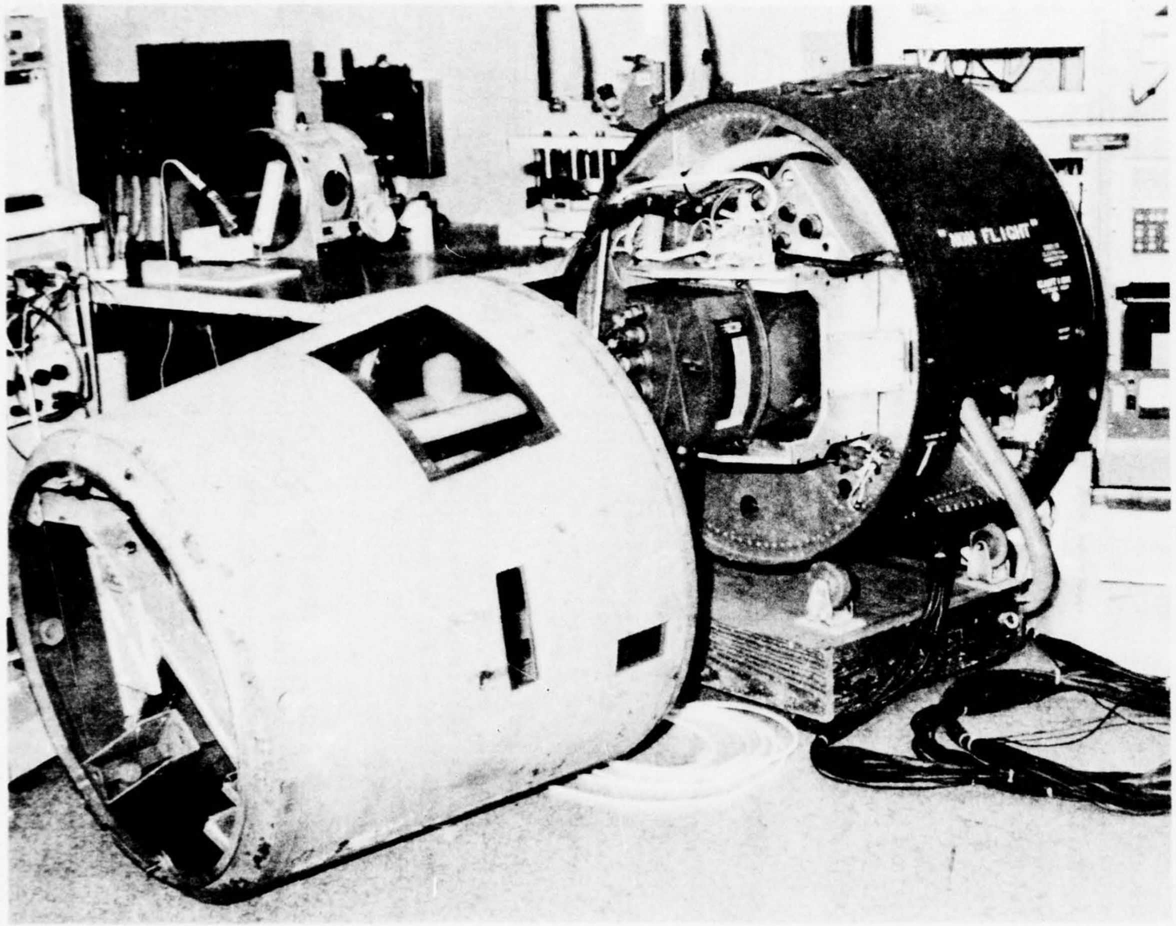

Figure 1. IMU installed in modified G&C section, normal position.

The test fixture incorporates a rotatable member which is dowel-pinned and fastened with bolts at the nominal azimuth orientation of the IMU case prior to entering the gyrocompass mode. At the completion of a gyrocompass run, the test fixture can be manually rotated through approximately 103° and dowel-pinned at this point. This rotation of the IMU allows acquisition of the cluster mounted mirror for obtaining accuracy data by optical means. Figure 2 shows the IMU at the 103° position with the optical access port in view.

The G&C section weight and center of gravity were adjusted to approximate that of an unmodified Pla G&C section with standard equipment on board, by the use of lead weights.

The section was installed on an EL-mounted missile. The system, complete with dummy warhead, is shown in Figure 3.

The test was performed in the vicinity of the PERSHING Modification Shop (Mod Shop), Building 5671.

Figure 4 shows a typical test setup in the Mod Shop area. A concrete pad, approximately 5 feet × 5 feet and 2 feet high, was installed to serve as a stable base for theodolite No. 2 (T2). T2 was used in conjunction with Theodolite No. 1(T1) and the Reference Monument Prism (RMP) to determine azimuth orientation of the X accelerometer input axis, via use of the IMU cluster mirror (CM) at the end of each gyrocompass run.

Figure 5 shows the missile G&C section as viewed from the T2 position. Figure 6 shows the RMP in the left foreground and the missile nose in the center background as viewed from the T1 area.

The complete test setup, except for meteorological instrumentation, is shown in Figure 7.

The test equipment van (TEV) in the foreground of Figure 7 housed all IMU test and instrumentation equipment. An interior view of the TEV is shown in Figure 8.

The heavy vehicle in Figure 7 was driven in the vicinity of the EL during certain of the test runs to impart disturbances to the system.

Meteorological instrumentation equipment used to provide ambient wind speed and direction is shown in Figure 9.

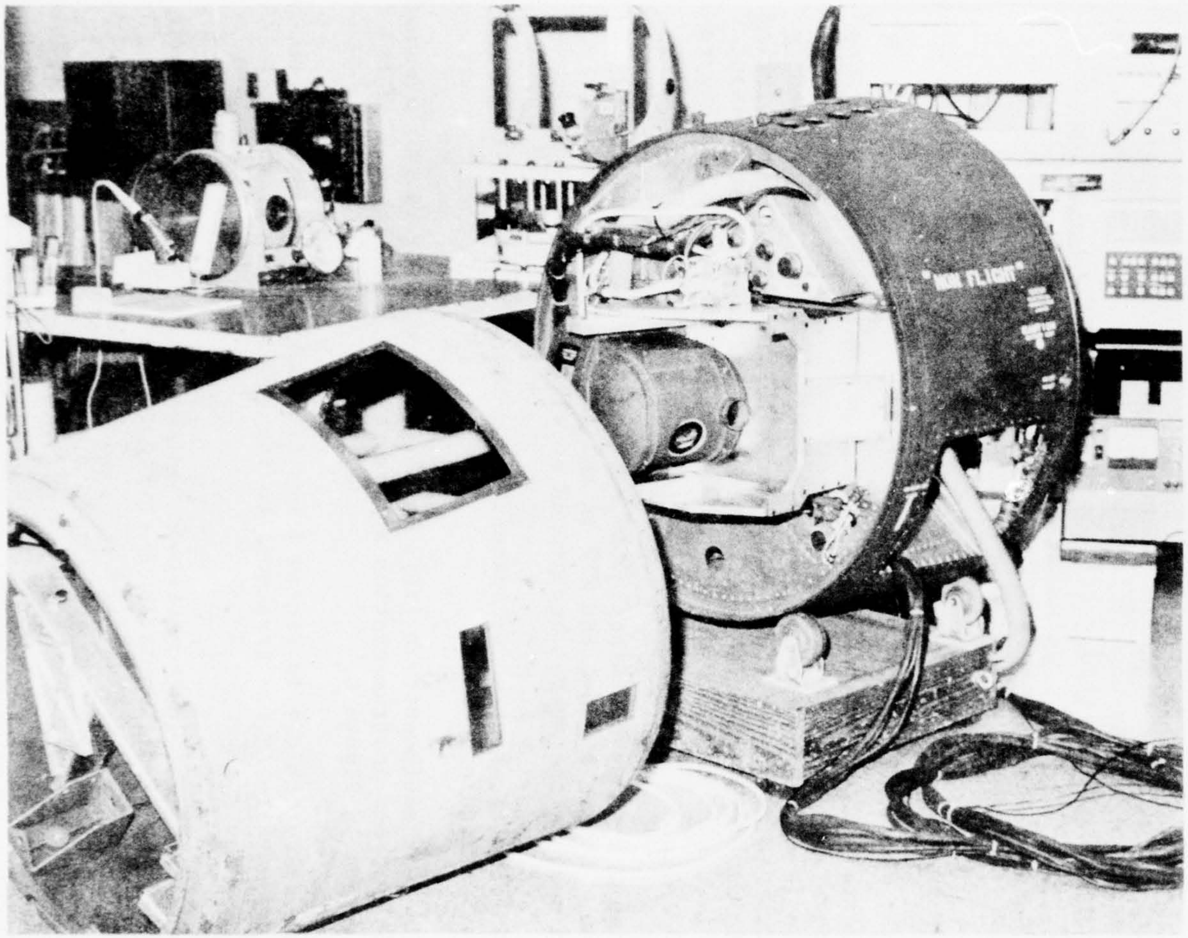

Figure 2. IMU rotated in mounting fixture, optical port exposed.

Figure 3. EL-mounted missile system ready for test.

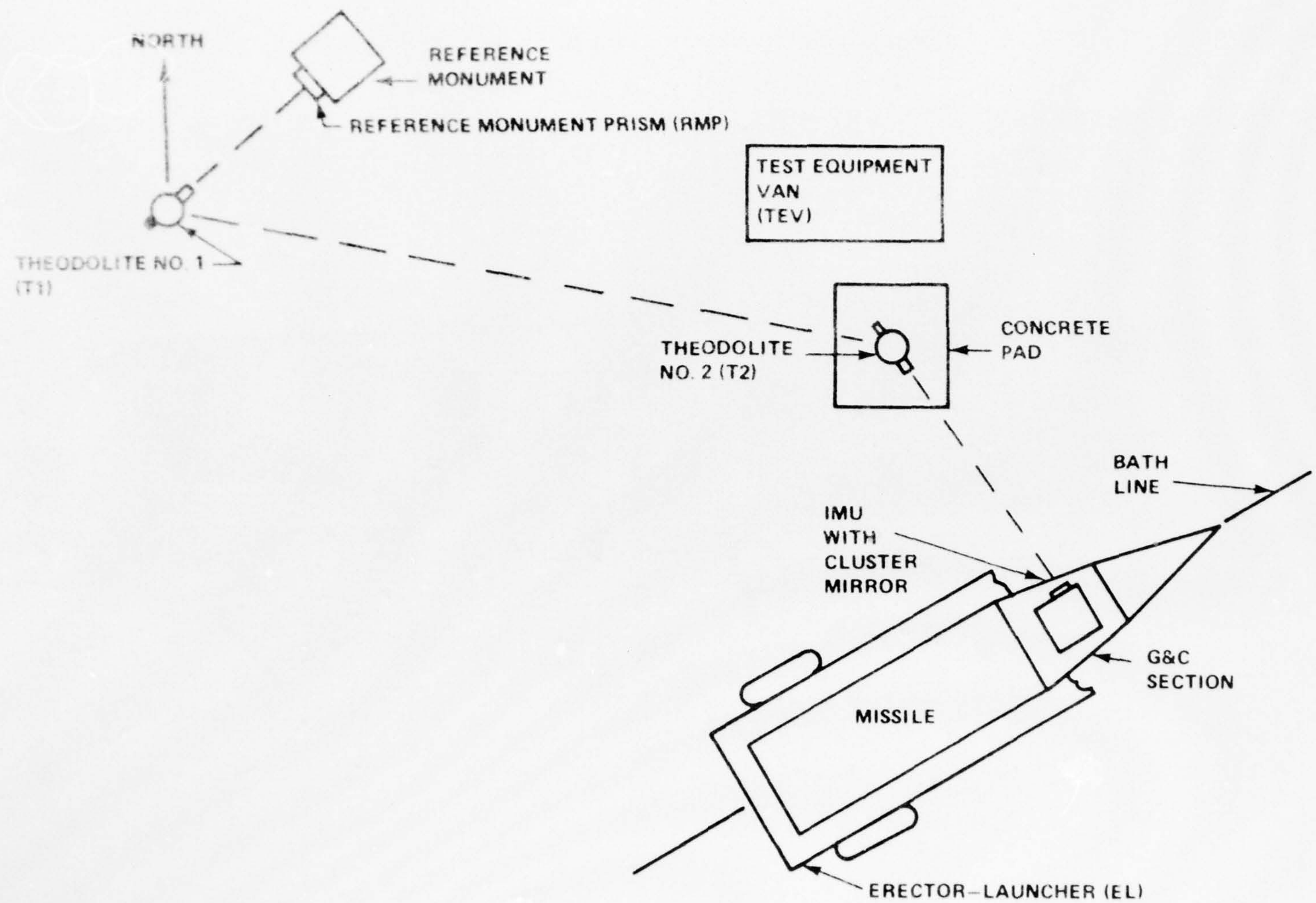

Figure 4. MOD shop area typical test setup.

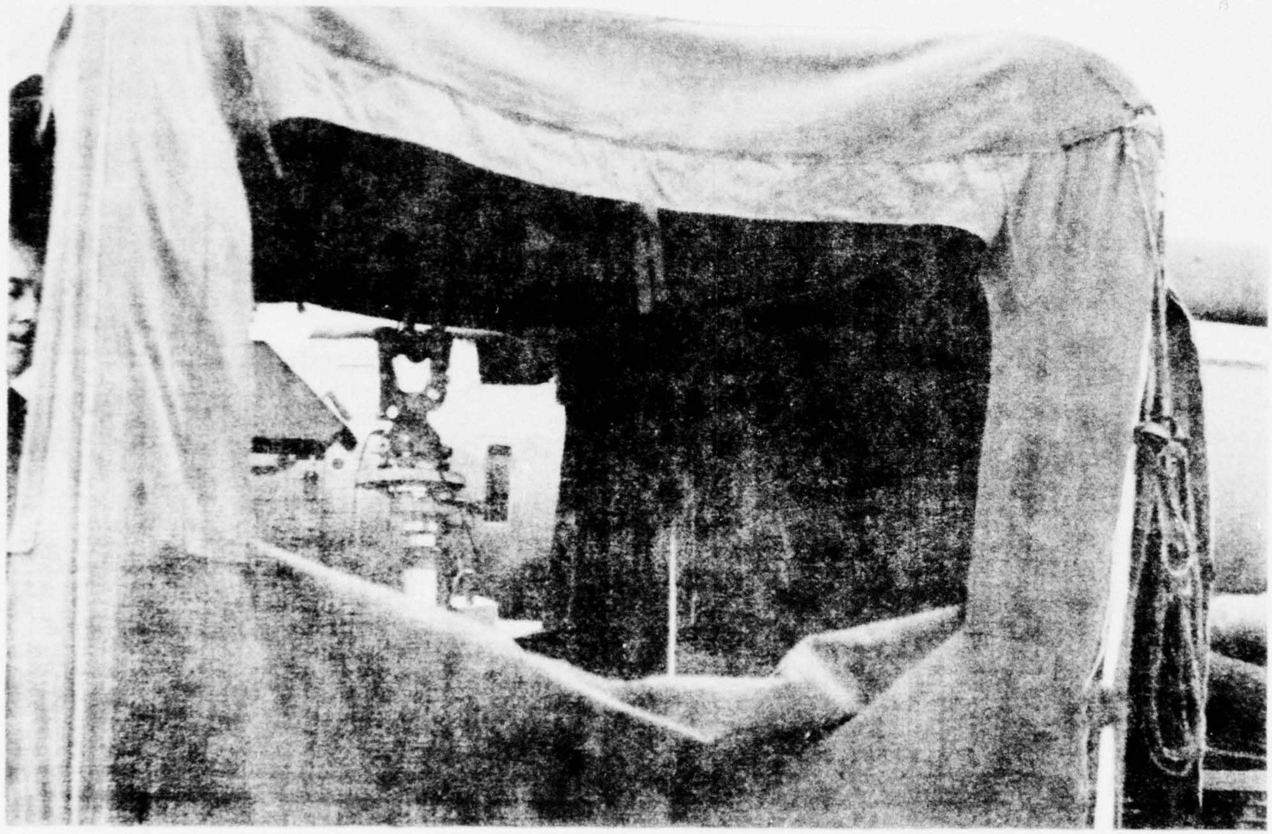

Figure 5. Missile G&C section viewed from T2 position.

Figure 6. Reference monument prism and nose of missile viewed from T1 area.

Figure 7. Field test setup.

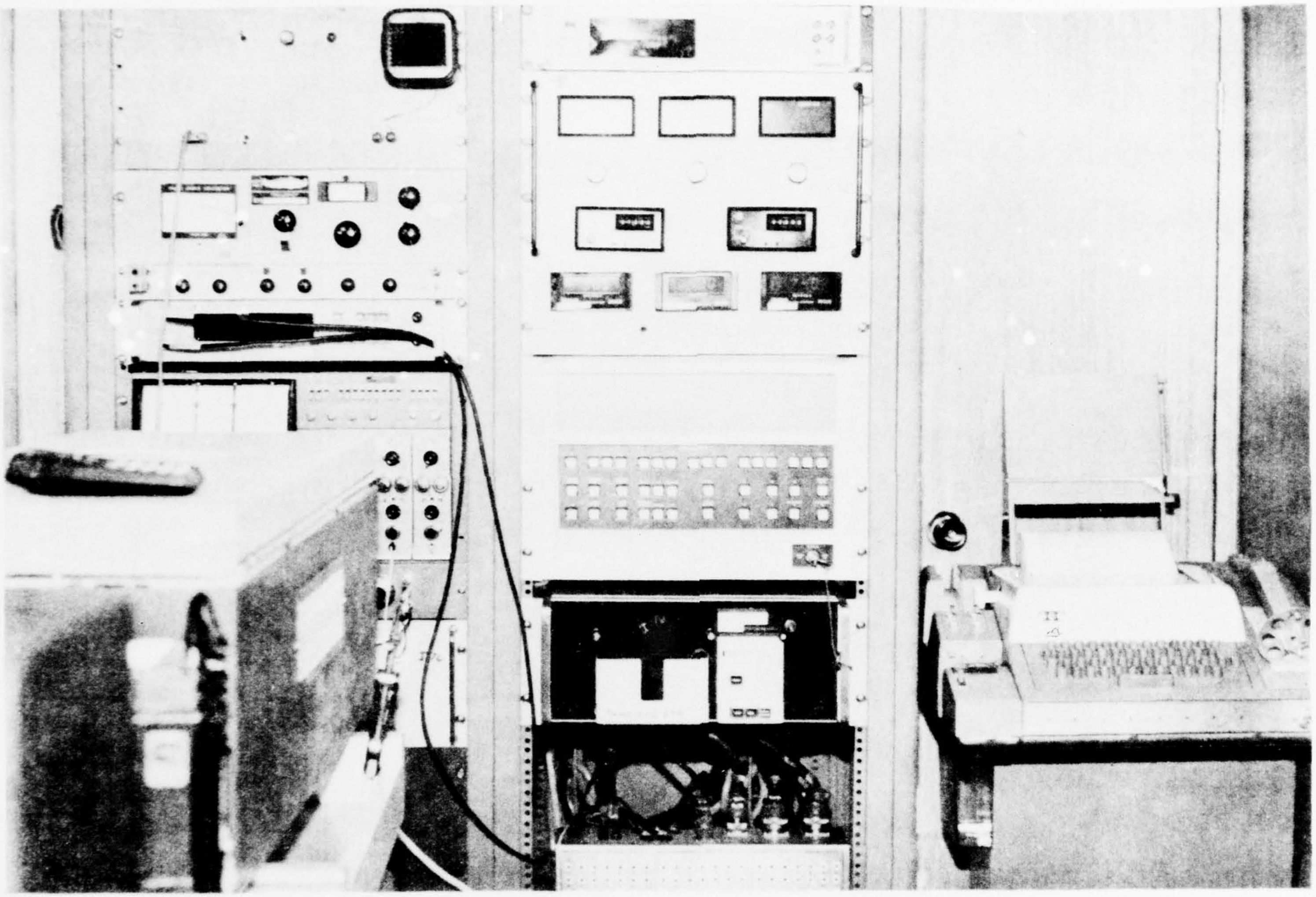

Figure 8. Interior of test equipment van.

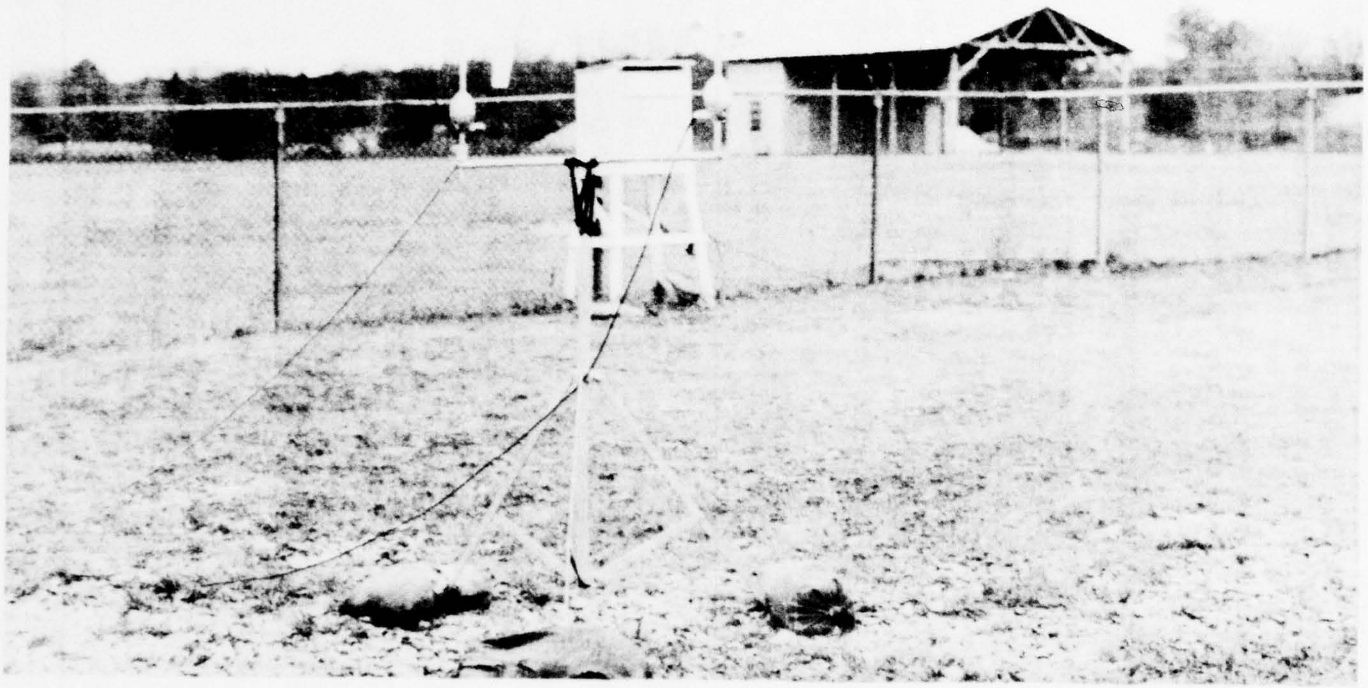

Figure 9. Meteorological instrumentation equipment.

Environmental disturbances imparted to the IMU case were monitored by an accelerometer triad with sensing axes nominally along the roll (X), pitch (Y), and yaw (Z) axes of the unit. The triad was mounted to the top of the IMU test fixture as shown in Figures 1 and 2.

Temperature was monitored at the IMU air inlet and at the accelerometer triad with a pair of quartz thermometer probes.

IV. TEST OPERATIONS AND CONDITIONS

A total of 64 gyrocompassing runs were made at 8 different headings approximately 45° apart. Azimuth data were taken optically using the same procedure as used in the laboratory. The detailed test procedure is given in Appendix A.

Testing was performed during the 2 to 14 December 1976 time period. The prevailing environmental conditions are summarized in Table 1. Corresponding laboratory conditions are included for comparison purposes.

TABLE 1. ENVIRONMENTAL CONDITIONS

Test Condition	Field Environment	Laboratory Environment
Soil condition	Large gravel spread over area (See Figure 7)	Isolated test pad
Weather	Sunny; partly cloudy; cloudy with light rain	Controlled environment
Temperature	29° - 67°F	Controlled at 72°F
Wind	1-13 mph, direction variable	None
Vehicular traffic	During 31 test runs	None
Vehicle idling Beside EL	During 24 test runs	
No vehicle operation	During 9 test runs	
IMU case orientation		
Pitch	0.4° fore axis down	0°
Roll	4.5° clockwise from aft	0°

V. TEST DATA

Optical, meteorological, and acceleration data were acquired for each of the 64 test runs. Appendix B presents a sample of raw data for each of these parameters. A heading of 180° was arbitrarily chosen as the position for which the raw data are given.

Average power spectra of accelerometer data were determined for each of the three axes monitored. A discussion of average power spectra and results from each of 8 runs at 180° heading are presented in Appendix C. Average power spectra for each of the three accelerometer channels operating in the laboratory are also presented.

Appendix D contains a summary of gyrocompass accuracy test results. Detailed data obtained from each of 8 test runs at each of 8 azimuth headings are presented along with the statistical results. The 40° and 70° headings were used rather than 45° and 90° headings, respectively, because of difficulty in positioning the EL at these headings.

The reduced data are further summarized, compiled, and plotted for comparison with pretest and post-test laboratory performance. Composite statistics are presented for the 64 pretest runs, the 64 field-test runs, and the 64 post-test runs for comparison purposes.

Pretest and post-test calibration data are also presented as part of Appendix D.

VI. DISCUSSION OF RESULTS

Figures D-1 and D-2 of Appendix D readily show the increase in RMS and average errors resulting from field-test runs over pretest and post-test runs. At a given heading, however, Figure D-3 of Appendix D shows that no great variations in standard deviations exist among the three test conditions. When the composite statistics for the field test, as shown in Table D-10 of Appendix D, are examined it is noted that if the average error had been near zero (as for pretest or post-test average error) the RMS error would approximate the one-sigma value of 66 arc sec. This is indicative of the fact that even though the standard deviation about the average at an individual heading is comparable to laboratory data, the peak error swings in the field are significantly greater. This can be visualized by drawing a horizontal axis at 40 arc sec average error on Figure D-2 of Appendix D and comparing the peak swings about this offset to those of the other two test conditions with offsets near zero. Thus, without an offset, the field RMS error would still be larger than the laboratory errors.

The exact cause of increased error in the field is undetermined; however, in the discussion that follows potential sources are examined.

It is noted from Table D-10 of Appendix D that during certain of the test runs the laboratory latitude rather than the test site latitude was mistakenly entered into the gyrocompass program. It can be shown that a reasonable approximation of azimuth error, σ_L, due to misbiasing the west gyro caused by a small incorrect latitude input is given by

$$|\sigma_L| = |\Delta\lambda \tan \lambda| \tag{1}$$

in which λ is the correct latitude and $\Delta\lambda$ is the difference between correct and incorrect latitute inputs. For the local latitude and $\Delta\lambda = 41$ arc sec

$$|\sigma_L| = |28| \text{ arc sec} \quad . \tag{2}$$

The composite field statistics of Table D-10 of Appendix D are repeated in Table 2 along with the resulting values when the correction of equation (2) is applied in both a positive and negative sense.

TABLE 2. COMPOSITE FIELD STATISTICS

Table D-10 (arc sec)		Positive Sense (arc sec)	Negative Sense (arc sec)
RMS	77	85	71
Avg	40	54	26
σ	66	66	66

The general shape of the pretest and the post-test average error curves of Figure D-3 of Appendix D suggests that the correction should be applied in the negative sense.

Another complicating factor is the non-extension of EL jacks during the same runs for which incorrect latitude setting was applied. An examination of instrumentation accelerometer data reveals that base motions were generally slightly higher when the jacks were supporting the EL; however, it is shown that measured base motions, whether the jacks were extended or not, contribute an insignificant amount of azimuth error.

It can be shown to a reasonable approximation, that gyro drift rate error ($D\epsilon$), due to base vibratory acceleration inputs of the form $G = G_{PN} \sin (N\omega_o t + \phi)$, is given by

$$D\epsilon = \frac{30\sqrt{2}}{t^3 \omega_o^2} \left(\sum_{N=1}^{k} \frac{G_{PN}^2}{N^4} \right)^{1/2} \text{ rad/sec} \qquad (3)$$

where

$G_{PN}(g)$ = peak sinusoidal acceleration at frequency $N\omega_o$

t(sec) = time duration of gyro bias/fine gyrocompass sequence

ω_o(rad/sec) = lowest sinusoidal base motion frequency present

N = 1, 2, 3, ..., k such that $k\omega_o$ is the highest acceleration frequency of interest.

An examination of accelerometer average power spectra (180° heading) in Figures D-3 through D-26 of Appendix D shows the variation of the square of peak acceleration input as a function of frequency. Equation (3) indicates that gyro drift rate due to high frequency inputs is insignificant. This, along with the fact that IMU vibration isolators start attenuating case inputs at 40 to 50 hertz, sets the highest frequency of interest at

$$k\omega_o = 2\pi f = 2\pi(50) = 100\pi \text{ rad/sec} \quad . \qquad (4)$$

Determination of the lowest frequency present is more difficult because uncompensable DC amplifier offset tended to swamp out amplitudes at other frequencies. To obtain reasonable scaling, the spectrum plots were started at 0.5 hertz. Except for the DC component, very little amplitude was noted below 0.5 hertz and for analytical purposes a low frequency of this value was chosen. This gives

$$\omega_o = 2\pi f = 2\pi(0.5) = \pi \text{ rad/sec} \qquad (5)$$

and from Equation (4)

$$k = 100 \quad . \qquad (6)$$

The maximum peak acceleration as determined by the average power spectrum analysis in either the X or Y channel never exceeded 2×10^{-3} g's for any of the 64 test runs.

An extreme worst case condition can be analyzed by assuming that this peak value was present over the total frequency range from 0.5 to 50 hertz. Under this assumption equation (3) can be written as

$$D_{\epsilon} = \frac{30\sqrt{2}\, G_{PN}}{t^3\, \omega_o^2} \left(\sum_{N=1}^{k} \frac{1}{N^4} \right)^{1/2} \text{ rad/sec} \tag{7}$$

where

$G_{PN} = 2 \times 10^{-3}$ g

$t = 240$ sec

$\omega_o = \pi$ rad sec

$k = 100$.

By actual computation

$$\sum_{N=1}^{100} \frac{1}{N^4} = 1.082323 \tag{8}$$

so that the square root of the term is taken as unity.

With this approximation and with the values shown substituted into Equation (7)

$$D_{\epsilon} = 6.22 \times 10^{-10} \text{ rad/sec} = 1.28 \times 10^{-4} \text{ deg/hr} \quad . \tag{9}$$

Making the assumption that the X and Y gyro error drift rates are equal at both the 0° and 90° positions, a composite drift rate, $D_{\epsilon T}$, is given by

$$D^2_{\epsilon T} = D^2_{\epsilon x}(0°) + D^2_{\epsilon y}(0°) + D^2_{\epsilon x}(90°) + D_{\epsilon y}(90°) \tag{10}$$

$$D^2_{\epsilon T} = 4\, D^2_{\epsilon} \tag{11}$$

$$D_{\epsilon T} = 2\, D_{\epsilon} \quad . \tag{12}$$

The ratio of the composite drift error of equation (12) and local horizontal component of earth's rate ($\Omega \cos \lambda$) gives azimuth error, σ_G, as indicated:

$$\sigma_G = \frac{2 D_\epsilon}{\Omega \cos \lambda} = 2.07 \times 10^{-5} \text{ rad} = 4.28 \text{ arc sec} \quad . \tag{13}$$

This is a negligible error even though extreme worst case conditions were assumed. Vehicular traffic and ambient winds therefore apparently contributed an insignificant amount to the errors shown in Table D-10, Appendix D.

Another error source could be possible inaccuracy in the accuracy of line-of-sight heading to the prism which was used as a reference for all test runs.

The line-of-sight heading was established by measuring the angle relative to Polaris. The heading was verified by a gyrocompass which was carefully calibrated in the laboratory, before and after the verification run, at the heading determined by theodolite readings on Polaris. Verification results differed from the original heading by 11 arc seconds and the uncertainty in the reference heading is judged to be in no greater error than this amount.

Operator error is always a possible error source. A review of the raw optical data, however, indicates repeatability comparable to that obtained in laboratory measurements. The fact that the optical measurement equipment was subjected to essentially the same environmental conditions as the test specimen, however, cannot be overlooked.

Re-setup of the system, as described in Appendix D at 225° heading which gave results very similar to those obtained the previous day, gives added confidence that the test setup and measurement operations were performed properly.

The fact that the IMU case was rotated approximately 4.5° about the roll axis and 0.4° about the pitch axis should theoretically cause no azimuth error. A speculation is, however, that some measurement error may have accrued because the optical line-of-sight to the IMU cluster mirror was not perpendicular to the glass in the optical access post.

Pretest and post-test calibration runs as shown in Tables D-11 and D-12, Appendix D, indicate that no unusual parameter changes occurred during the field-test period. This is further evidenced by pretest and post-test gyrocompass performance.

VII. CONCLUSIONS AND RECOMMENDATION

This test has provided the first PERSHING PII IMU gyrocompass accuracy data outside the laboratory. Although RMS and average errors increased by significant amounts, no catastrophic performance breakdown was experienced. Repeatability at each heading did not deviate significantly from laboratory performance.

The most readily identifiable error source which, if corrected, significantly decreases the composite average error and slightly decreases the composite RMS error is the incorrect latitude input for four of the headings. The data in the third column of Table 2, which is corrected in the negative sense, are believed to be the proper representation of system performance.

Little, if any, of the error can be attributed to base motions caused by either vehicular traffic or ambient winds.

Other measurement errors such as operator, reference, and possibly optical glass errors contribute to the system error to some degree but cannot fully account for the rather large swings about the average error.

A significant finding is that the error from the first run in the morning from a cold start differs substantially from the succeeding runs. This phenomenon occurred when the first run was made after only a 9-minute system warm-up as required by the IMU specification. The error does not appear to belong to the succeeding population of errors and is most likely connected with IMU thermal characteristics. The phenomenon can be observed in Tables D-1 through D-8, Appendix D, by noting unusual error values and the accompanying remarks.

It is recommended that this phenomenon be carefully monitored during up-coming tests to be performed with PII hardware by the system contractor.

Use of IMU EM S/N 001 is recommended for the full-scale test for data comparison, particularly in the area of average errors as a function of heading.

It is recognized that the foregoing test results are by no means conclusive; however, the indications are that errors grow when the system is operated outside a benign laboratory environment. This is sufficient reason for non-relaxation of current performance specifications.

Appendix A. TEST PROCEDURE

A. Equipment List

The following equipment is required for performance of the outdoor gyrocompass test:

1) Pla missile

2) Erector-launcher

3) G&C section and shroud modified to accept PII IMU and mounting fixture and to provide access for routing cables, cooling air hose and for manual rotation of IMU case.

4) PII IMU

5) PII IMU mounting fixture

6) PII IMU test equipment

7) Cable set, 40 ft long

8) Shop vacuum for cooling air

9) Magnetic compass, or equivalent, for obtaining best available true heading (BATH)

10) Theodolite, 3 each

11) Anemometer

12) Accelerometer triad for instrumentation

13) Thermometer

14) Test equipment van

15) Tent or umbrella shelters for theodolites

16) Multichannel chart recorder

17) Multichannel tape recorder

B. Pretest Activities

Prior to start of outdoor testing, a full checkout of the system will be performed in the laboratory.

The IMU mounting fixture will be equipped with an accelerometer triad for measurement of vibrational disturbances, nominally along the three principal axes of the IMU. A quartz thermometer probe will be installed in the IMU cooling air inlet and the accelerometer triad mounting block.

The IMU and mounting fixture will be installed in the G&C section and its weight and center of gravity will be adjusted to approximate Pla values.

Test equipment will be connected to the IMU, through the long (40 ft) cable set and pretest gyrocompass runs will be made very similar to those to be made outdoors, to determine if use of long cables affects gyrocompass performance. Accelerometer triad and thermometer instrumentation will be checked at this time.

The IMU will then be removed from the G&C section and reinstalled on the laboratory test table. A final pretest calibration run will be made, using the long cables to determine if use of long cables produces any significant effect on IMU calibration results.

Pretest activities in the Mod Shop area will involve the laying off of eight lines in the vicinity of the concrete pad at nominal azimuth headings of 0°, 45°, 90°, 135°, 180°, 225°, 270°, and 315°. This will be accomplished by use of a magnetic compass or equivalent device to provide a BATH. The EL will be parked, in turn, with its longitudinal axis nominally along a line to provide gyrocompass data at each of the previously mentioned nominal headings. Combined accuracy of the line layout and EL parking operations will be held within the range of approximately ±5°.

Following these activities, the G&C section will be taken to the Mod Shop and installed on the missile. The complete system will then be set up outdoors in the typical configuration shown in Figure A-1.

C. Operational Procedure

The procedure for performing gyrocompass tests is outlined as follows:

1) Park EL nominally along 0° line in such a manner that the G&C section optical access window can be viewed by T2.

2) Connect IMU test cables to test set in TEV, connect accelerometer triad, thermometer and anemometer to test instrumentation equipment, and connect IMU cooling vacuum hose.

3) Set up T1 and T2; acquire RMP with T1 and IMU optical port with T2.

4) Turn on all power to the TEV and allow instrumentation (accelerometers, thermometer electronics, recording equipment, etc.) to warm up at least 30 minutes.

5) Turn on IMU power and vacuum source and proceed into a preliminary gyrocompass run using laboratory operating procedure set forth in Singer, Kearfott Division (SKD) document number E100F547E110, Revision E. Check for proper operation of accelerometer triad, thermometer, anemometer and recording equipment.

6) When "ALIGN HOLD" event is reached (as printed out by the teletype) remove bolts holding test fixture rotatable member in place and rotate IMU case through approximately 103°. Pin fixture at this point with dowel pin.

7) Acquire IMU cluster mirror with T2. T2 is now positioned such that gyrocompass runs for record can be performed at a nominal heading of 0°.

8) Rotate IMU case to original position (fore axis nominally along missile longitudinal fore axis) and secure with bolts.

9) Set up recording equipment for runs for record (set zeros, scale factors, etc.)

10) Commence gyrocompass run using laboratory operating procedure set forth in SKD document number E100F547E110, Revision E. Start heavy vehicle traffic in vicinity of EL.

11) Record the following parameters starting at the beginning of the gyrocompass run.

a) Air inlet temperature

b) Wind speed and direction

c) Accelerometer triad outputs (chart and tape recorders). Voice annotate tape recording, with date, heading, run number, start of run, end of run, etc.

d) Other remarks such as rapid change in temperature, wind gusts, and other unusual occurrences.

12) Near the end of the gyrocompass run, set up T1 and T2 so that a minimum amount of releveling and other adjustments are required at "ALIGN HOLD".

13) When "ALIGN HOLD" event is reached, stop vehicle traffic, and carefully rotate IMU case through 103° as in step 6. The operator performing this manual task should avoid imparting disturbances to the missile body.

14) Repeat step 11 at the end ("ALIGN HOLD") of gyrocompass run.

15) At "ALIGN HOLD", immediately commence taking optical data by sighting on the IMU cluster mirror with T2, and by sighting on RMP with T1.

16) Complete optical meaaurements by collimating T1 and T2.

17) Repeat steps 8 through 16 for a total of eight runs.

The procedure outlined previously is to be repeated at each 45° nominal heading increment of the EL and missile, and will likely entail movement of the TEV for each heading.

D. Data Acquisition

Gyrocompass accuracy data will be acquired using T1, T2, RMP, and the IMU CM. The measurement diagram is shown in Figure A-2 in which the following definitions apply:

1) R1 = T1 horizontal scale reading when sighting from T1 to RMP

2) R2 = T1 horizontal scale reading when sighting from T1 to T2

3) R3 = T2 horizontal scale reading when sighting from T2 to T1

4) R4 = T2 horizontal scale reading when sighting from T2 to CM

Using Figure A-2 and the foregoing definitions, the following angles are known or can be calculated as indicated:

1) A = Known angle between North and line-of-sight (LOS) to RMP

2) $B = R_2 - R_1$

3) $C = R_3 - R_4$

4) $D = A + B$

5) $\bar{D} = 180° - D$

6) E = LOS heading to CM

$E = 180° - C + D$

7) γ = Known angle between LOS to CM and X accelerometer input axis

8) $\bar{\gamma} = 180° - \gamma$

9) α_o = Azimuth heading of X accelerometer input axis (the required angle)

$\alpha_o = E - \bar{\gamma}$

Optical readings R1, R2, R3, and R4 will each be calculated as the average of a minimum of two sets of forward and reverse measurements made with the applicable theodolite.

The measurement diagram of Figure A-3 applies when the missile interferes with the LOS between T1 and T2.

Entries necessary for calculation of α_o will be made on attached Data Sheet No. 1.

Data Sheet No. 2 will be used when the missile interferes with the LOS between T1 and T2.

Accelerometer triad data will be acquired using a chart recorder for quick-look purposes and will also be tape recorded for off-line processing.

Temperature and wind data will be recorded during each gyrocompass run as well as any unusual occurrences during a test.

At the end of each gyrocompass run a computed value of azimuth heading, α, is printed out by the teletype. North channel drift rate (DN), west channel drift rate (DW), and azimuth resolver readout (RSV) are also printed out. These parameters along with α_o as computed on Data Sheet No. 1 or Data Sheet No. 2 will be entered on attached Data Sheet No. 3. Other pertinent data will be entered as indicated at the top of Data Sheet No. 3.

E. Data Reduction

With reference to Data Sheet No. 3, the error in a gyrocompass run is computed as

$$\epsilon_o = \alpha - \alpha_o \text{ (arc sec)}$$

and will be entered in the indicated column.

The root mean square (RMS), average (AVG), and standard deviation (σ) of the errors determined in the series of eight runs at a particular heading will be calculated in the conventional manner:

$$\text{RMS} = \left(\frac{\sum_{i=1}^{N} \epsilon_{oi}^2}{N} \right)^{1/2}$$

$$AVG = \frac{\sum_{i=1}^{N} \epsilon_{oi}}{N}$$

$$\sigma = \left(\frac{\sum_{i=1}^{N} (\epsilon_{oi} - AVG)^2}{N - 1} \right)^{1/2} .$$

N = Number of runs = 8

The results will be entered on Data Sheet No. 3.

Tape recorded accelerometer triad data will be processed off-line to determine the average power spectra of environmental disturbances coupled to the IMU mounting fixture and case.

F. Post-Test Activities

At the completion of outdoor gyrocompass testing the IMU will be returned to the laboratory test setup and a calibration run will be made.

Eight gyrocompass runs will be made at each heading for which tests were performed outdoors:

Pretest data, outdoor data, and post-test data will be compiled on attached Data Sheet No. 4. Data Sheet No. 4 will be used to analyze pretest and post-test data versus outdoor data to determine if significant differences exist. Plots will be made showing RMS, AVG, and standard deviation of error values versus heading for each of three test conditions.

Pretest and post-test calibration data will also be examined.

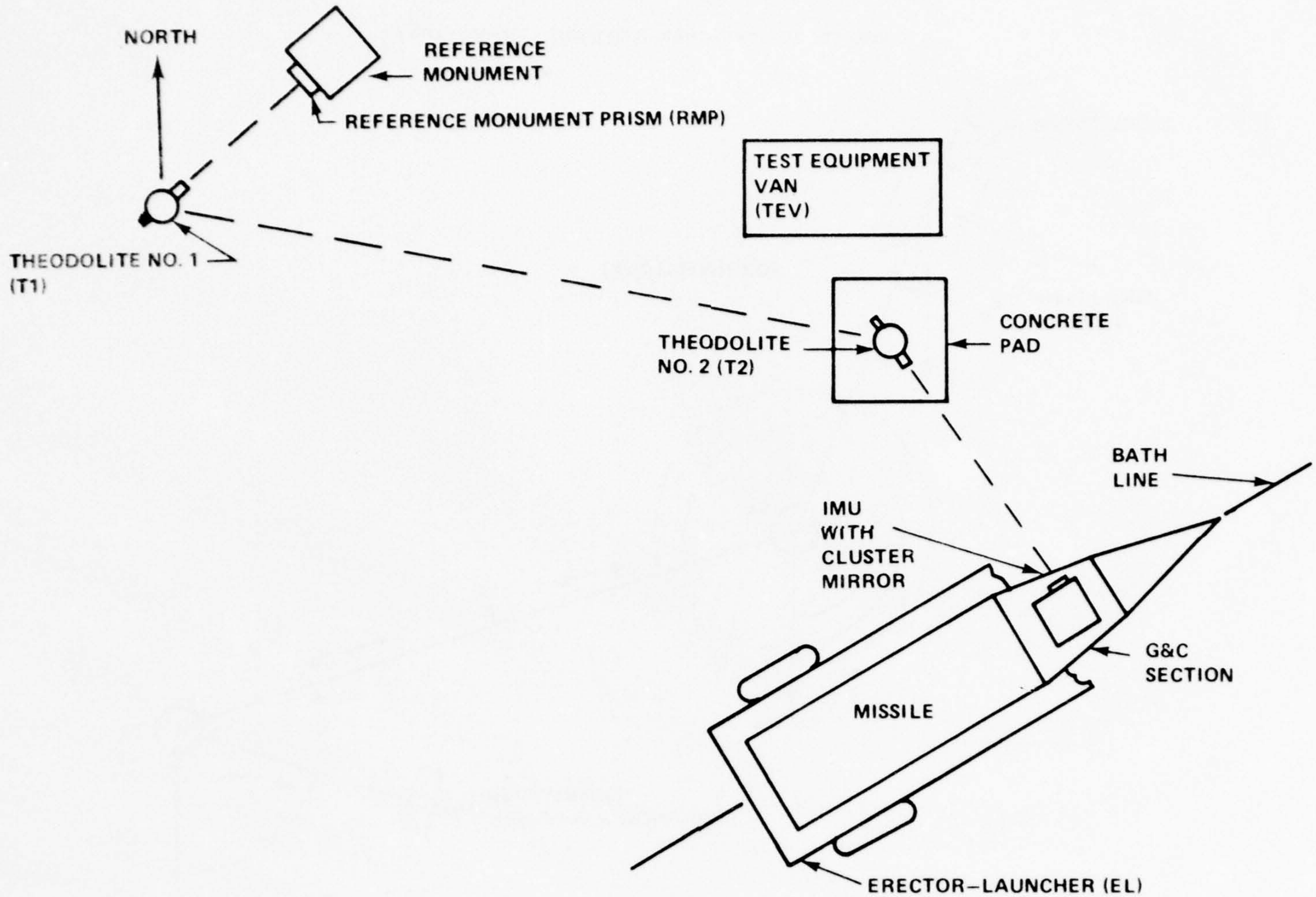

Figure A-1. Mod Shop area typical test setup.

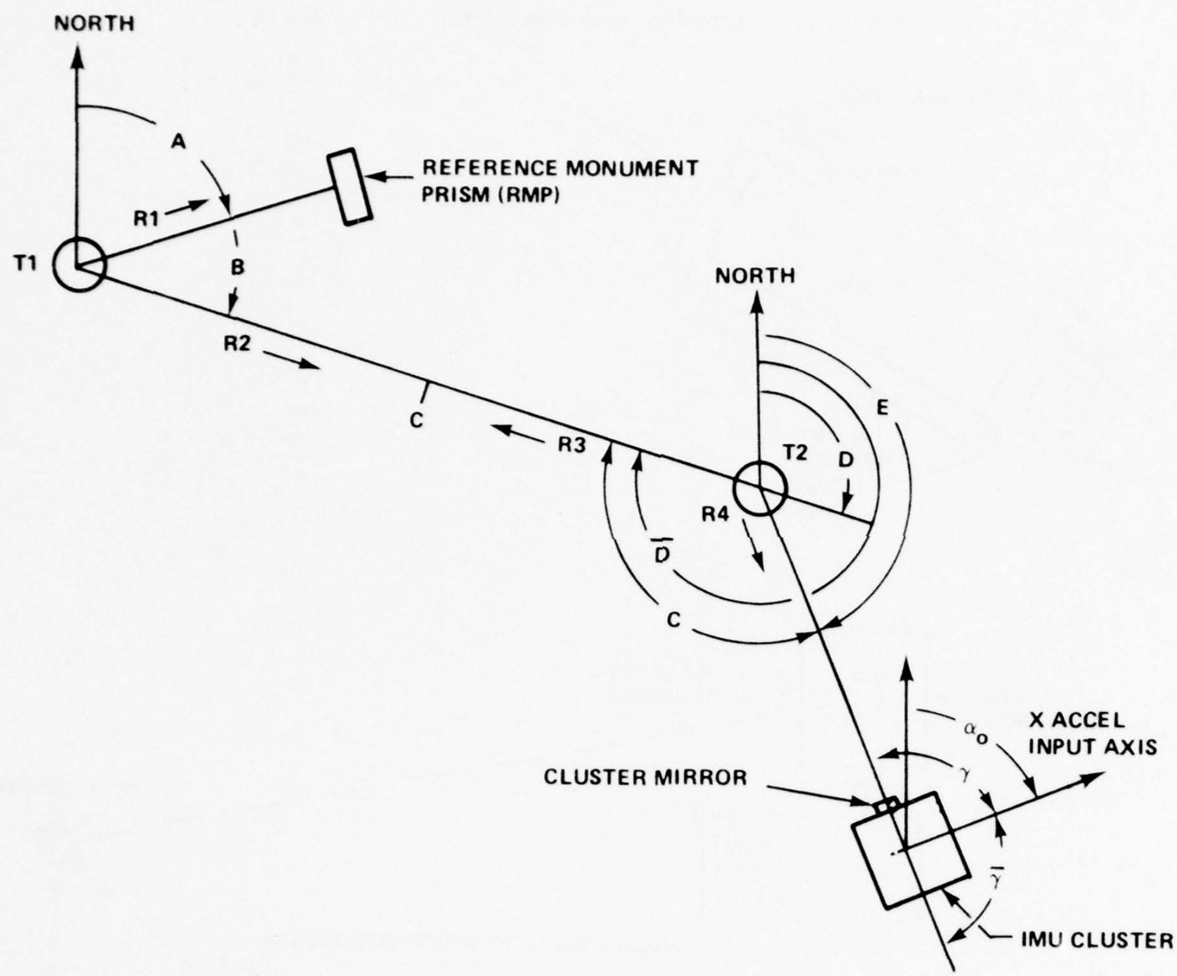

Figure A-2. Optical measurement diagram.

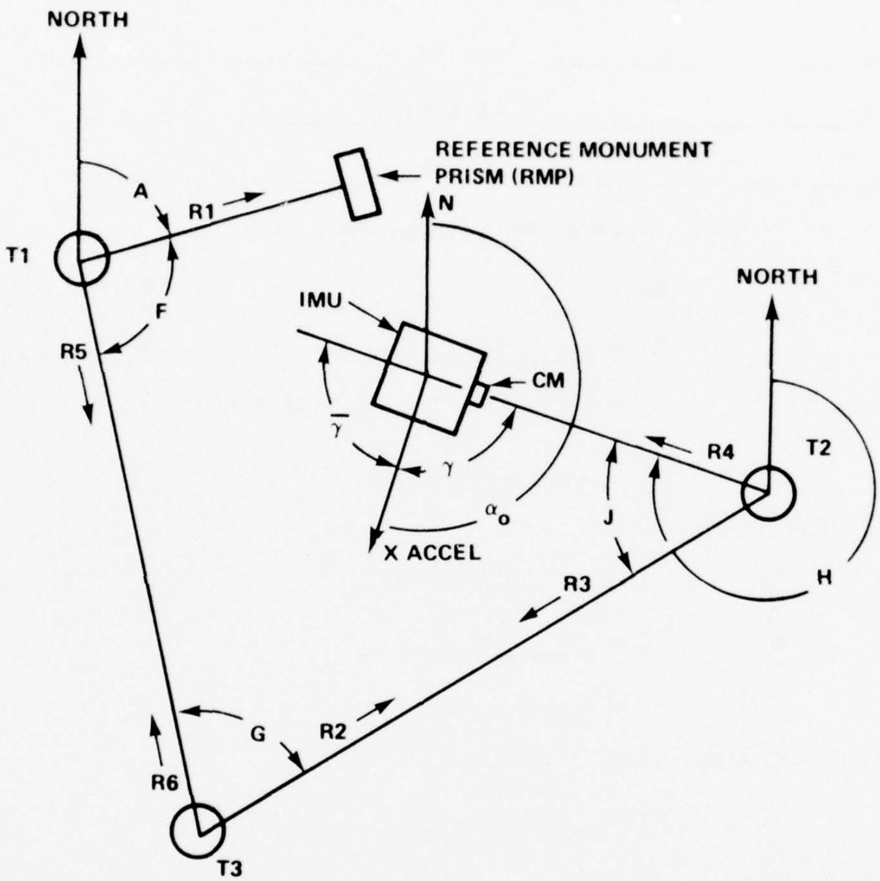

Figure A-3. Optical measurement diagram when missile interferes with LOS between T1 and T2.

DATA SHEET No. 1

PII IMU MISSILE-MOUNTED GYROCOMPASS TEST

Heading:____________________ Run No.:____________________

IMU S/N:____________________ T1 S/N:____________________

Date:____________________ T2 S/N:____________________

OPTICAL DATA (deg, min, sec)

R2 = R3 =

R1 = __________ R4 = __________

(B = R2 - R1): B = (C = R3 - R4): C =

A = __________

(D = A + B): D =

$180° = 179° 59' 60''$

C = __________

D = __________

(E = 180° - C + D): E =

$\bar{\gamma}$ = __________

($\alpha_0 = E - \bar{\gamma}$): α_0 =

TEMPERATURE AND WIND DATA

Temperature (°F)

	Accel Triad	IMU Air Inlet	Wind Speed/Direction (mph/deg)
Start:	__________	__________	Start:____________________
End:	__________	__________	End:____________________

DATA SHEET NO. 2

PII IMU MISSILE-MOUNTED GYROCOMPASS TEST

Heading:____________________ Run No.:____________________

IMU S/N:____________________ T1 S/N:____________________

Date:____________________ T2 S/N:____________________

T3 S/N:____________________

OPTICAL DATA (deg, min, sec)

	R5 =		A =
	R1 =		F =
(F = R5 - R1):	F =		G =
	R2 =		J =
	R6 =	(H = A + F + G + J):	H =
(G = R2 - R6):	G =		$\bar{\gamma}$ =
	R4 =	(α_o = H - $\bar{\gamma}$):	α_o =
	R3 =		α =
(J = R4 - R3):	J =		α_o =
		ϵ_o = (α - α_o):	ϵ_o =

TEMPERATURE AND WIND DATA

Temperature (°F)

	Accel Triad	IMU Air Inlet	Wind Speed/Direction (mph/deg)
Start:			Start:
End:			End:

DATA SHEET NO. 3

PII IMU MISSILE-MOUNTED GYROCOMPASS FIELD TEST

IMU S/N: ______________ Remarks Legend: (1) Temperature (°F) Range

Date: ______________ (2) Wind speed (mph), and direction (deg) range

Heading: ______________ (3) Other

Weather: ______________

Run No.	α (arc sec) (deg, min, sec)	α_o (arc sec) (deg, min, sec)	ϵ_o (arc sec)	DN(°/hr) / DW(°/hr)	RSV (deg, min, sec)	Remarks
1						
2						
3						
4						
5						
6						
7						
8						
		RMS				
		AVG				
		σ				

DATA SHEET NO. 4

PII IMU GYROCOMPASS FIELD TEST RESULTS

IMU S/N 001: COMPILATION OF PRETEST, FIELD TEST AND POST-TEST DATA

Heading (deg)	Statistics for 8 Runs	Pretest Error (arc sec)	Field Test Error (arc sec)	Post-Test Error (arc sec)
0	RMS AVG σ			
45	RMS AVG σ			
90	RMS AVG σ			
135	RMS AVG σ			
180	RMS AVG σ			
225	RMS AVG σ			
270	RMS AVG σ			
315	RMS AVG σ			
Composite Statistics for 64 runs for Each Test Condition	RMS AVG σ			

Appendix B. RAW DATA SAMPLE

The following raw data were taken at a nominal missile heading of 180°F. At this heading, the missile blocked the line-of-sight between T1 and T2 requiring the use of an auxiliary theodolite, T3.

Raw optical data (theodolite readings) corresponding to the requirements (minimum of two sets of forward and reverse measurements) of Appendix A, Test Procedure are presented in Table B-1. Tables B-2 through B-9 present results of raw data reduction using the optical measurement diagram of Figure A-3, Appendix A. Temperature and wind data are also shown in Tables B-2 through B-9.

Detailed meteorological data are shown in Table B-10 at 1-minute intervals during each of the 8 gyrocompass tests at this heading.

Samples of accelerometer output data as recorded with a multichannel chart recorder for each of the 8 runs are shown in Figures B-1 through B-8. All recordings were made with a chart speed of 100 mm/sec and a scale factor or 100 μV/mm. The accelerometer scale factor is 0.4 μg/mm so that the chart recorder scale factor in terms of acceleration is 400 μg/mm.

Channel 4 of the recorder was not used.

TABLE B-1. THEODOLITE READINGS

Date: 14 Dec 76 Heading: 180°												
Run No.	R1: T1 to prism		R2: T3 to T2		R3: T2 to T3		R4: T2 to CM		R5: T1 to T3		R6: T3 to T1	
	Fwd	Rev	Fwd	Rev	Fwd	Rev	Fwd	Rev	Fwd	Rev	Fwd	Rev
1	097 48 02	277 48 00	044 47 31	224 47 29	000 00 55	180 00 43	104 31 46	284 31 34	138 23 42	318 23 41	001 01 33	181 01 36
	03	47 59	33	34	51	44	40	29	44	50	35	37
	Avg: 097 48 01		044 47 32		000 00 48		104 31 37		138 23 44		001 01 35	
2	097 47 58	277 48 03	044 47 33	224 47 40	000 01 02	180 00 50	104 34 08	284 33 54	138 23 43	33 23 44	001 01 37	181 01 42
	59	03	35	36	00 55	48	33 48	44	48	49	40	42
	Avg: 097 48 01		044 47 36		000 00 54		104 33 54		138 23 47		001 01 40	
3	097 48 04	277 48 01	044 47 40	224 47 42	001 01 02	180 00 48	104 53 54	284 33 42	138 23 36	318 23 42	001 01 38	181 01 36
	00	02	39	43	00	50	45	30	38	42	40	39
	Avg: 097 48 02		044 47 41		000 00 55		104 33 43		138 23 40		001 01 38	
4	097 48 00	277 47 54	044 47 41	224 47 47	001 01 12	180 01 05	104 33 36	284 33 17	138 23 40	318 23 48	001 01 15	181 01 10
	04	48 01	44	49	11	03	17	10	36	41	16	14
	Avg: 097 48 00		044 47 45		000 01 08		104 33 20		138 23 41		001 01 14	
5	097 47 57	277 47 51	044 47 44	224 47 48	000 01 12	180 01 09	104 33 38	284 33 28	138 23 28	318 23 27	001 01 12	181 01 17
	56	59	47	45	10	05	28	14	25	27	14	13
	Avg: 097 47 56		044 47 46		000 01 09		104 33 27		138 23 27		001 01 14	
6	097 48 12	227 48 04	044 47 51	224 47 51	000 01 09	180 01 00	104 33 23	284 33 12	138 23 36	318 23 22	001 01 12	181 01 16
	17	16	46	51	05	00 55	09	32 53	35	37	11	13
	Avg: 097 48 12		044 47 50		000 01 02		104 33 09		138 23 25		001 01 13	
7	097 48 13	227 48 12	044 47 51	224 47 58	000 01 14	180 01 08	104 32 55	284 32 41	138 23 30	318 23 33	001 01 13	181 01 15
	16	15	56	56	13	11	43	28	31	32	10	15
	Avg: 097 48 14		044 47 55		000 01 12		104 32 42		138 23 32		001 01 13	
8	097 48 12	227 48 08	044 48 01	224 48 05	000 01 24	180 01 16	104 32 20	284 32 11	138 23 39	318 23 41	001 01 11	181 01 05
	15	14	47 59	00	20	14	07	31 55	39	42	10	04
	Avg: 097 48 12		044 48 01		000 01 18		104 32 08		138 23 40		001 01 08	

Note: Entries are in deg, min, sec.

TABLE B-2. PII IMU MISSILE-MOUNTED GYROCOMPASS TEST, HEADING 180°, RUN NO. 1

IMU S/N: 001 T1 S/N: 119678

Date: 14 Dec 76 T2 S/N: 55939

T3 S/N: 116699

OPTICAL DATA (deg, min, sec)

	R5 = 137 83 44		A = 094 33 18
	R1 = 097 48 01		F = 040 35 43
(F = R5 - R1):	F = 040 35 43		G = 043 45 57
	R2 = 044 46 92		J = 104 30 43
	R6 = 001 01 35	(H = A + F + G + J):	H = 283 25 41
(G = R2 - R6):	G = 043 45 57		$\bar{\gamma}$ = 102 02 19
	R4 = 104 30 91	($\alpha_o = H - \bar{\gamma}$):	α_o = 181 23 22
	R3 = 000 00 48		α = 181 24 28
(J = R4 - R3):	J = 104 30 43		α_o = 181 23 22
		($\epsilon_o = \alpha - \alpha_o$):	ϵ_o = 000 01 06
			ϵ_o = 66 arc sec

TEMPERATURE AND WIND DATA

	Temperature (°F) Accel Triad	IMU Air Inlet	Wind Speed/Direction (mph/deg)
Start:	39	39	5/130
End:	42	41	5/110

TABLE B-3. PII IMU MISSILE-MOUNTED GYROCOMPASS TEST
HEADING 180°, RUN NO. 2

IMU S/N: 001

Date: 14 Dec 76

T1 S/N: 119678

T2 S/N: 55939

T3 S/N: 116699

OPTICAL DATA (deg, min, sec)

	R5 =	137	83	47
	R1 =	097	48	01
(F = R5 - R1):	F =	040	35	46
	R2 =	044	46	96
	R6 =	001	01	40
(G = R2 - R6):	G =	043	45	56
	R4 =	104	33	54
	R3 =	000	00	54
(J = R4 - R3):	J =	104	33	00

	A =	094	33	18
	F =	040	35	46
	G =	043	45	56
	J =	104	33	00
(H = A + F + G + J):	H =	283	27	60
	$\bar{\gamma}$ =	102	02	19
($\alpha_o = H - \bar{\gamma}$):	α_o =	181	25	41
	α =	181	26	76
	α_o =	181	25	41
($\epsilon_o = \alpha - \alpha_o$):	ϵ_o =	000	01	35

ϵ_o = 95 arc sec

TEMPERATURE AND WIND DATA

Temperature (°F)

	Accel Triad	IMU Air Inlet	Wind Speed/Direction (mph/deg)
Start:	48	46	Start: 8/130
End:	50	48	End: 4/120

TABLE B-4. PII IMU MISSILE-MOUNTED GYROCOMPASS TEST, HEADING 180°, RUN NO. 3

IMU S/N: 001 T1 S/N: 119678

Date: 14 Dec 76 T2 S/N: 55939

T3 S/N: 116699

OPTICAL DATA (deg, min, sec)

	R5 = 137 83 40		A = 094 33 18
	R1 = 097 48 02		F = 040 35 38
(F = R5 - R1):	F = 040 35 38		G = 043 46 03
	R2 = 044 47 41		J = 104 32 48
	R6 = 001 01 38	(H = A + F + G + J):	H = 283 27 47
(G = R2 - R6):	G = 043 46 03		$\bar{\gamma}$ = 102 02 19
	R4 = 104 32 103	($\alpha_o = H - \bar{\gamma}$):	α_o = 181 25 28
	R3 = 000 00 55		α = 181 25 85
(J = R4 - R3):	J = 104 32 48		α_o = 181 25 28
		($\epsilon_o = \alpha - \alpha_o$):	ϵ_o = 000 00 57
			ϵ_o = 57 arc sec

TEMPERATURE AND WIND DATA

Temperature (°F)

	Accel Triad	IMU Air Inlet	Wind Speed/Direction (mph/deg)
Start:	50	48	Start: 6/110
End:	55	52	End: 5/130

TABLE B-5. PII IMU MISSILE-MOUNTED GYROCOMPASS TEST, HEADING 180°, RUN NO. 4

IMU S/N: 001 T1 S/N: 119678

Date: 14 Dec 76 T2 S/N: 55939

T3 S/N: 116699

OPTICAL DATA (deg, min, sec)

	R5 =	137	83	41
	R1 =	097	48	00
(F = R5 - R1):	F =	040	35	41
	R2 =	044	47	45
	R6 =	001	01	14
(G = R2 - R6):	G =	043	46	31
	R4 =	104	33	20
	R3 =	000	01	08
(J = R4 - R3):	J =	104	32	12

	A =	094	33	18
	F =	040	35	41
	G =	043	46	31
	J =	104	32	12
(H = A + F + G + J):	H =	283	27	42
	$\bar{\gamma}$ =	102	02	19
($\alpha_o = H - \bar{\gamma}$):	α_o =	181	25	23
	α =	181	25	61
	α_o =	181	25	23
	ϵ_o =	000	00	38
($\epsilon_o = \alpha - \alpha_o$):	ϵ_o =	38 arc sec		

TEMPERATURE AND WIND DATA

	Temperature (°F) Accel Triad	IMU Air Inlet	Wind Speed/Direction (mph/deg)
Start:	55	52	Start: 3/120
End:	56	52	End: 3/090

TABLE B-6. PII IMU MISSILE-MOUNTED GYROCOMPASS TEST, HEADING 180°, RUN NO. 5

IMU S/N: 001 T1 S/N: 119678

Date: 14 Dec 76 T2 S/N: 55939

T3 S/N: 116699

OPTICAL DATA (deg, min, sec)

	R5 = 137 82 87		A = 094 33 18
	R1 = <u>097 47 56</u>		F = 040 35 31
(F = R5 - R1):	F = 040 35 31		G = 043 46 32
	R2 = 044 47 46		J = <u>104 32 18</u>
	R6 = <u>001 01 14</u>	(H = A + F + G + J):	H = 283 27 39
(G = R2 - R6):	G = 043 46 32		$\bar{\gamma}$ = <u>102 02 19</u>
	R4 = 104 33 27	($\alpha_o = H - \bar{\gamma}$):	α_o = *181 25 20*
	R3 = <u>000 01 09</u>		α = 181 25 10
(J = R4 - R3):	J = 104 32 18		α_o = <u>181 25 20</u>
			ϵ_o = 000 00 10
		($\epsilon_o = \alpha - \alpha_o$):	ϵ_o = -10 arc sec

TEMPERATURE AND WIND DATA

	Temperature (°F) Accel Triad	IMU Air Inlet		Wind Speed/Direction (mph/deg)
Start:	56	53	Start:	6/120
End:	57	54	End:	6/120

TABLE B-7. PII IMU MISSILE-MOUNTED GYROCOMPASS TEST, HEADING 180°, RUN NO. 6

IMU S/N: 001 T1 S/N: 119678

Date: 14 Dec 1976 T2 S/N: 55939

T3 S/N: 116699

OPTICAL DATA (deg, min, sec)

	R5 = 137 83 35		A = 094 33 18
	R1 = 097 48 12		F = 040 35 23
(F = R5 - R1):	F = 040 35 23		G = 043 46 37
	R2 = 044 47 50		J = 104 32 07
	R6 = 001 01 13	(H = A + F + G + J):	H = 283 26 85
(G = R2 - R6):	G = 043 46 37		$\bar{\gamma}$ = 102 02 19
	R4 = 104 33 09	($\alpha_o = H - \bar{\gamma}$):	α_o = 181 24 66
	R3 = 000 01 02		α = 181 25 63
(J = R4 - R3):	J = 104 32 07		α_o = 181 25 06
		($\epsilon_o = \alpha - \alpha_o$):	ϵ_o = 000 00 57
			ϵ_o = 57 arc sec

TEMPERATURE AND WIND DATA

	Temperature (°F) Accel Triad	IMU Air Inlet	Wind Speed/Direction (mph/deg)
Start:	58	55	4/120
End:	59	55	3/150

TABLE B-8. PII IMU MISSILE-MOUNTED GYROCOMPASS TEST, HEADING 180°, RUN NO. 7

IMU S/N: 001 T1 S/N: 119678

Date: 19 Dec 1976 T2 S/N: 55939

T3 S/N: 116699

OPTICAL DATA (deg, min, sec)

	R5 =	137	83	32
	R1 =	097	48	14
(F = R5 - R1):	F =	040	35	18
	R2 =	044	47	55
	R6 =	001	01	13
(G = R2 - R6):	G =	043	46	42
	R4 =	104	32	42
	R3 =	000	01	12
(J = R4 - R3):	J =	104	31	30

	A =	094	33	18
	F =	040	35	18
	G =	043	46	42
	J =	104	31	30
(H = A + F + G + J):	H =	283	26	48
	$\bar{\gamma}$ =	102	02	19
($\alpha_o = H - \bar{\gamma}$):	α_o =	181	24	29
	α =	181	24	87
	α_o =	181	24	29
$\epsilon_o = (\alpha - \alpha_o)$:	ϵ_o =	000	00	58

ϵ_o = 58 arc sec

Temperature and Wind Data

Temperature (°F)

	Accel Triad	IMU Air Inlet	Wind Speed/Direction (mph/deg)
Start:	59	56	Start: 4/120
End:	59	56	End: 5/120

TABLE B-9. PII IMU MISSILE-MOUNTED GYROCOMPASS TEST, HEADING 180°, RUN NO. 8

IMU S/N: 001 T1 S/N: 119678

Date: 19 Dec 1976 T2 S/N: 55939

T3 S/N: 116699

Optical Data (deg, min, sec)

	R5 = 137 83 40		A = 094 33 18
	R1 = 097 48 12		F = 040 35 28
(F = R5 - R1):	F = 040 35 28		G = 043 46 53
	R2 = 044 47 61		J = 104 30 50
	R6 = 001 01 08	(H = A + F + G + J):	H = 283 26 29
(G = R2 - R6):	G = 043 46 53		$\bar{\gamma}$ = 102 02 19
	R4 = 104 31 68	($\alpha_o = H - \bar{\gamma}$):	α_o = 181 24 10
	R3 = 000 01 18		α = 181 25 34
(J = R4 - R3):	J = 104 30 50		α_o = 181 24 10
		($\epsilon_o = \alpha - \alpha_o$):	ϵ_o = 01 24
			ϵ_o = 84 arc sec

Temperature and Wind Data

Temperature (°F)

	Accel Triad	IMU Air Inlet	Wind Speed/Direction (mph/deg)
Start:	59	56	Start: 8/130
End:	59	57	End: 3/100

TABLE B-10. METEOROLOGICAL DATA, DATE 14 DEC 1976, HEADING 180°

Time (min)	Run No. 1	Run No. 2	Run No. 3	Run No. 4	Run No. 5	Run No. 6	Run No. 7	Run No. 8
0	5/130	8/130	6/110	3/120	6/120	4/120	4/120	8/130
1	5/110	5/120	6/120	3/120	8/110	4/120	6/130	8/140
2	5/120	3/120	5/110	3/120	7/130	3/110	5/150	7/130
3	5/120	5/120	6/120	5/120	5/110	4/120	4/150	7/150
4	3/090	5/120	5/110	3/120	7/100	6/120	3/140	5/140
5	3/120	7/110	5/130	3/120	4/090	7/130	5/120	5/130
6	4/120	7/110	5/130	5/150	3/090	8/120	4/140	5/120
7	5/100	4/110	6/110	4/110	6/100	3/130	6/130	4/110
8	6/120	6/100	7/110	4/110	4/110	5/110	6/120	5/120
9	3/100	4/120	7/120	7/110	3/120	3/120	6/120	6/120
10	3/110	9/100	4/130	4/120	2/110	7/130	4/120	5/110
11	3/110	6/100	6/140	3/120	6/120	7/120	7/130	4/110
12	3/100	5/120	4/140	5/110	4/130	7/120	5/130	7/130
13	4/100	7/130	5/120	5/120	7/120	8/130	5/100	5/120
14	4/110	3/110	4/130	4/100	6/120	4/140	5/120	4/100
15	5/110	4/120	5/130	3/090	6/120	3/150	5/120	3/100

Note: Entries are Wind Speed (mph)/Direction (deg).

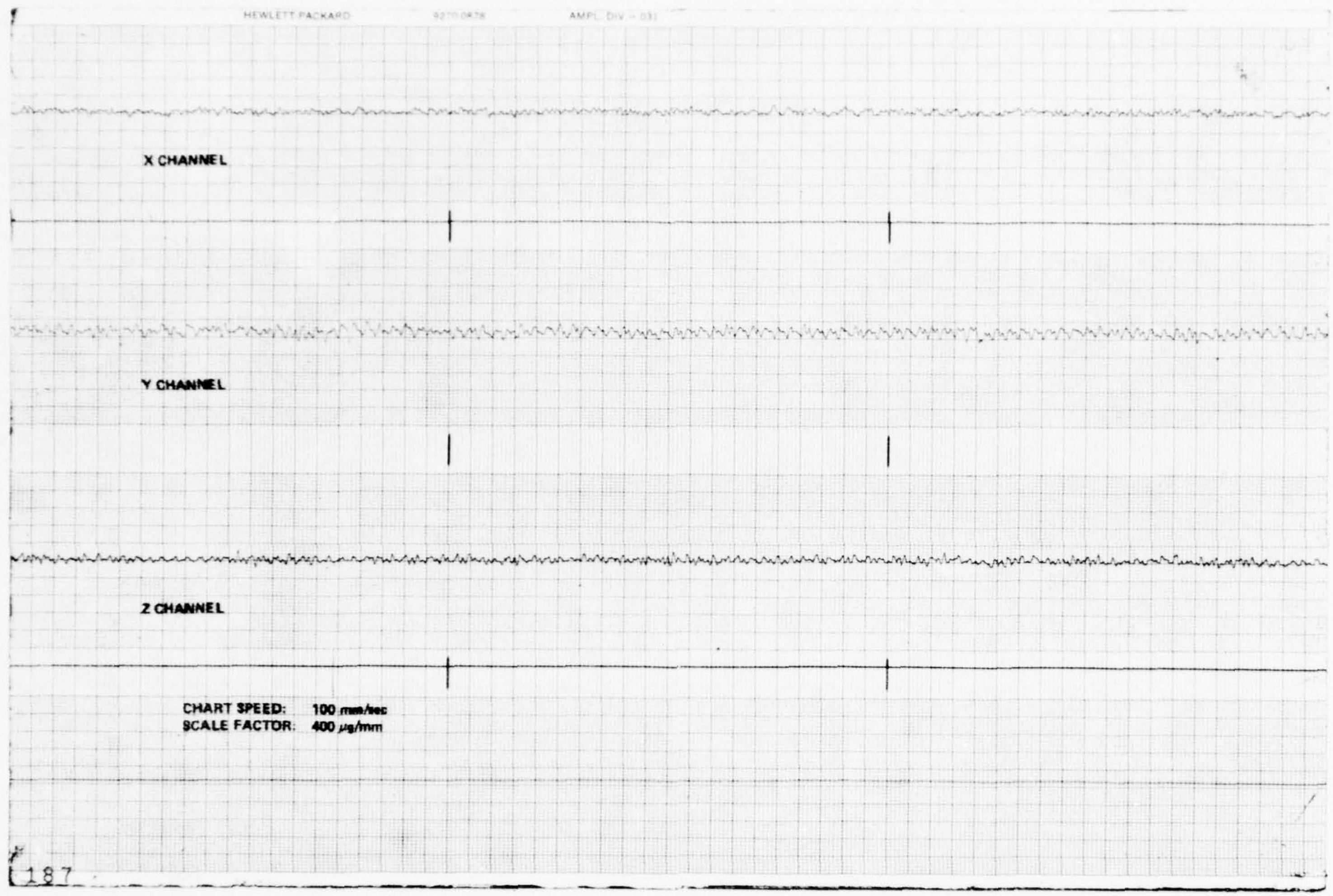

Figure B-1. Accelerometer data - 180° heading, run 1.

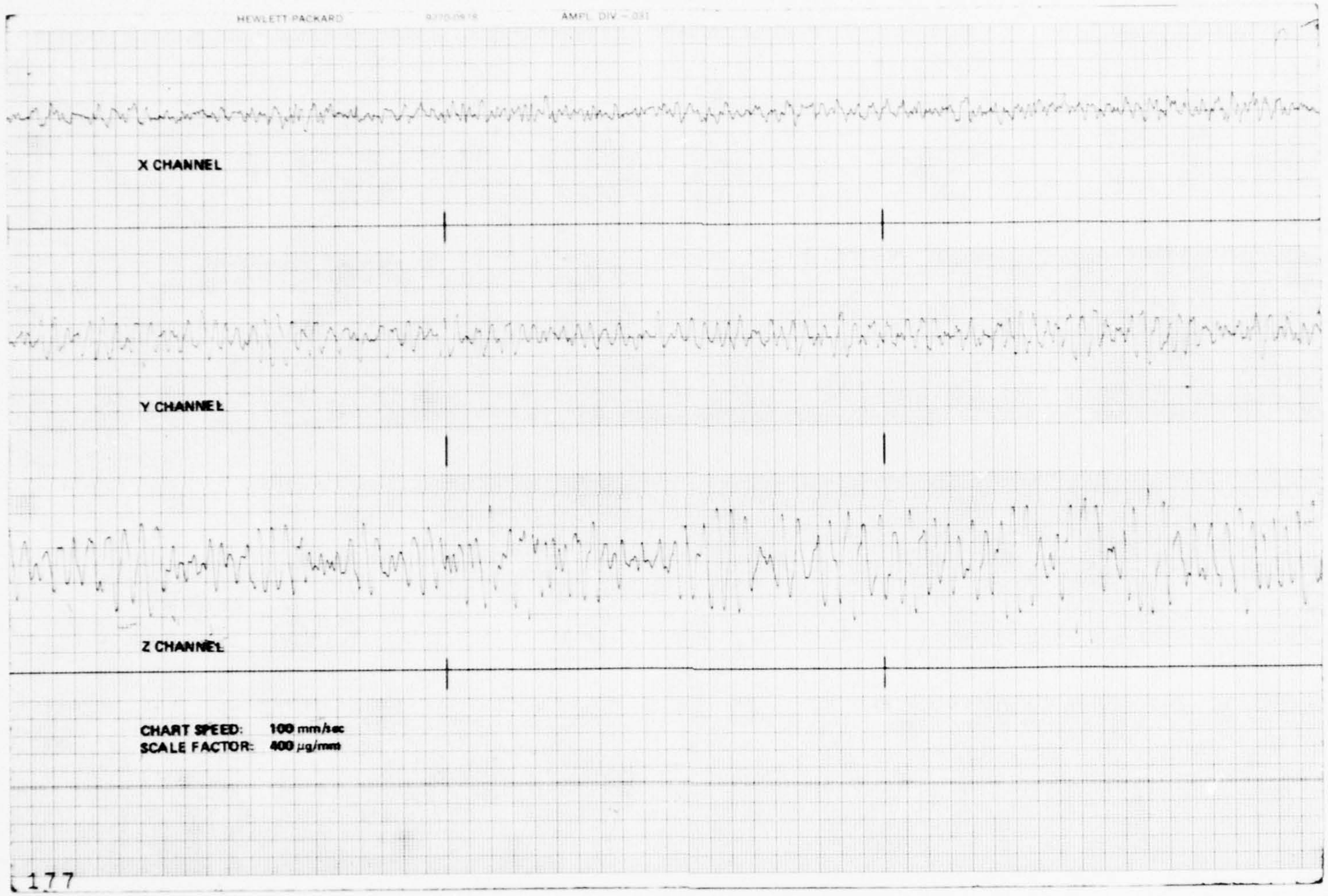

Figure B-2. Accelerometer data - 180° heading, run 2.

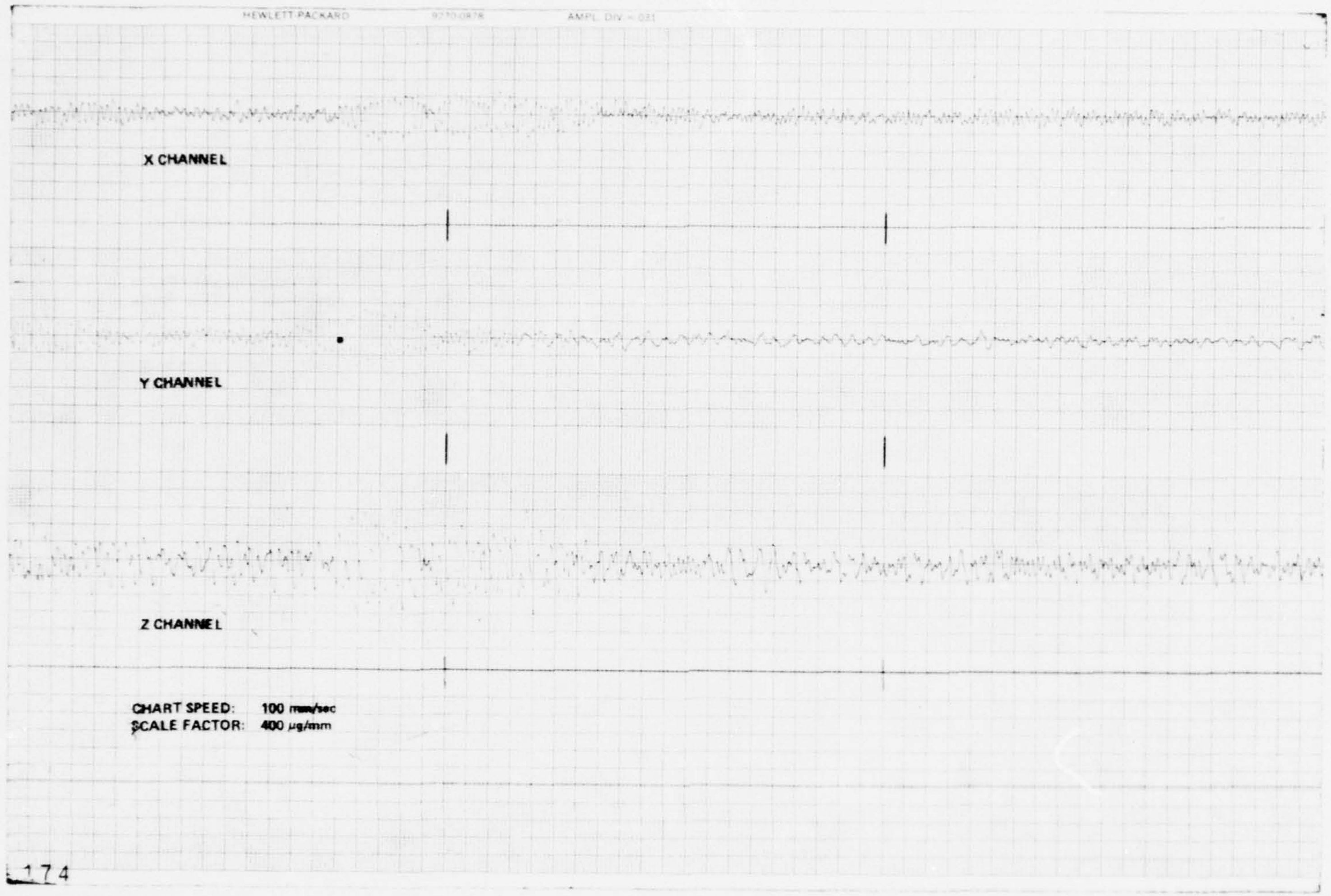

Figure B-3. Accelerometer data - 180° heading, run 3.

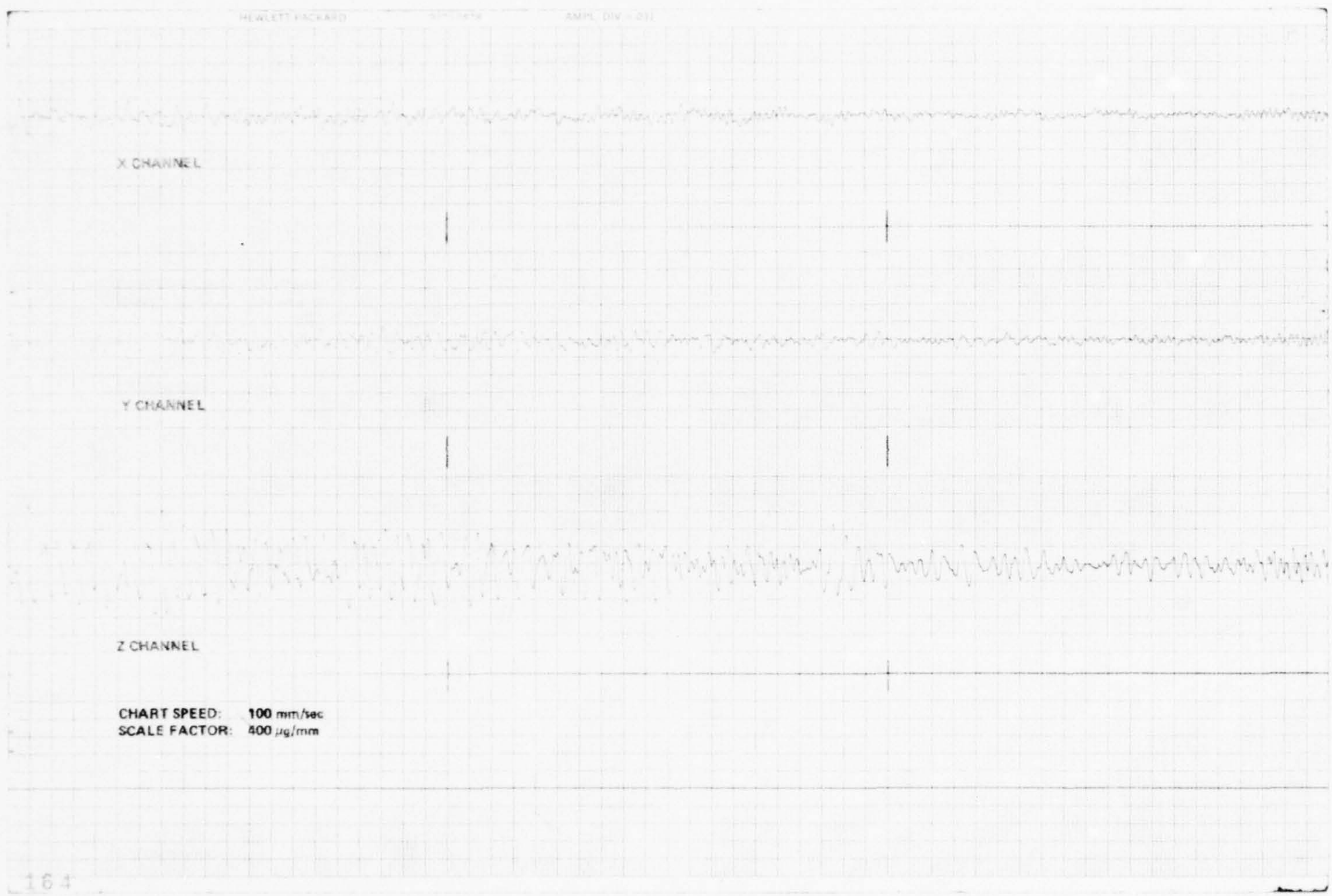

Figure B-4. Accelerometer data - 180° heading, run 4.

Figure B-5. Accelerometer data - 180° heading, run 5.

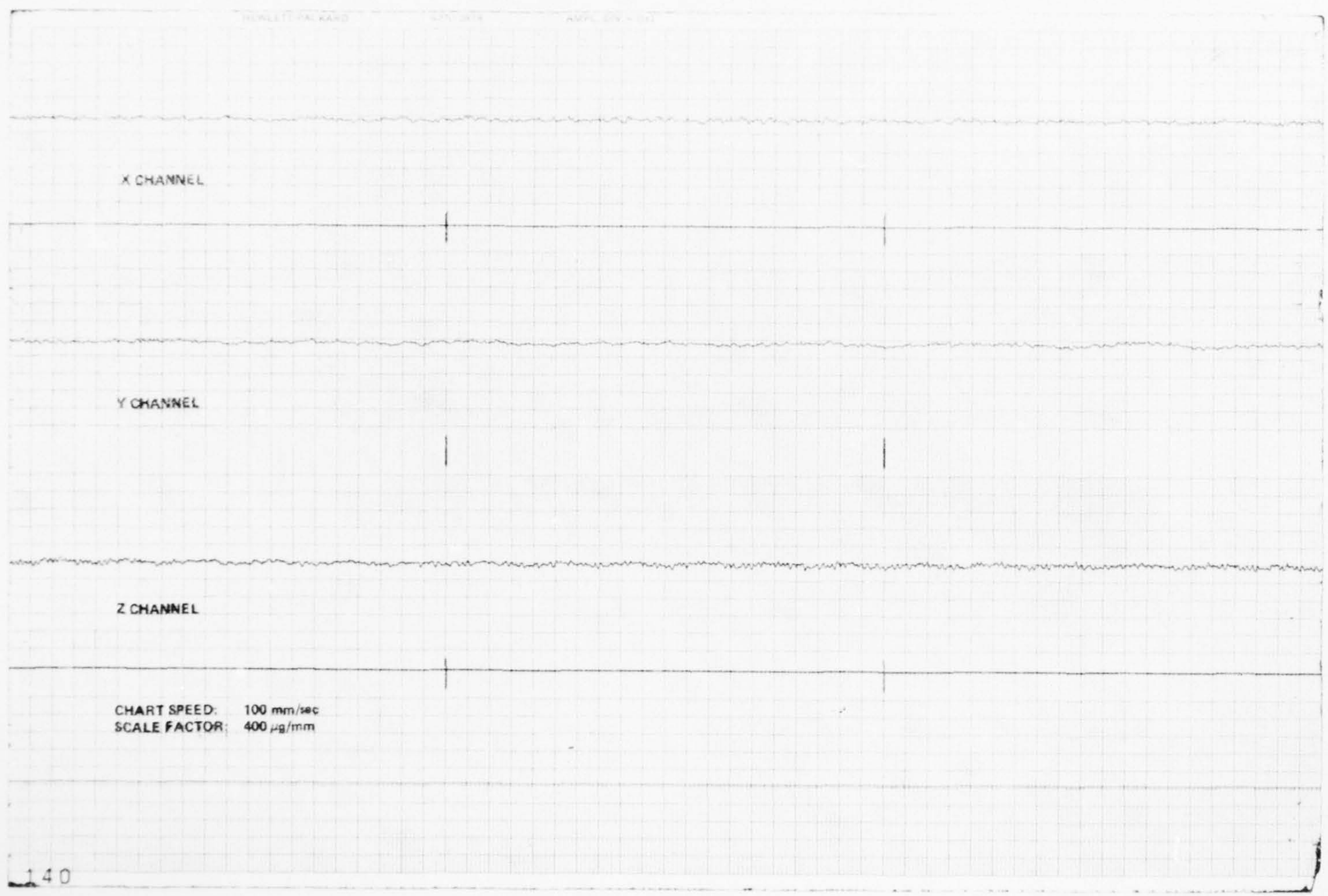

Figure B-6. Accelerometer data - 180° heading, run 6.

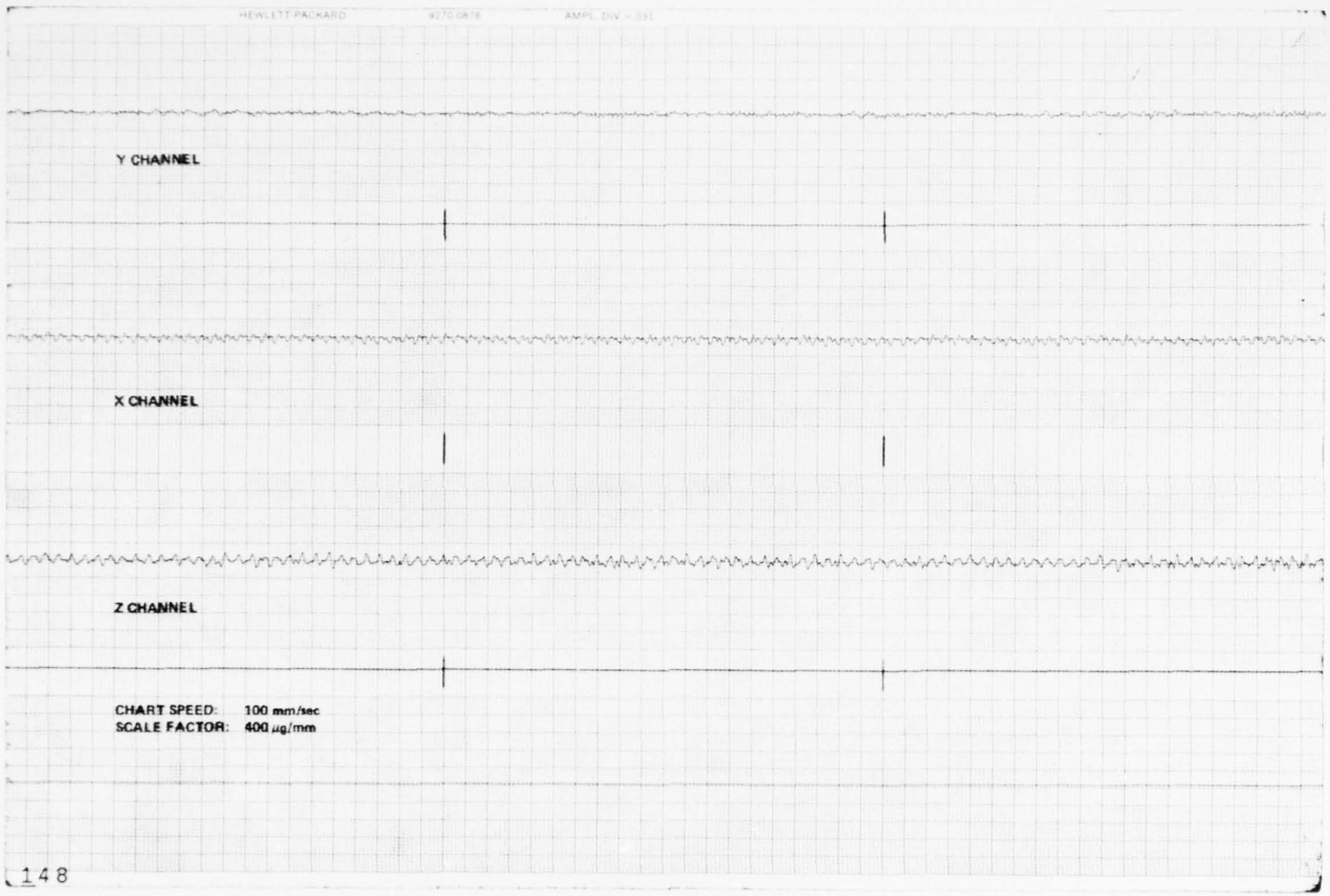

Figure B-7. Accelerometer data - 180° heading, run 7.

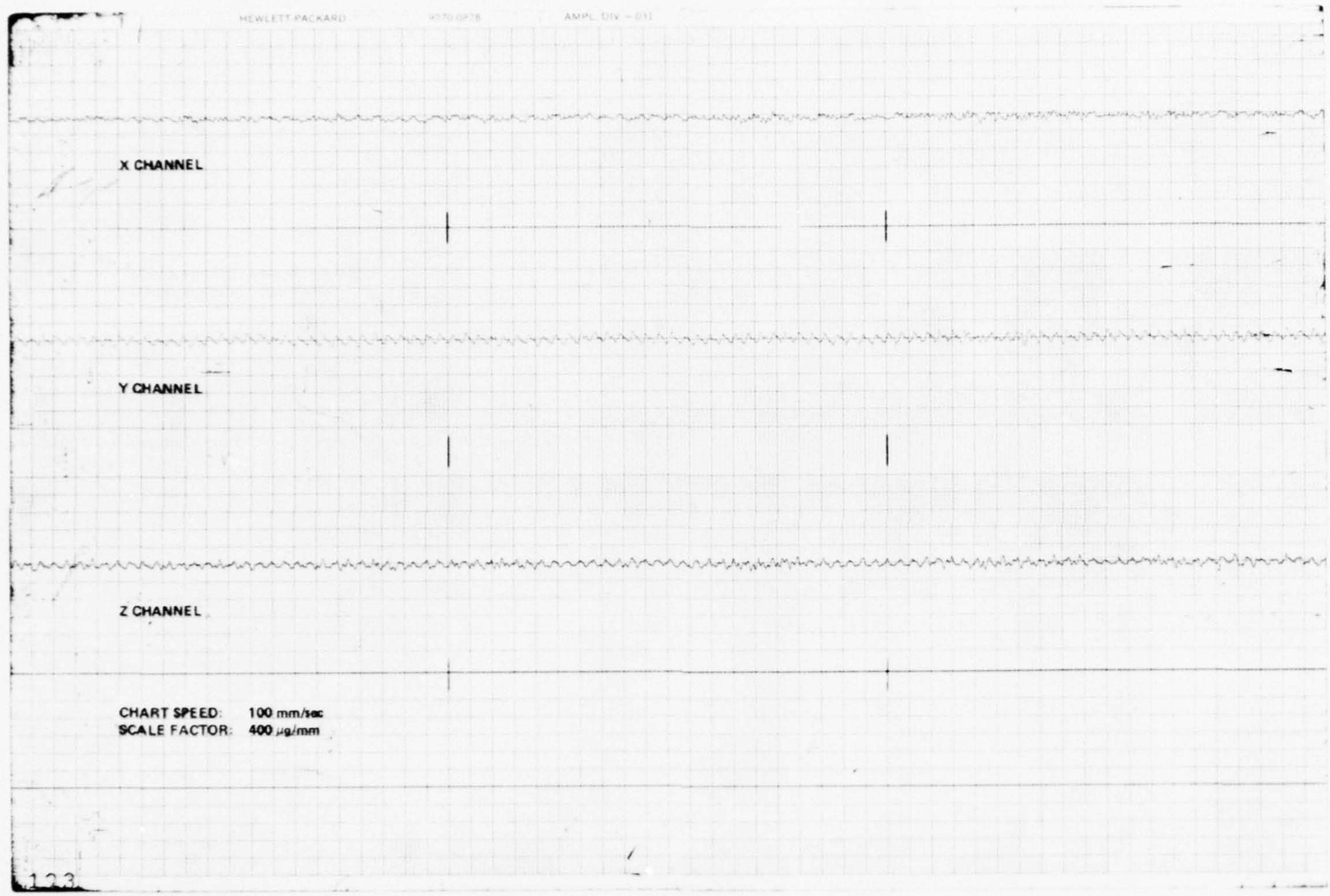

Figure B-8. Accelerometer data - 180° heading, run 8.

Appendix C. AVERAGE POWER SPECTRA OF ACCELEROMETER DATA

An accelerometer triad was used to monitor translational disturbances imparted to the IMU case. Accelerometer data were recorded with a multi-channel chart recorder, the preamplifiers of which were used to input data to the multi-channel tape recorder.

Chart recordings of only a few seconds duration were made for quick-look purposes. Tape recordings were made for the full 4-minute duration of Sequence 4 (90° position of IMU) and the full 4-minute duration of Sequence 7 (0° position of IMU) in the gyrocompass program.

Sequence 4 is the period during which IMU data are being acquired and processed by the computer for biasing the west gyro. During Sequence 7, data acquisition and processing is repeated for fine gyrocompassing. Since the IMU's accelerometers (not to be confused with the instrumentation accelerometers under discussion) are the principal sensors for performing the gyro bias and fine gyrocompass functions, any sensed extraneous accelerations due to base motions induced by whatever means are potential sources of azimuth error. This is particularly true if extraneous accelerations are sensed during Sequences 4 and 7, hence the choice of these sequences for recording purposes.

Tape recordings of each of the three accelerometer channels were made for all 64 test runs. The recordings were played back, off-line, into a digital Fourier analyzer capable of computing the average power spectrum of an arbitrary voltage signal and outputing the spectrum to a digital plotter for obtaining a hard copy of the result.

A block diagram of the complete instrumentation system is shown in Figure C-1.

The Fourier analyzer operates on the time domain signal, $V_3(t)$, as shown in Figure C-1 (one channel at a time) to obtain the Fourier transform, and subsequently computes the power spectrum. The Fourier analyzer output is scaled to give a spectral strength of $V_3^2(f)/4$ to signals of various frequencies that may be present in the input. The voltage axis of the digital plot, however, is labeled V^2 so that

$$V_3^2(f)/4 = V^2 \quad . \tag{C-1}$$

With reference to Figure C-1, the time domain input, $V_3(t)$, in terms of acceleration is given by

$$V_3(t) = K_t \; K \; K_a \; G(t) \tag{C-2}$$

where

K_t = Tape recorder scale factor (V/V)

K = Chart recorder preamplifier low frequency scale factor (V/V)

K_a = Accelerometer scale factor (V/g)

$G(t)$ = Input acceleration (g).

The corresponding frequency domain expression for Equation (C-3) is

$$V_3(f) = K_t \; K \; K_a \; G(f) \quad . \tag{C-3}$$

Substitution of Equation (C-3) into Equation (C-10) yields

$$(K_t \; K \; K_a)^2 \; G^2(f) = 4V^2 \tag{C-4}$$

or

$$G^2(f) = 4V^2 \; (K_t \; K \; K_a)^{-2} \tag{C-5}$$

so that the acceleration spectrum is directly related to the plotted voltage spectrum by the scale factor, $4 \; (K_t \; K \; K_a)^{-2}$.

The peak value of a sine wave function of acceleration of frequency f that may be a component of the input signal, is determined by taking the square root of Equation (C-5):

$$G(f) = 2V \; (K_t \; K \; K_a)^{-1} \quad , \tag{C-6}$$

where V^2 in Equation (C-5) is read directly from the plotted spectrum.

Nominal scale factor values for the system of Figure C-1 and Equation (C-5) are:

K_t = 1 V/V

K = 100 V/V (low frequency)

K_a = 2.5 V/g.

Frequency response of the system is limited by the chart recorder preamplifier and the frequency response curves in Figure C-2 should be used to more accurately specify this scale factor.

With K, as read from Figure C-2, and the values mentioned previously for K_t and K_a substituted into Equation (C-5), the result is

$$G^2(f) = 0.64\ V^2/K^2 \qquad \text{(C-7)}$$

as indicated on the average power spectrum plots shown in Figure C-3 through C-26. These plots are the results from each accelerometer channel for the eight test runs made at a heading of 180°.

The peak value of an acceleration sinusoid corresponding to Equation (C-7) is

$$G(f) = 0.8\ V/K \qquad \text{(C-8)}$$

with an error of approximately 7% of reading due mainly to gain and linearity errors of the tape recorder, chart recorder, and accelerometers.

The plots shown in Figures C-3 through C-26 were obtained by analyzing 30 data samples (15 from Sequence 4 and 15 from Sequence 7) each of 4.096 seconds duration. Thus, approximately 1 minute (61.44 seconds) of data from each of the two 4-minute sequences were analyzed and averaged to produce the plots. During a data processing run, the Fourier analyzer accepts data for 4.096 seconds, computes the transform and power spectrum, sums and stores the result in approximately 8 seconds and repeats these operations a total of 30 times. The final, summed power spectrum is divided by 30 to obtain an average value.

The plots shown in Figure C-3 through C-26 are good representations of the frequencies and average strengths of disturbances present at the IMU case. It should be noted, however, that slightly different average strengths would be computed if the data were analyzed beginning at a different starting point on the tape. To completely analyze a full 4-minute sequence the data would have to be replayed three times with successive starting times delayed by 4.096 seconds from the previous starting time.

The technique used is a compromise to provide representative data without complex synchronization equipment and the additional time required to make two more playback runs.

The raw data sample in Appendix B should be consulted forthe prevailing environmental stimuli during the eight test runs at a heading of 180°.

For reference purposes, the average power spectra for laboratory operation of the instrumentation accelerometers mounted on the IMU test fixture with the IMU running are presented in Figures C-27 through C-29. A value of K = 100 was used in the annotation of G^2 as a function of V^2.

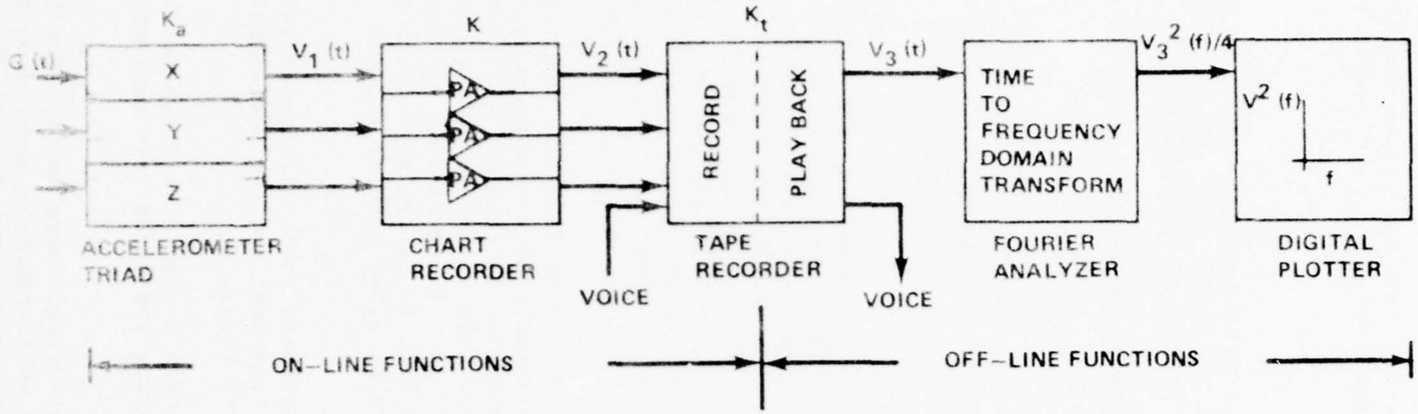

Figure C-1. Instrumentation accelerometer data acquisition and processing block diagram.

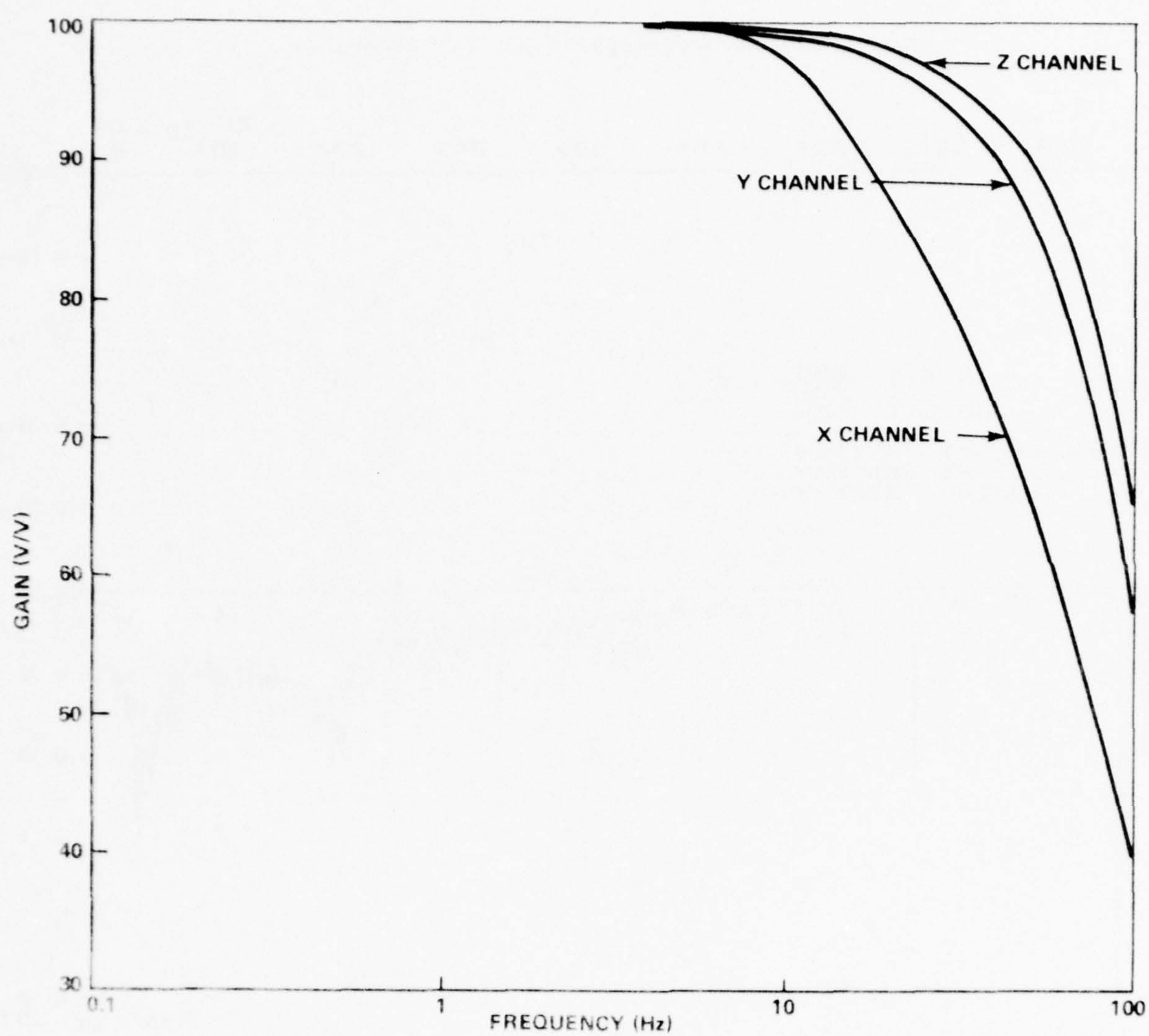

Figure C-2. Preamplifier frequency response.

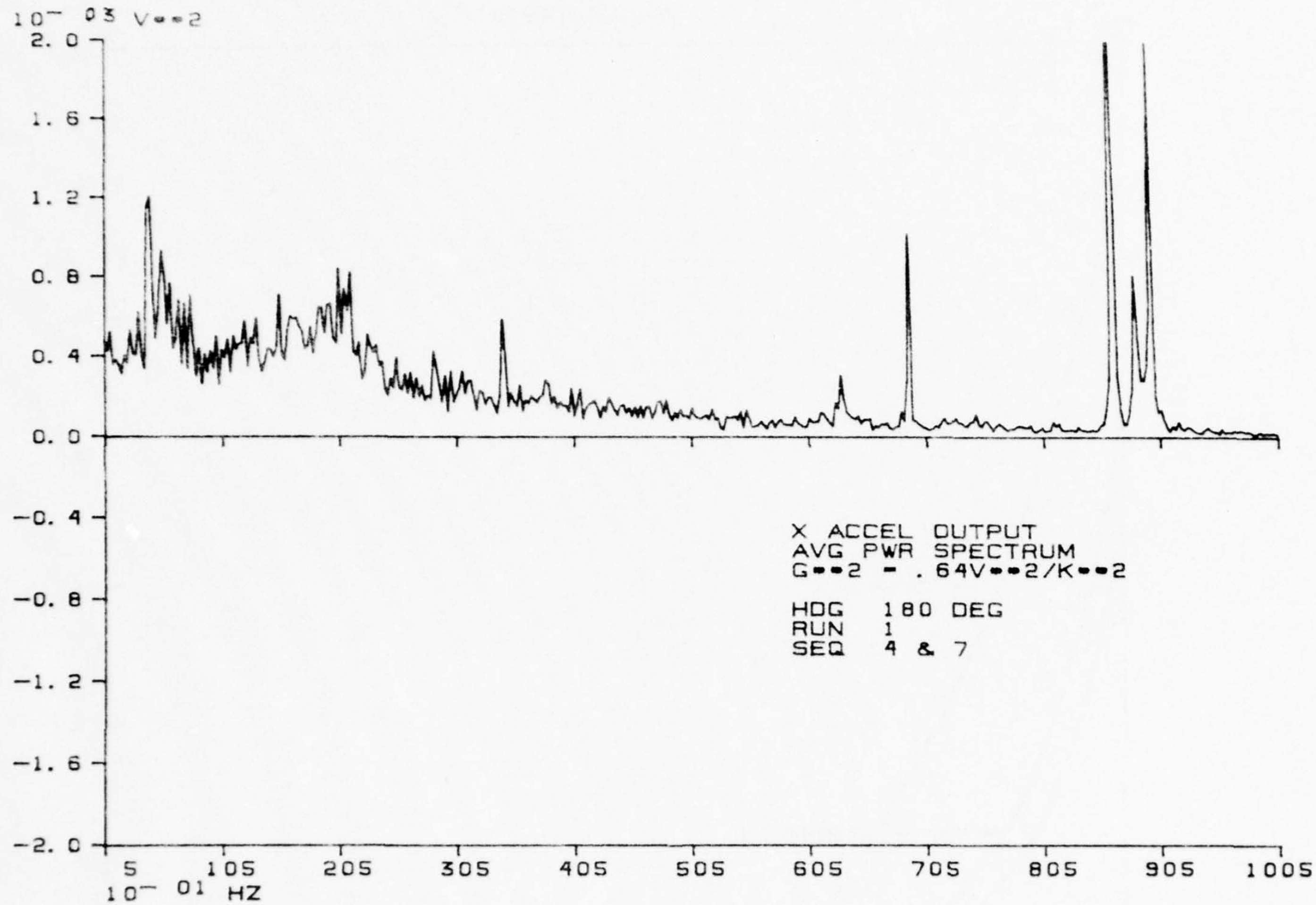

Figure C-3. X acceleration output for run 1.

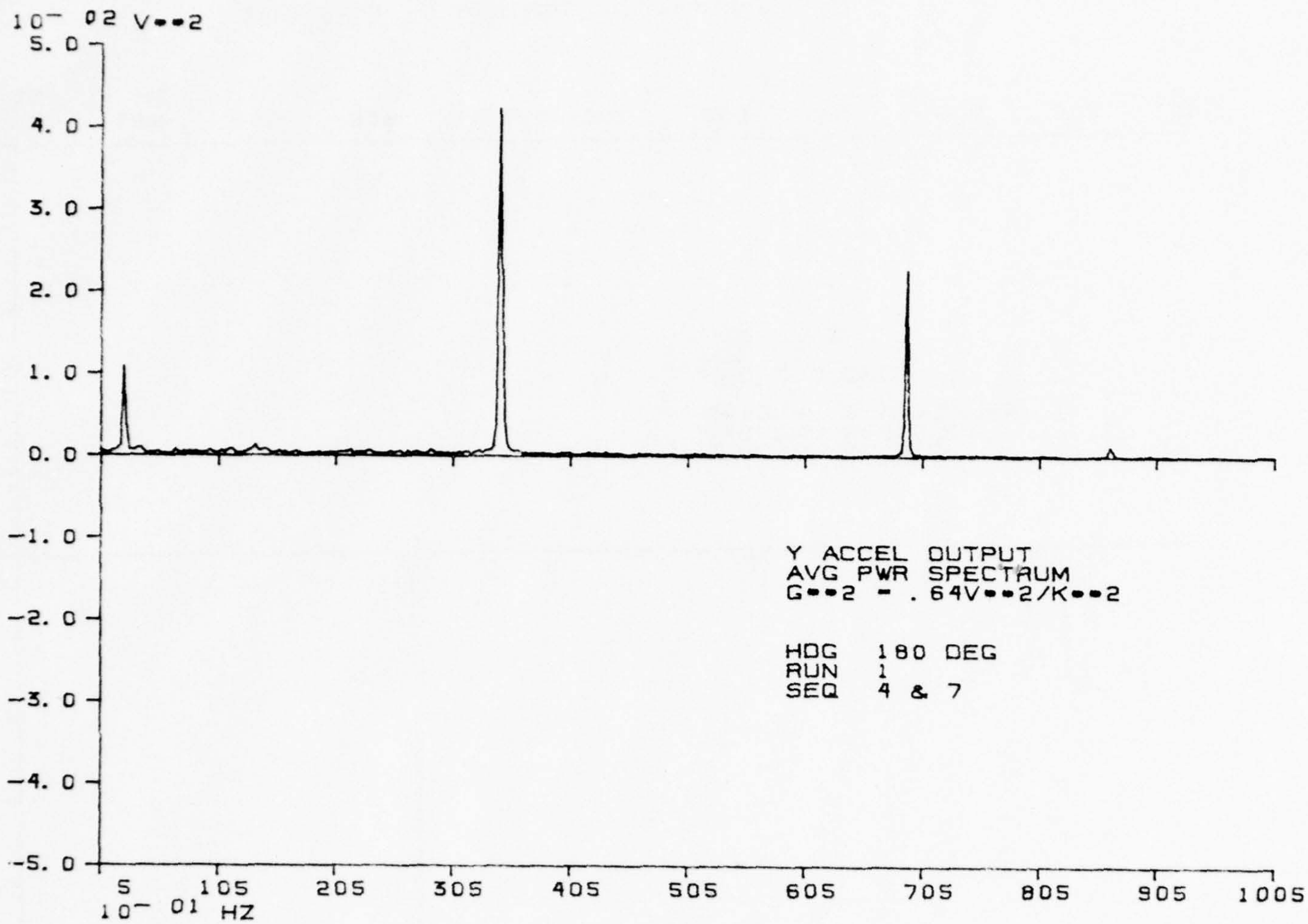

Figure C-4. Y acceleration output for run 1.

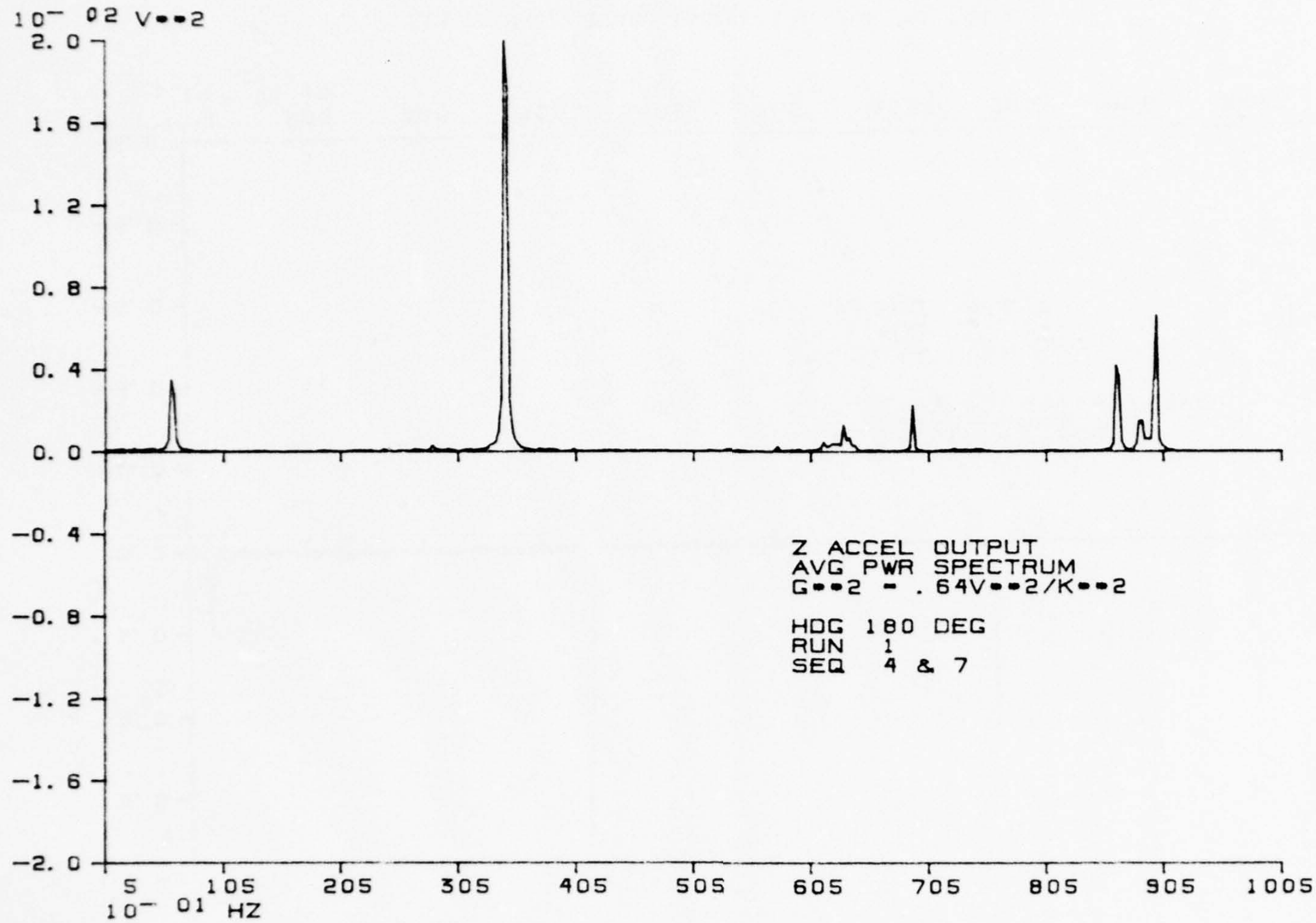

Figure C-5. Z acceleration output for run 1.

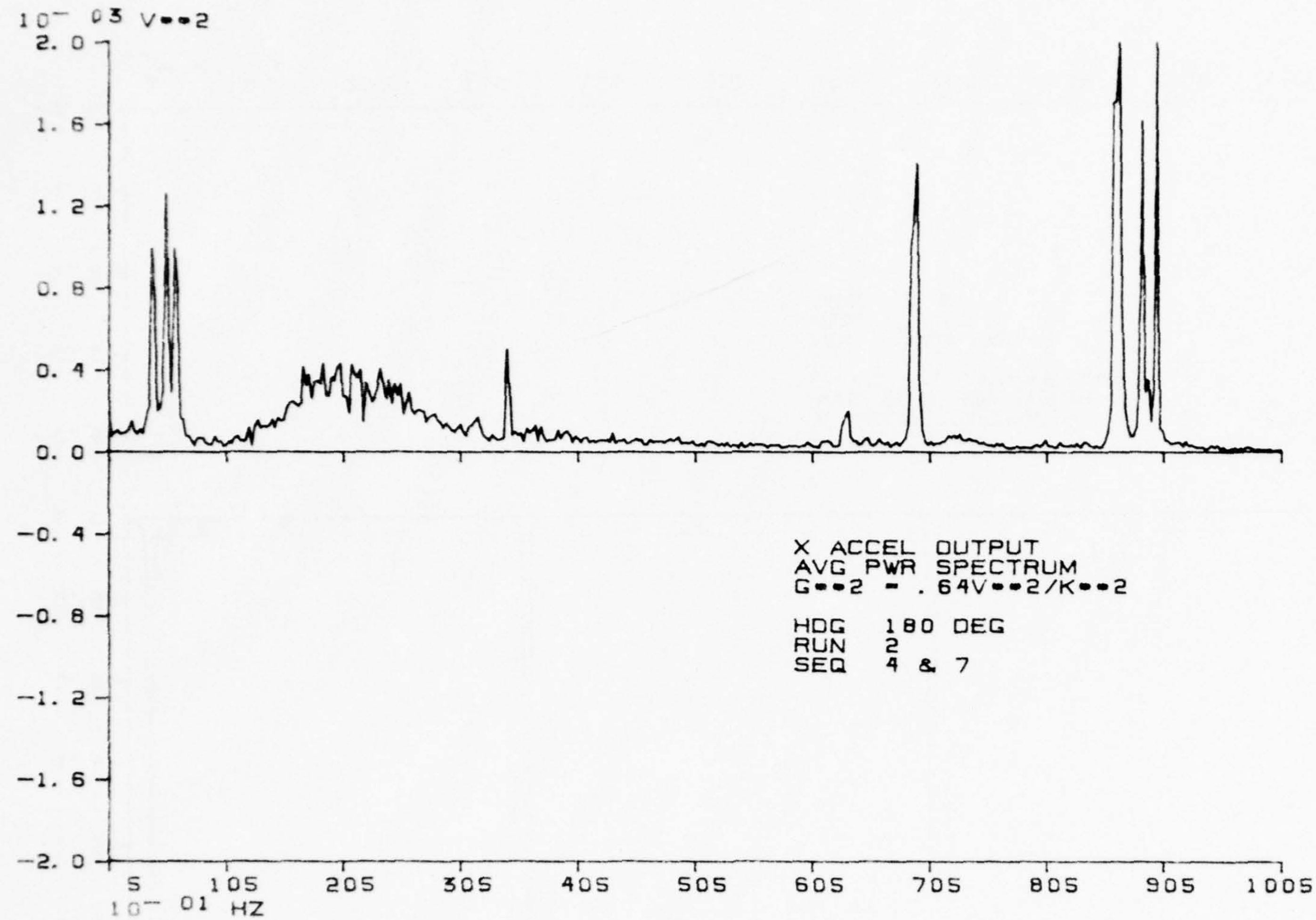

Figure C-6. X acceleration output for run 2.

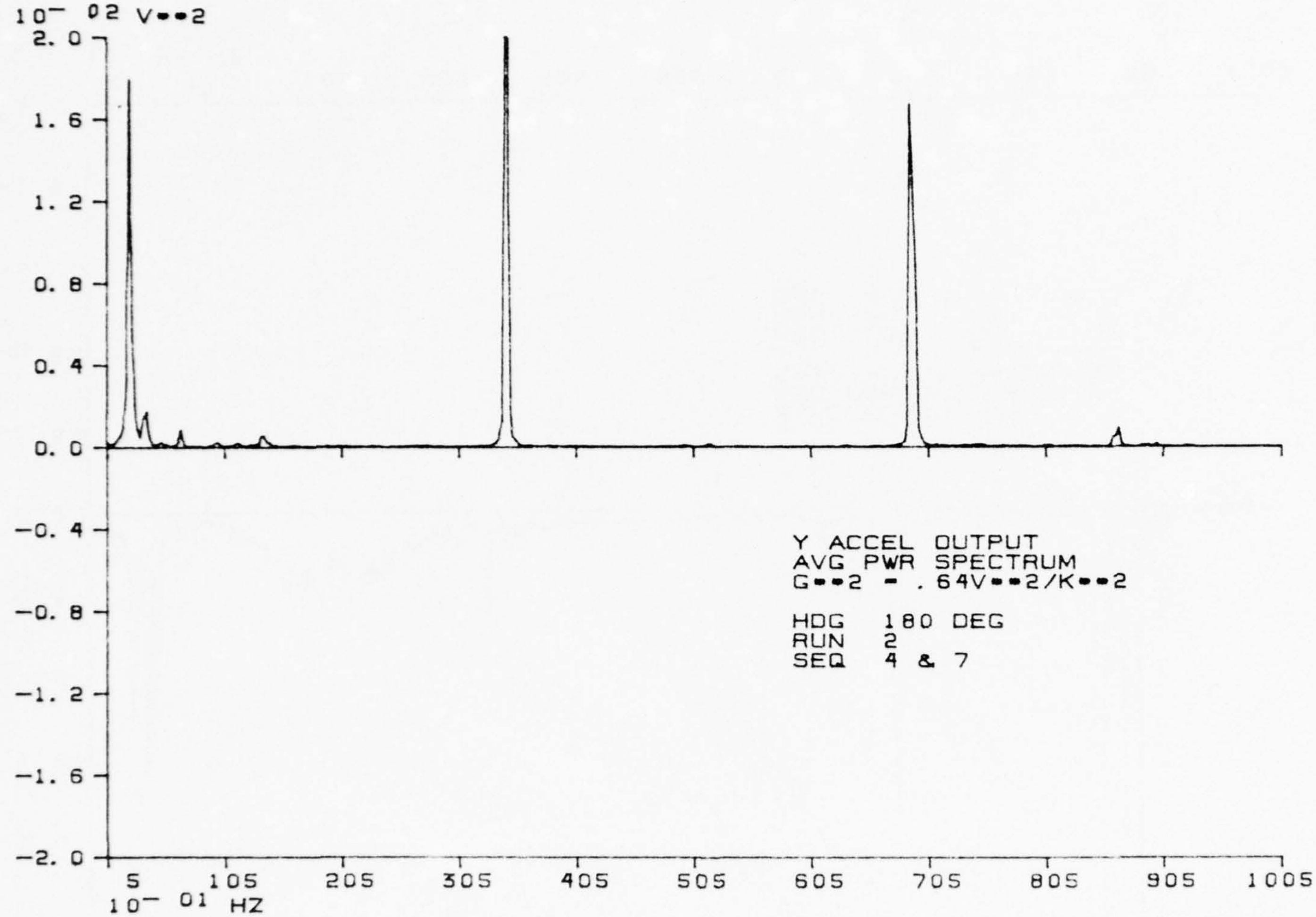

Figure C-7. Y acceleration output for run 2.

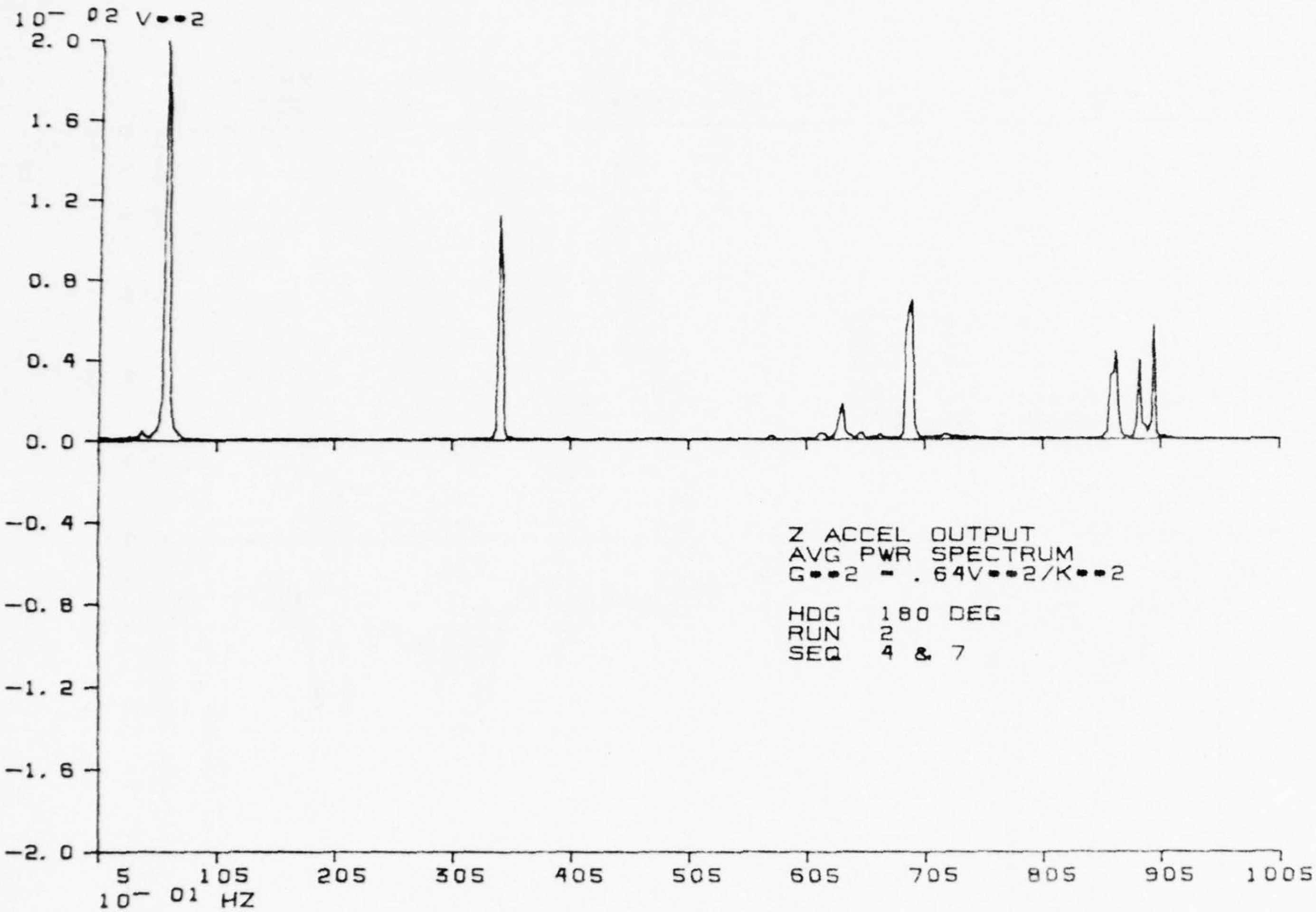

Figure C-8. Z acceleration output for run 2.

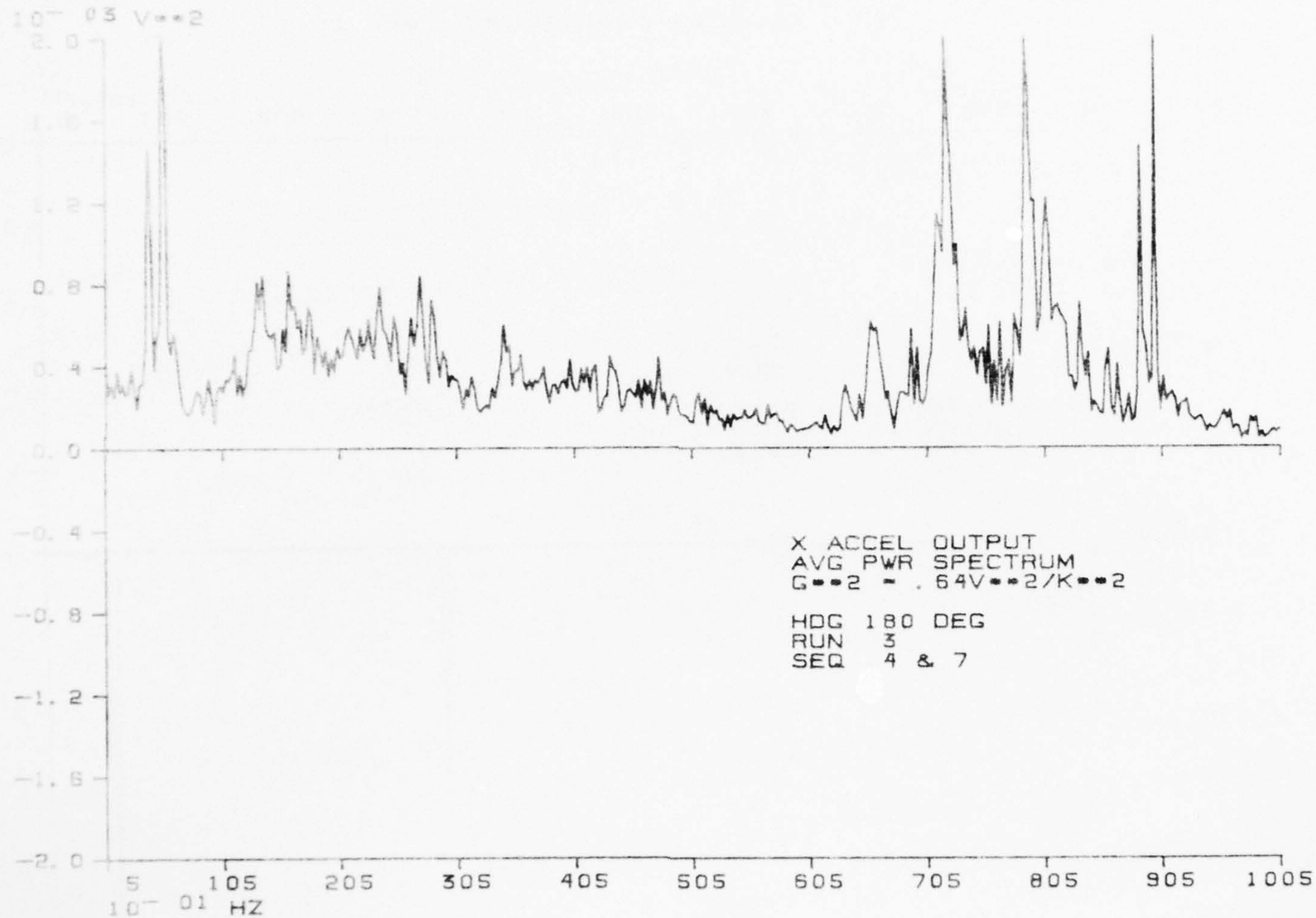

Figure C-9. X acceleration output for run 3.

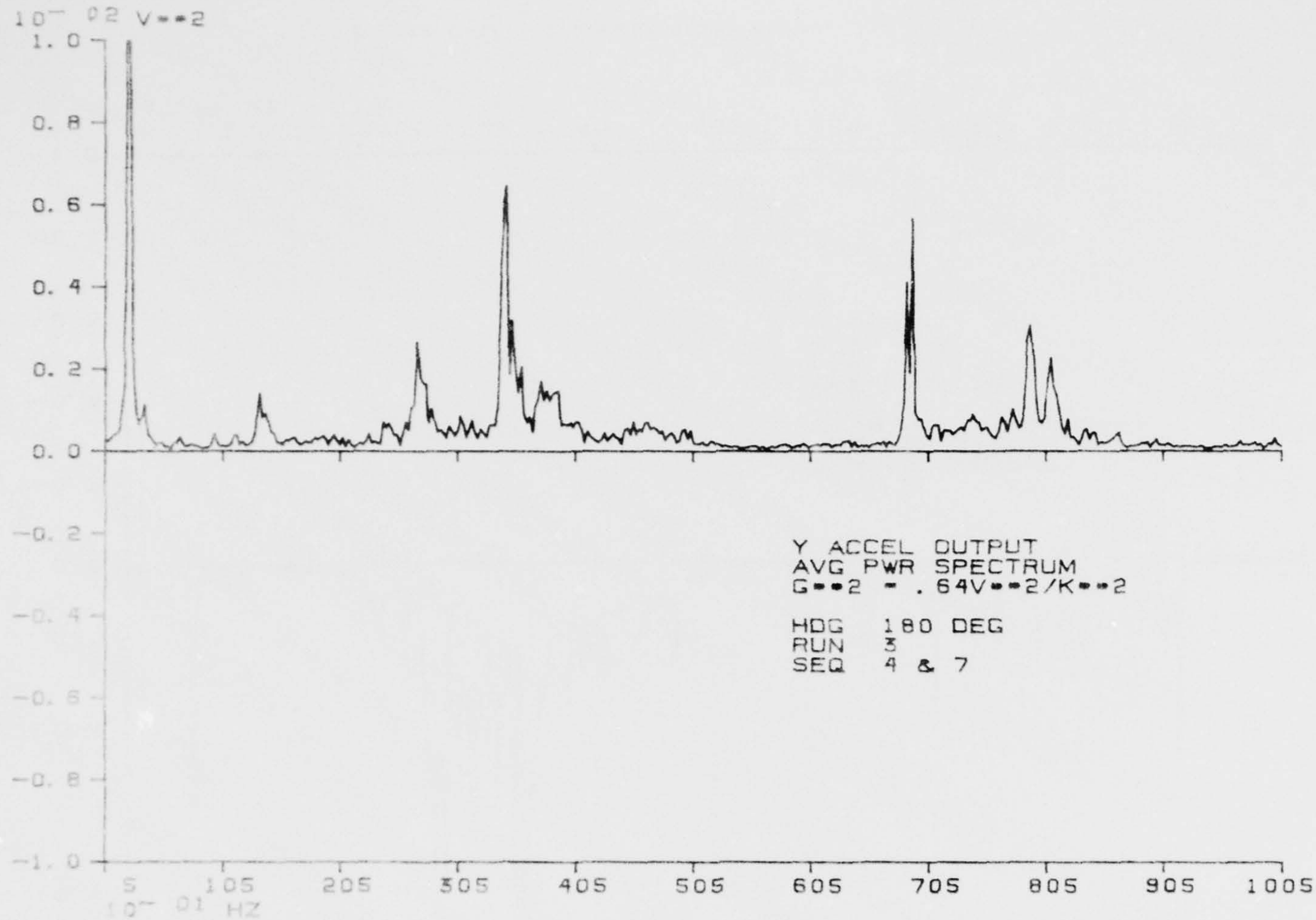

Figure C-10. Y acceleration output for run 3.

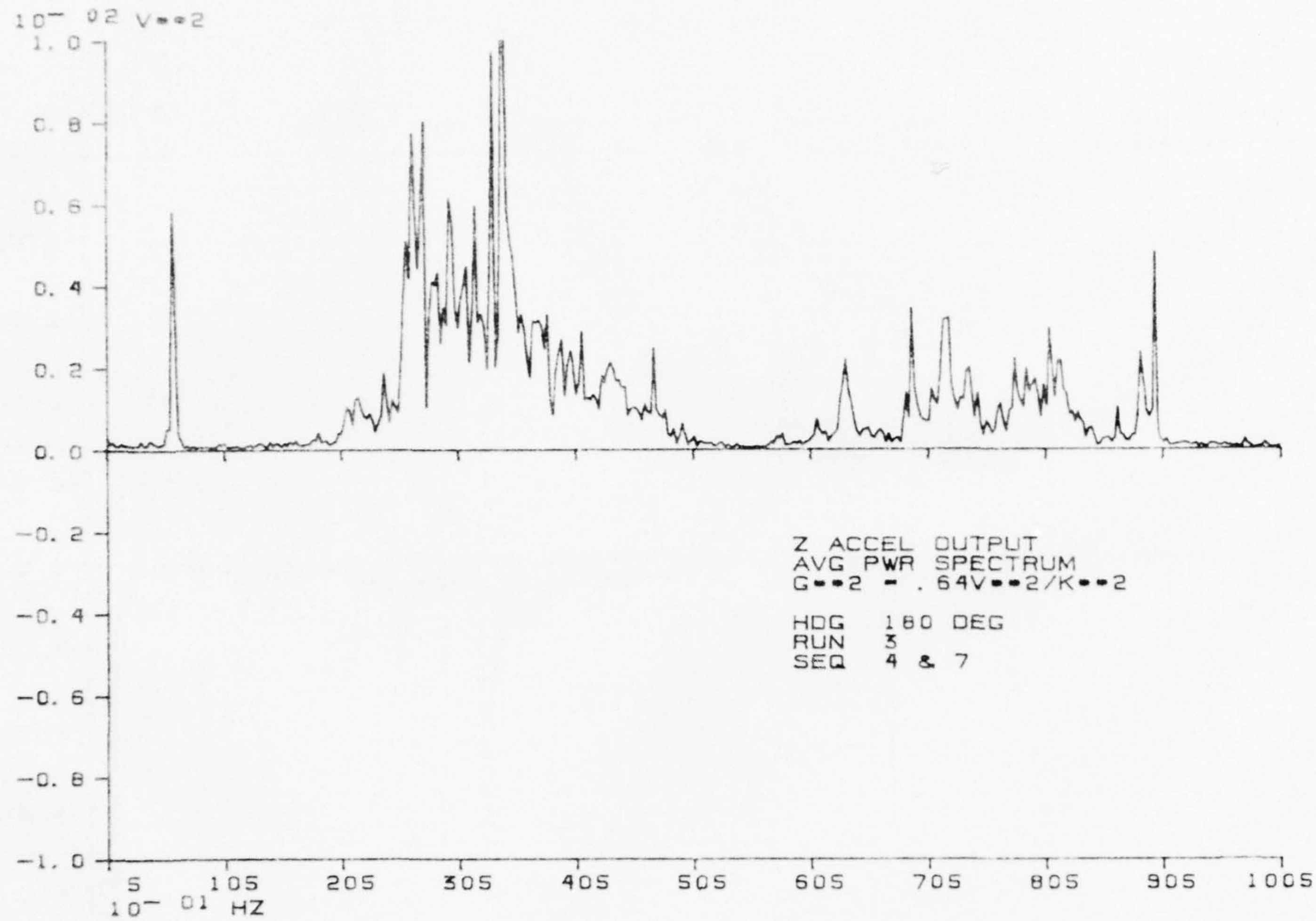

Figure C-11. Z acceleration output for run 3.

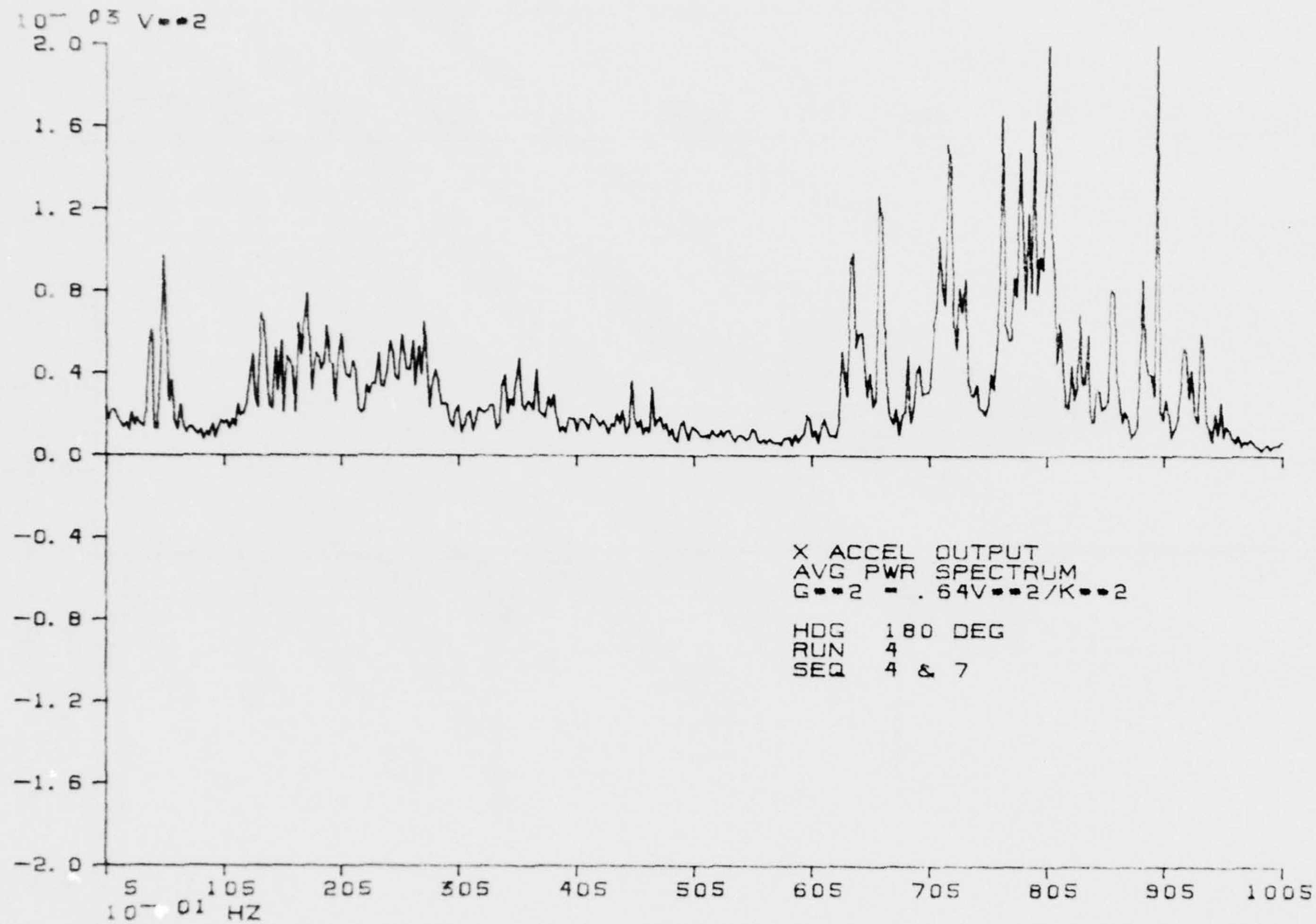

Figure C-12. X acceleration output for run 4.

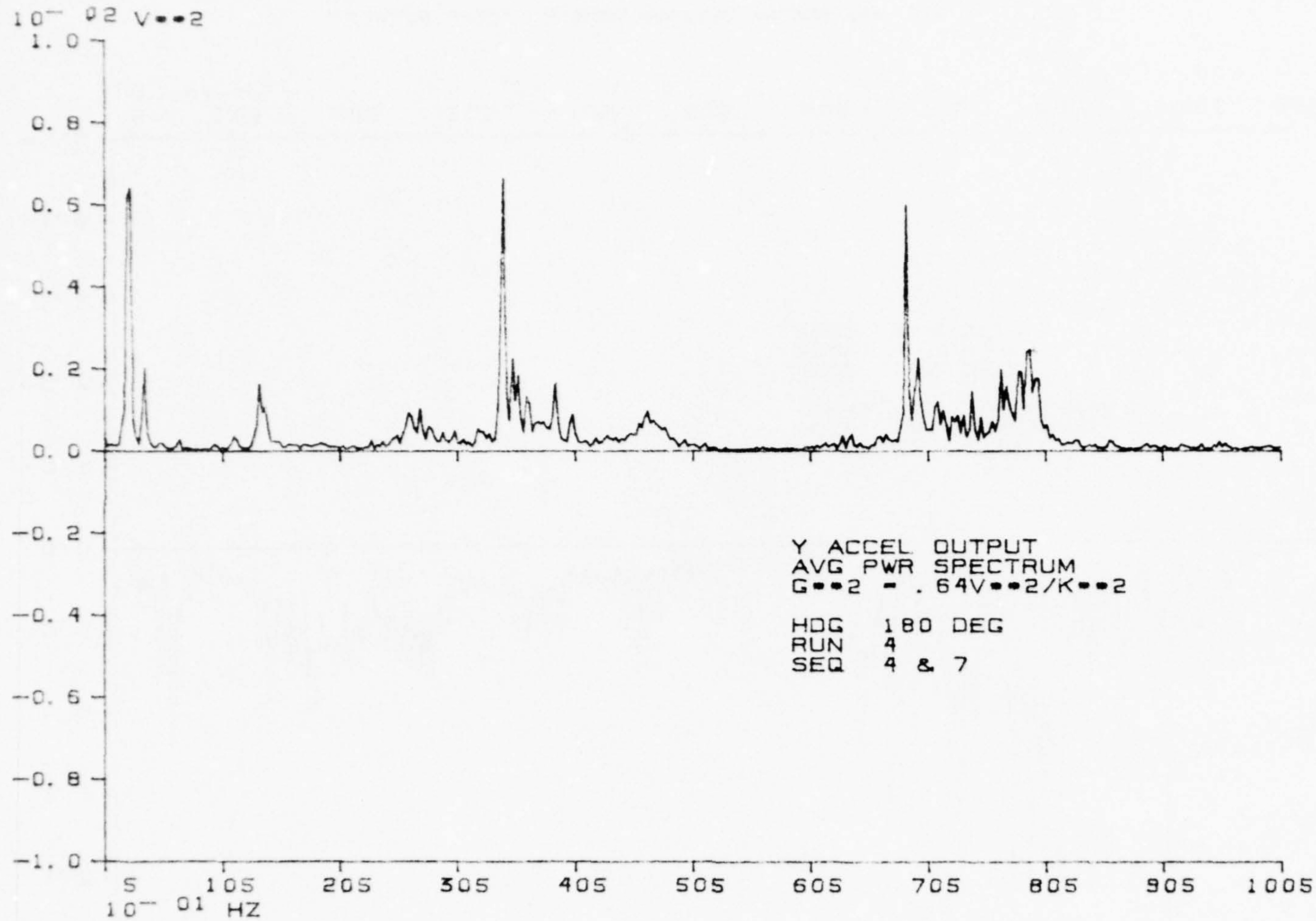

Figure C-13. Y acceleration output for run 4.

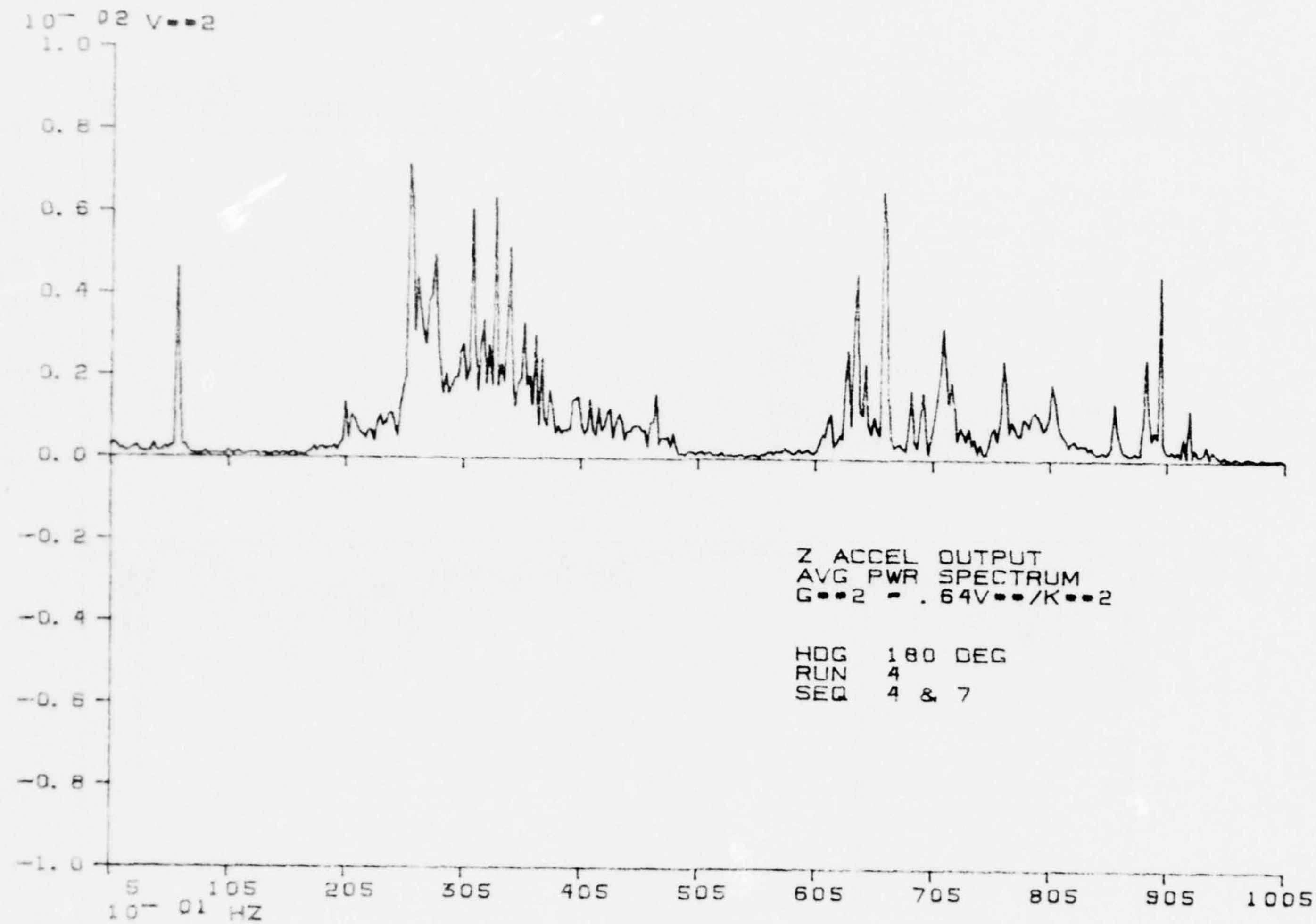

Figure C-14. Z acceleration output for run 4.

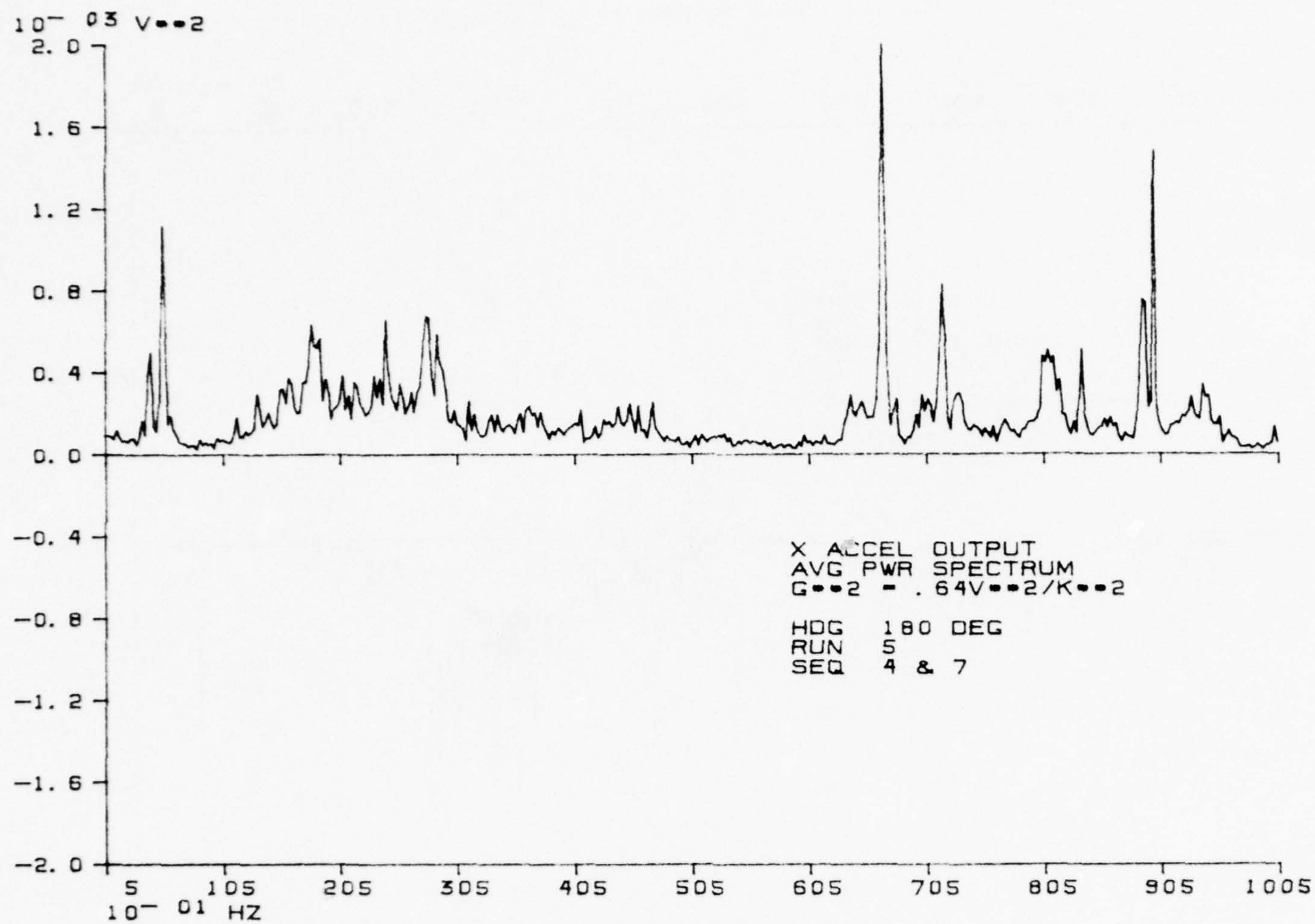

Figure C-15. X acceleration output for run 5.

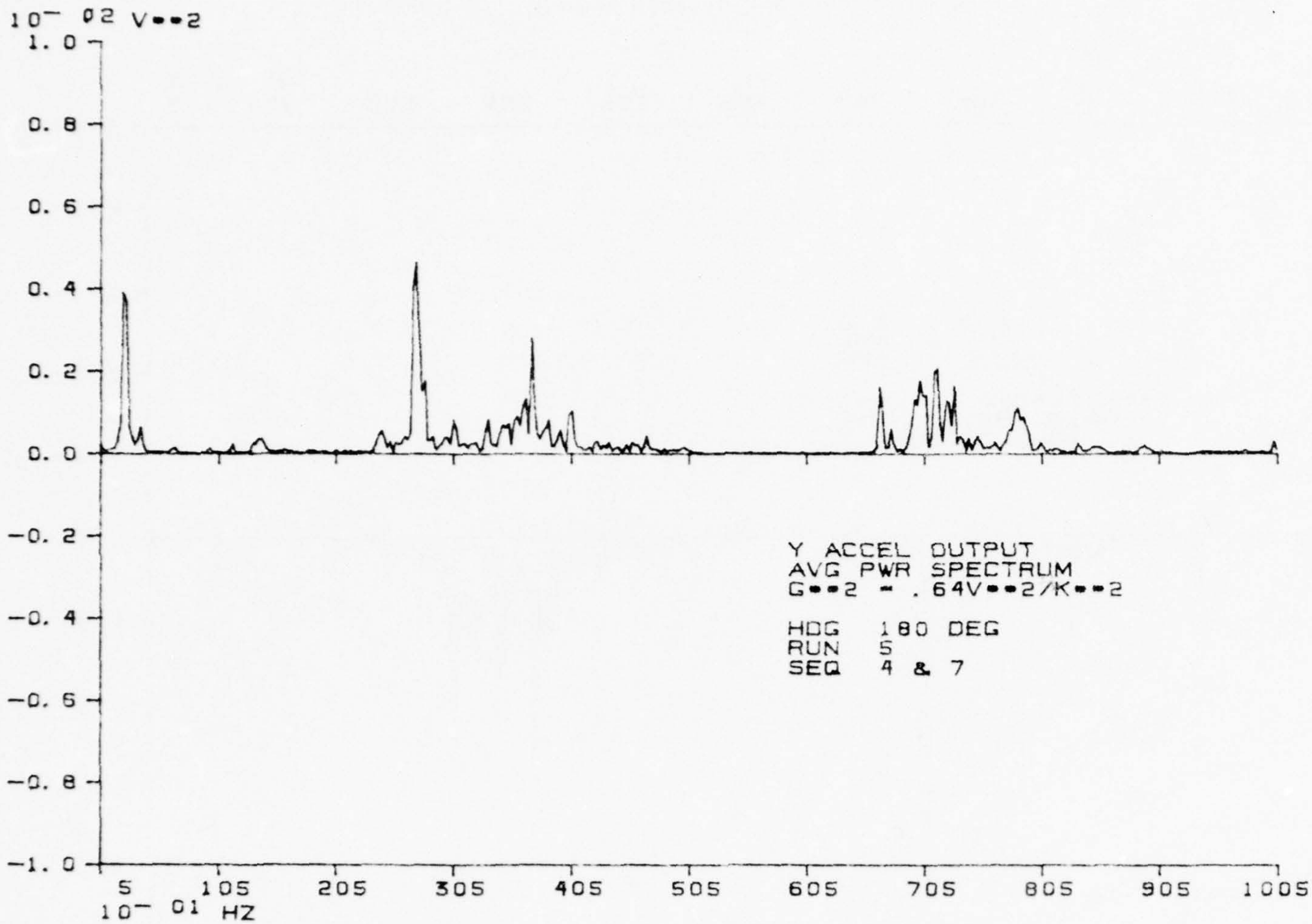

Figure C-16. Y acceleration output for run 5.

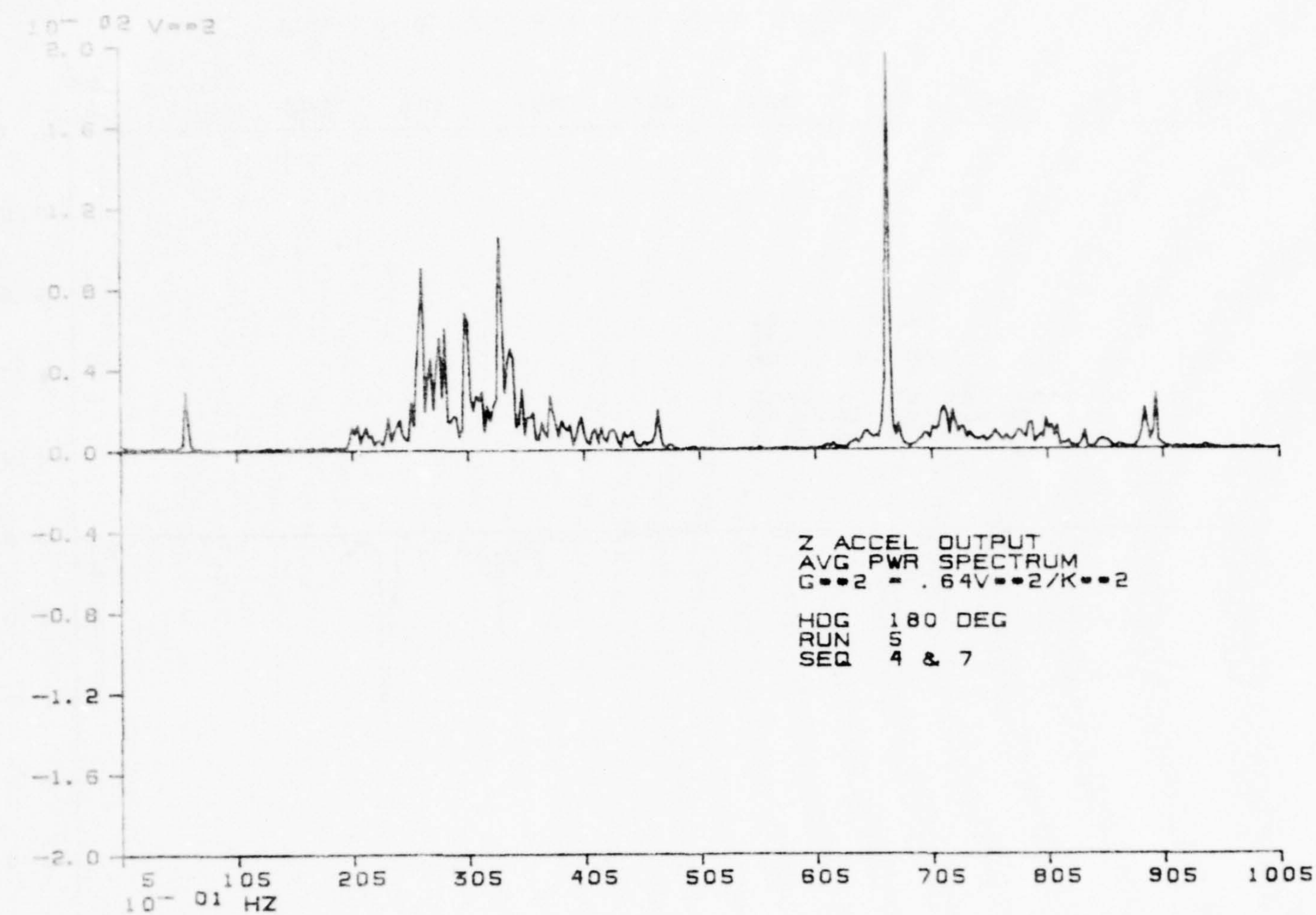

Figure C-17. Z acceleration output for run 5.

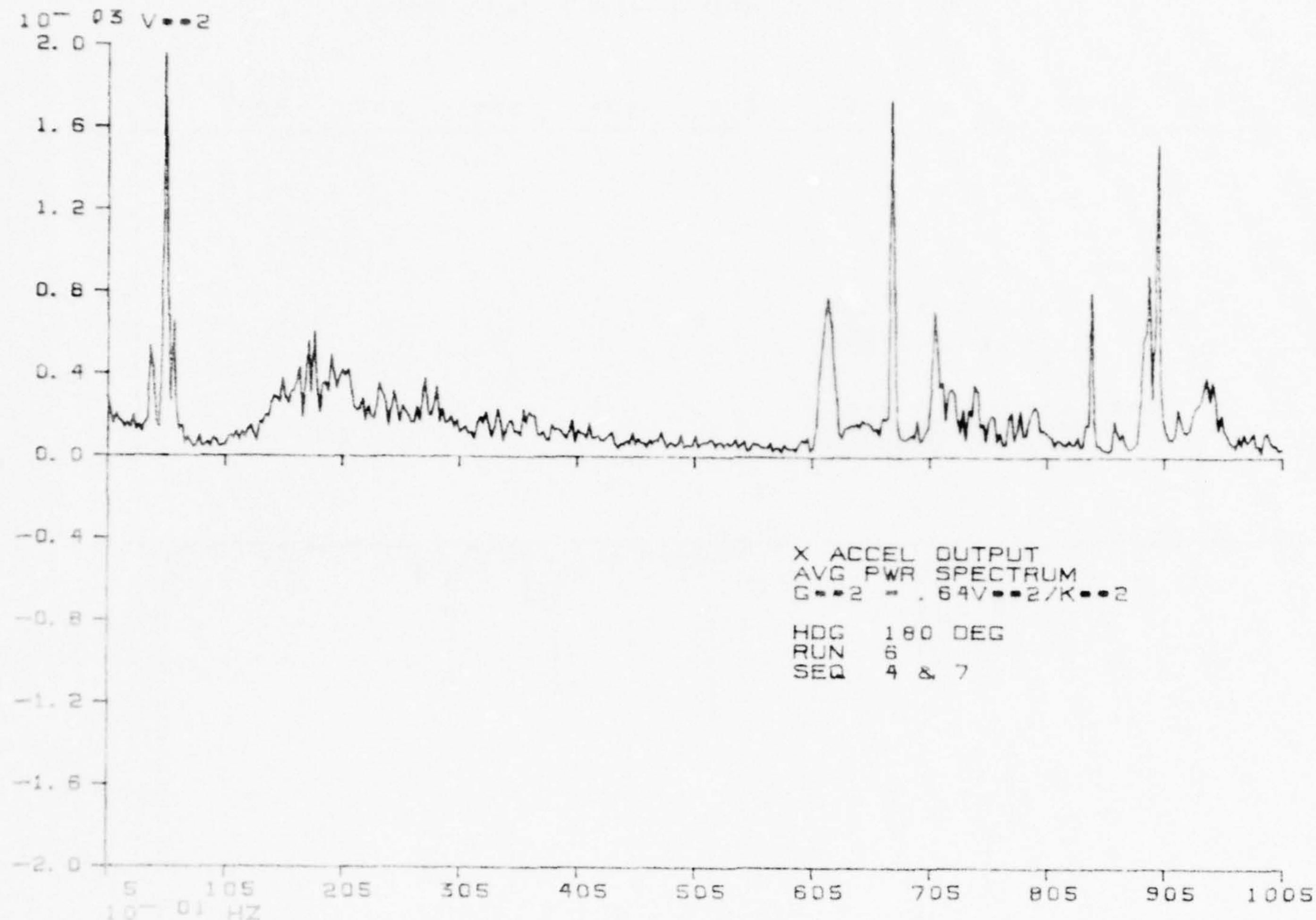

Figure C-18. X acceleration output for run 6.

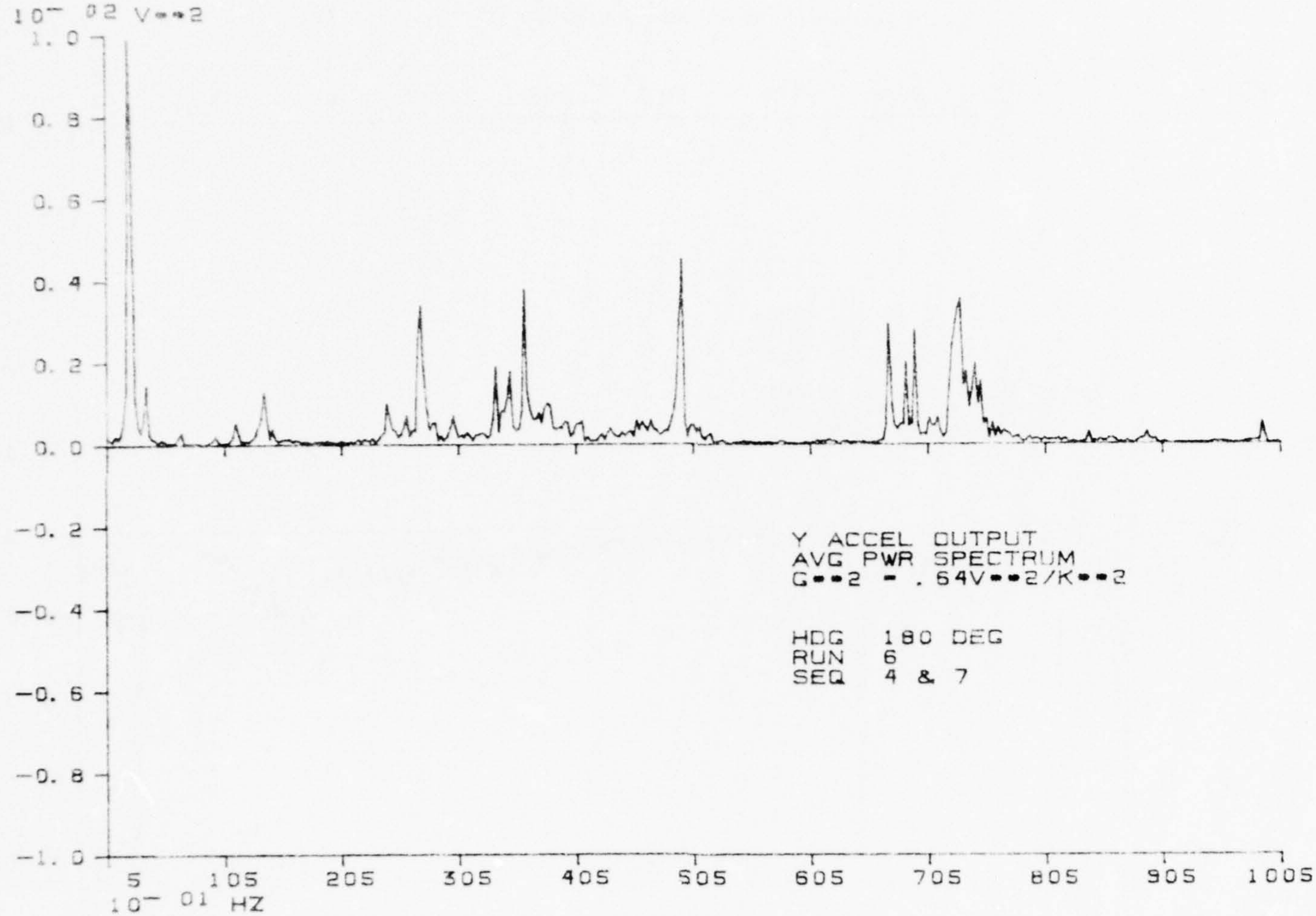

Figure C-19. Y acceleration output for run 6.

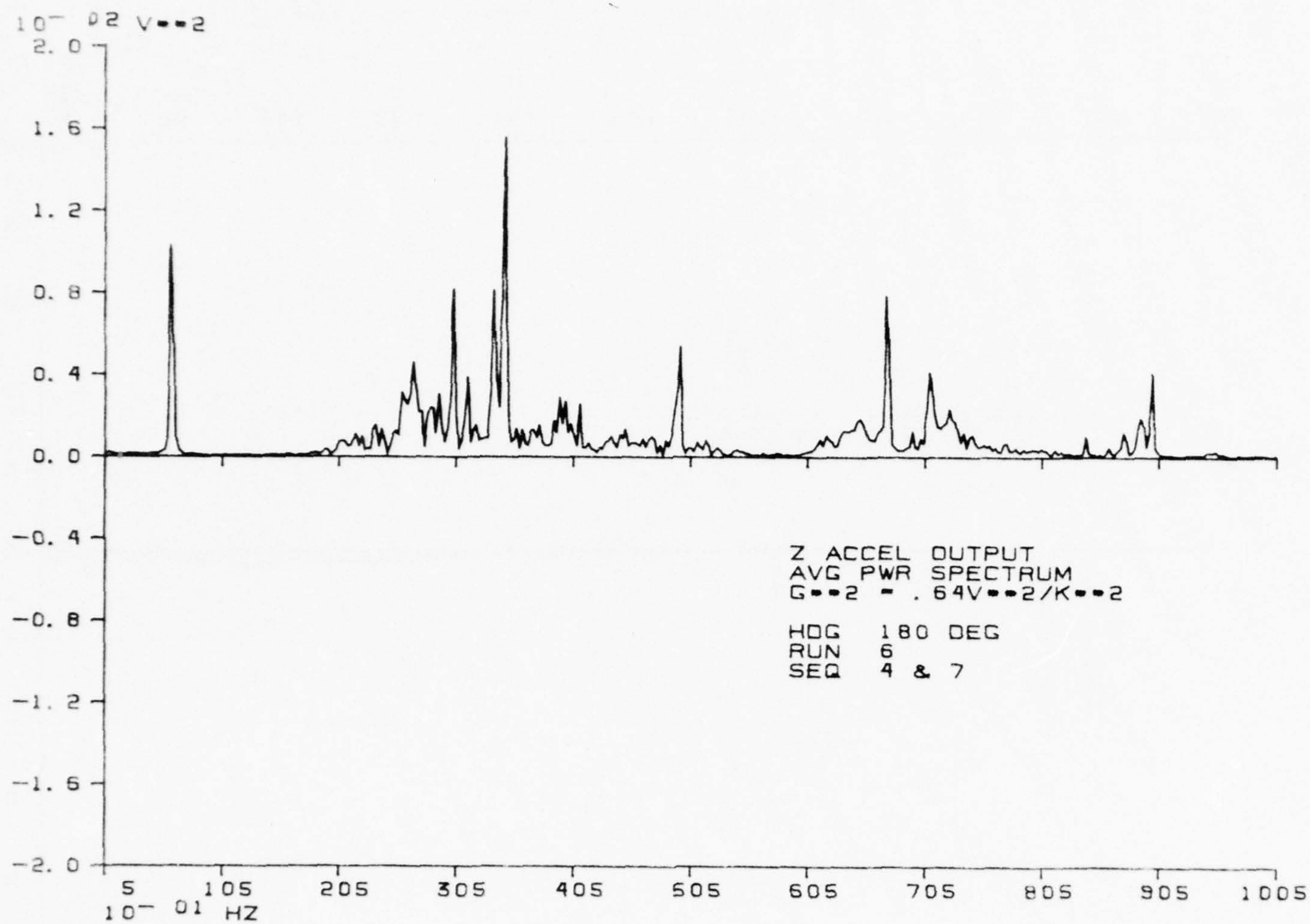

Figure C-20. Z acceleration output for run 6.

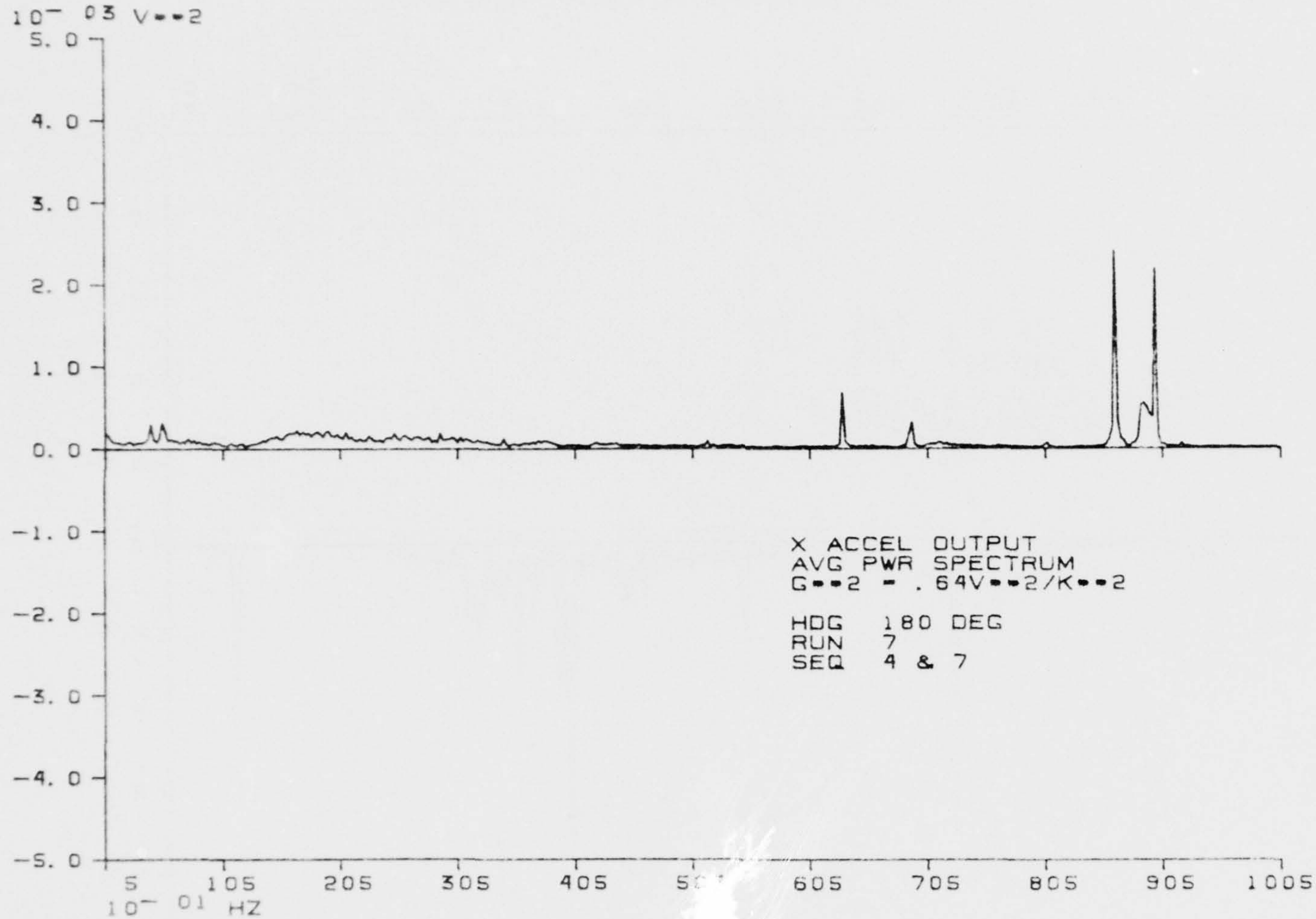

Figure C-21. X acceleration output for run 7.

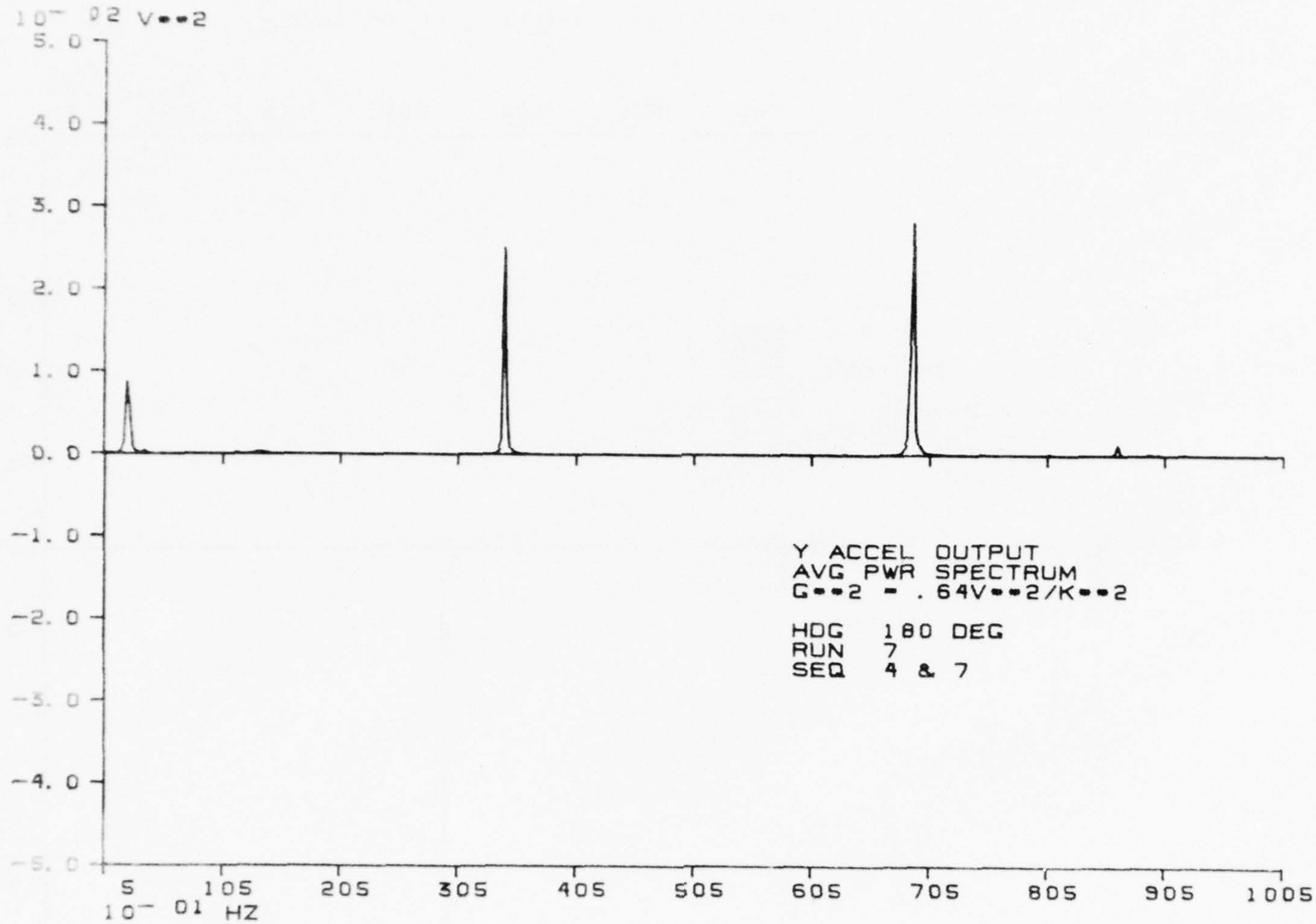

Figure C-22. Y acceleration output for run 7.

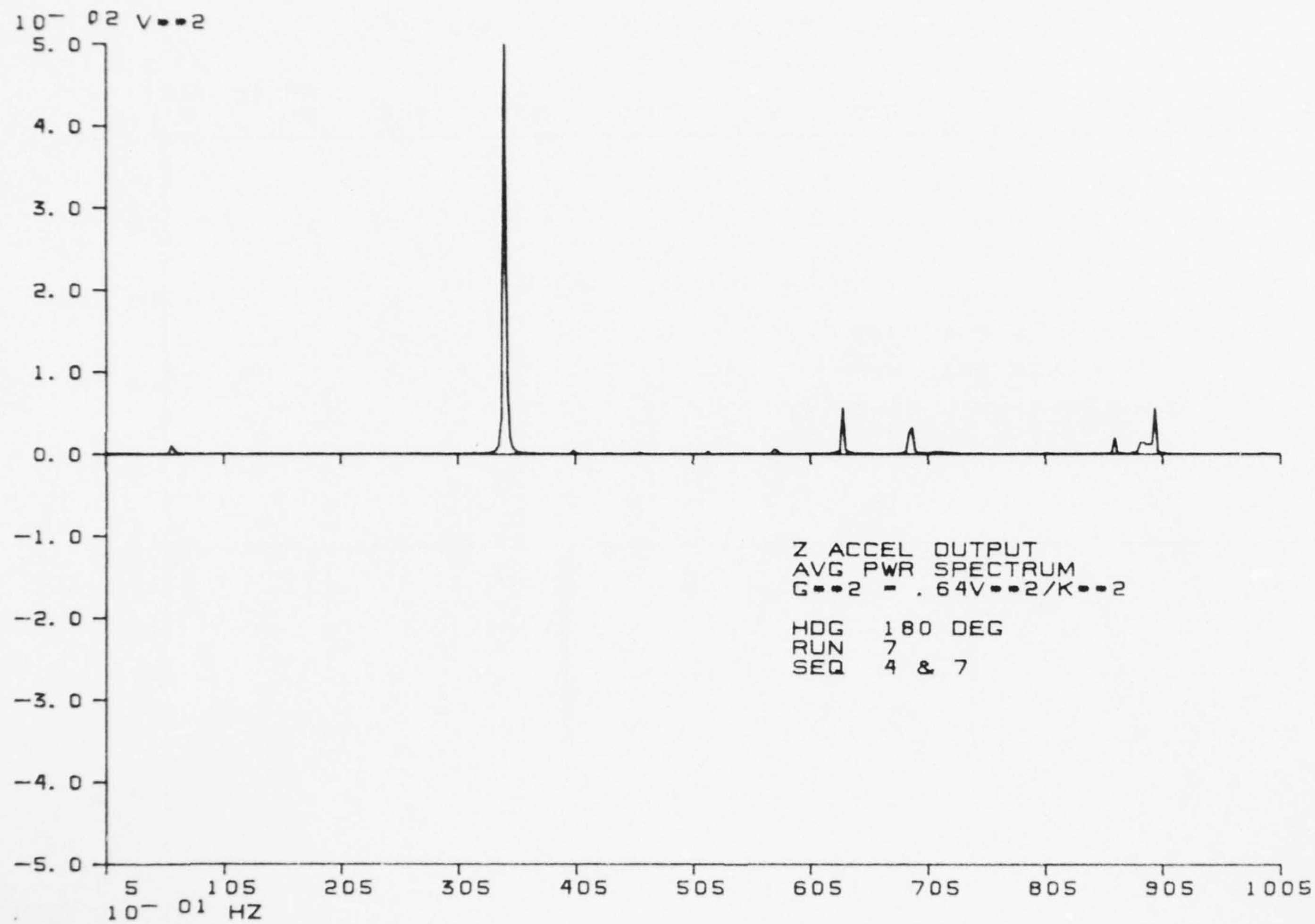

Figure C-23. Z acceleration output for run 7.

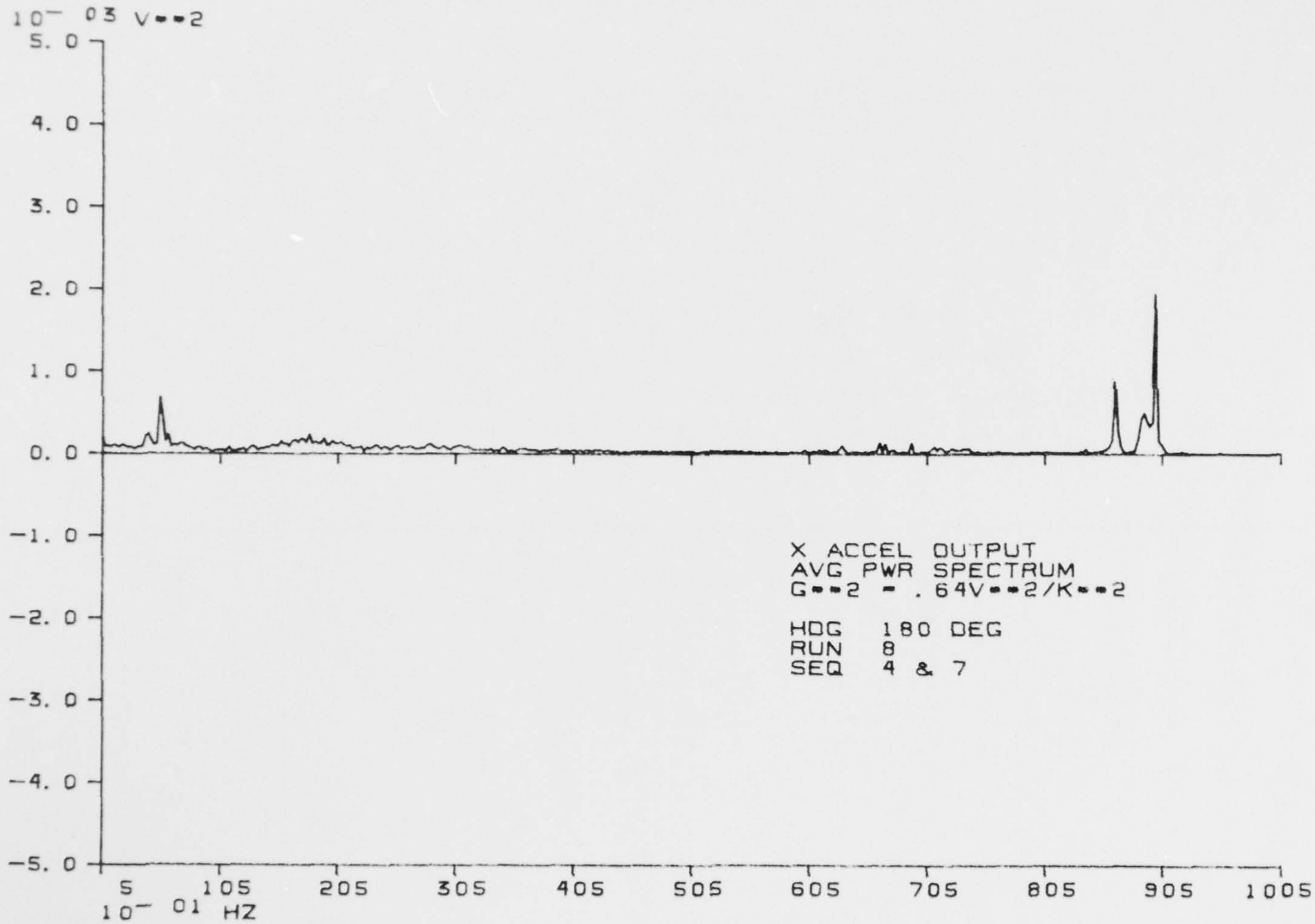

Figure C-24. X acceleration output for run 8.

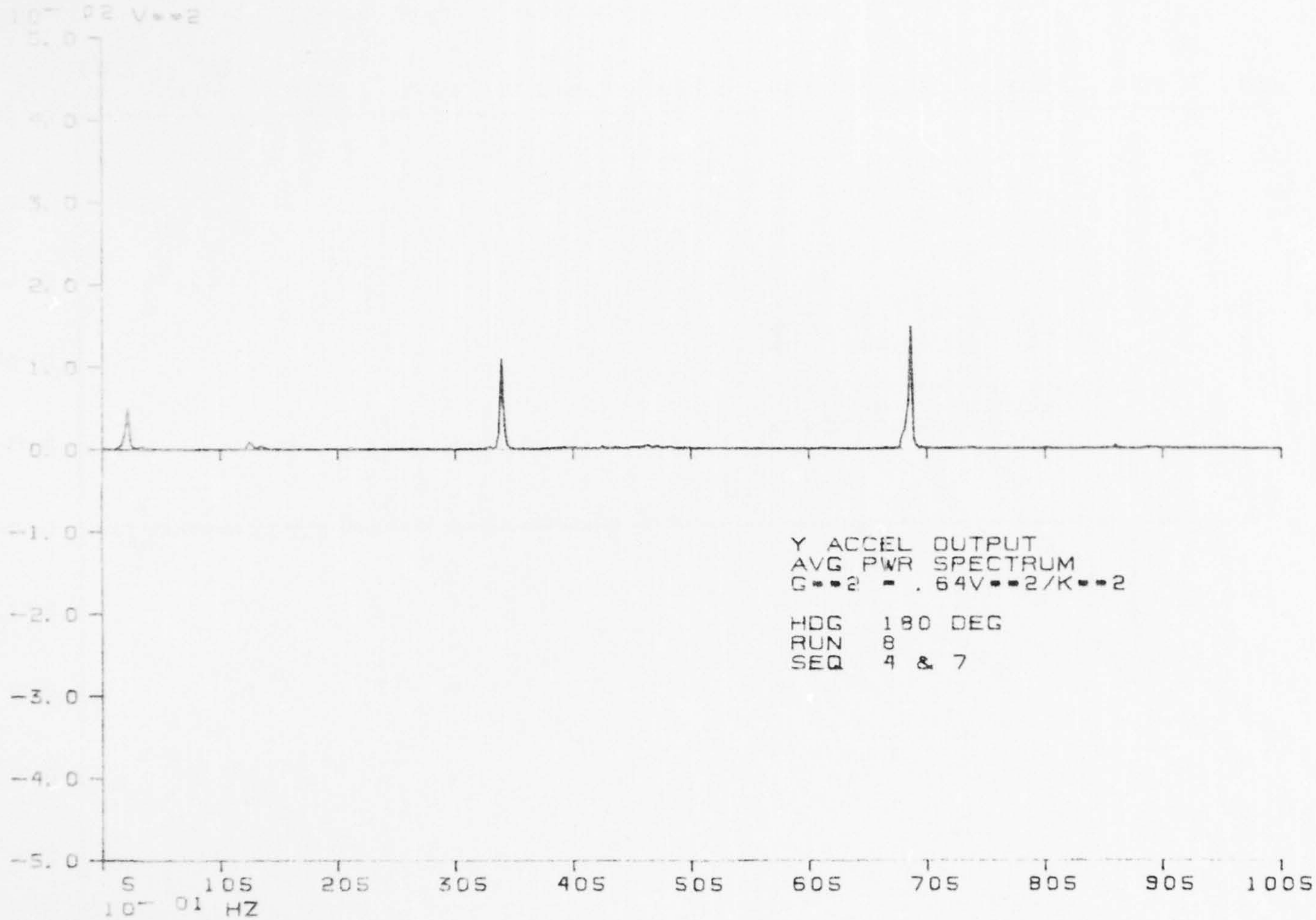

Figure C-25. Y acceleration output for run 8.

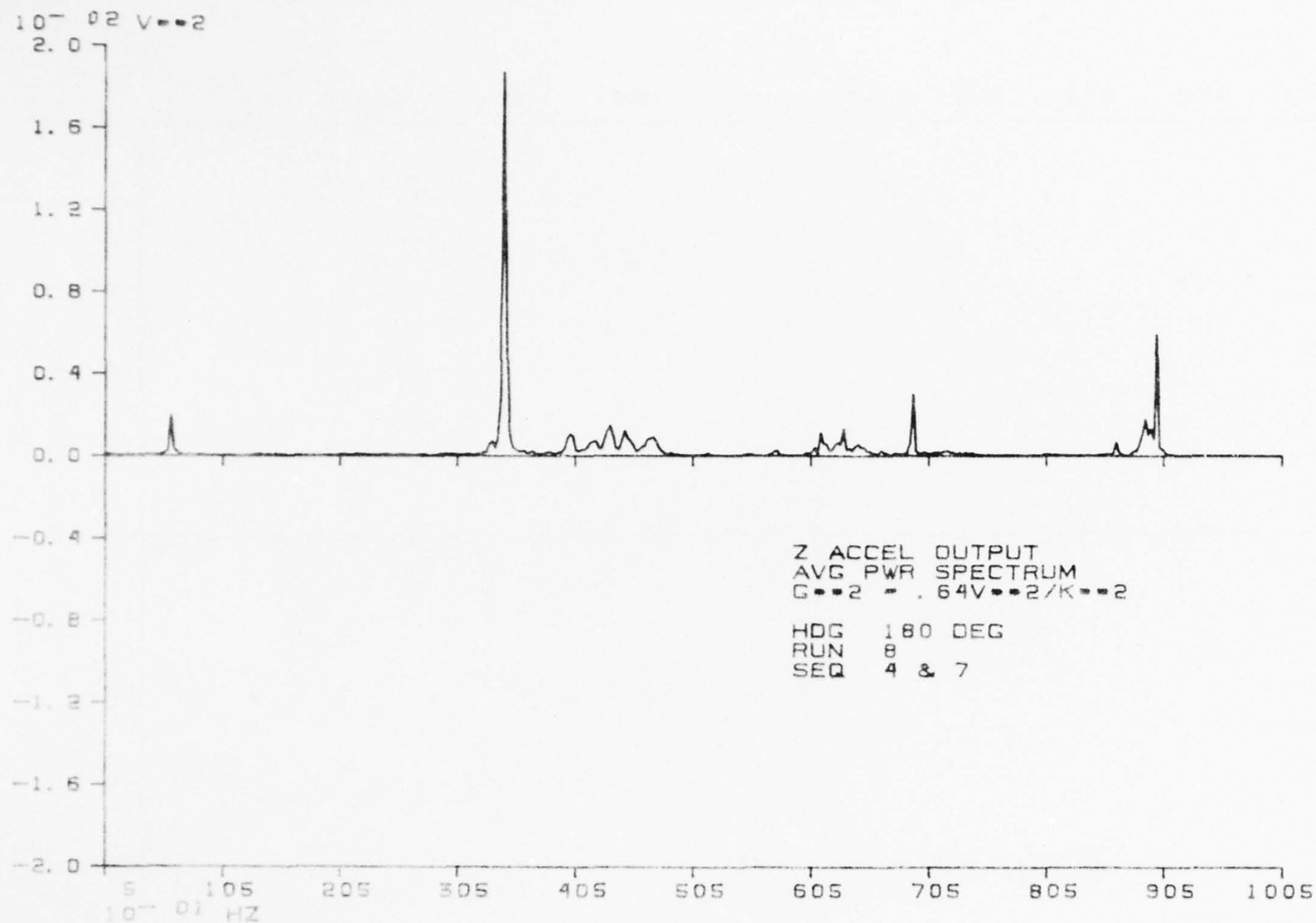

Figure C-26. Z acceleration output for run 8.

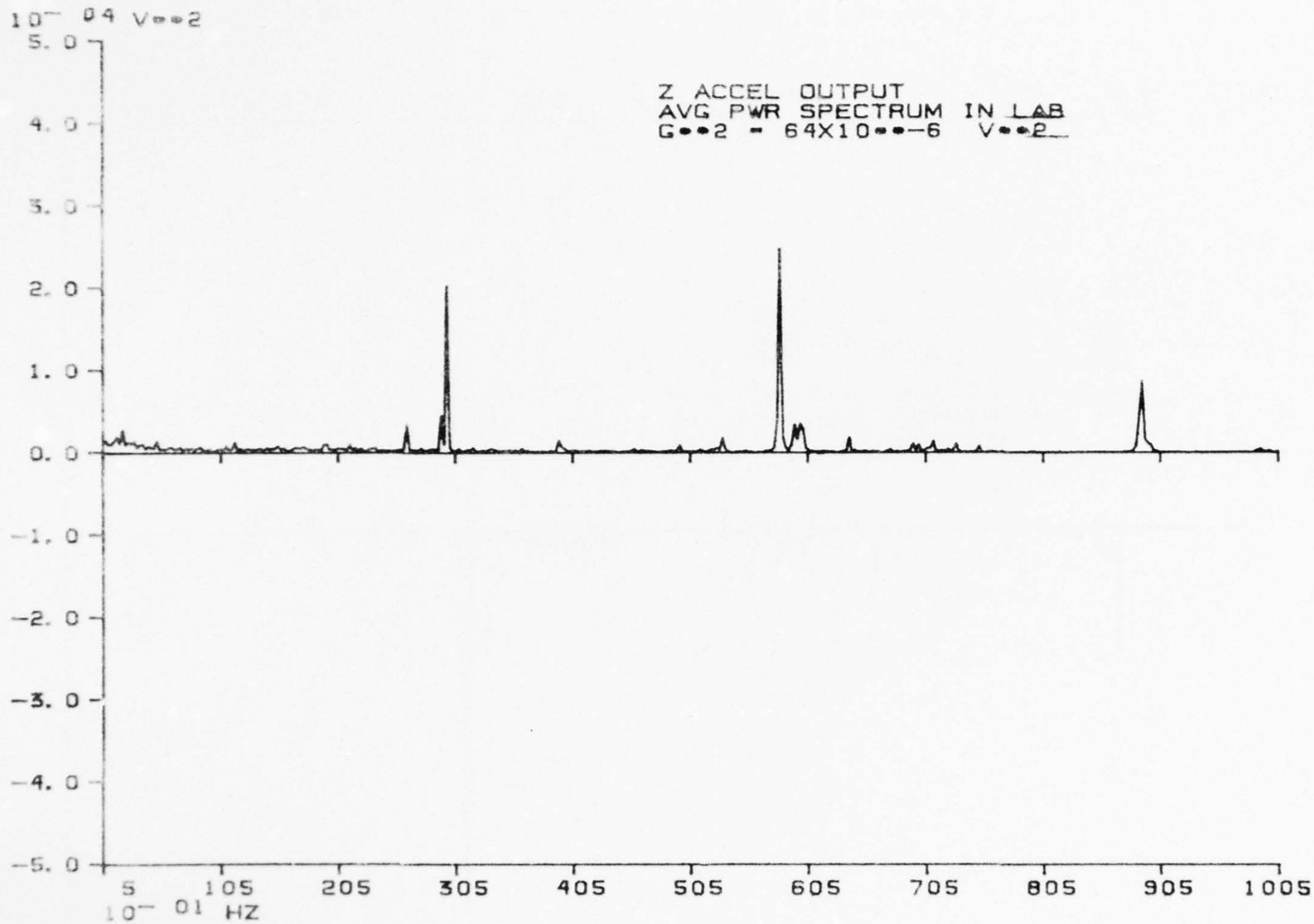

Figure C-27. Z acceleration output for laboratory operation.

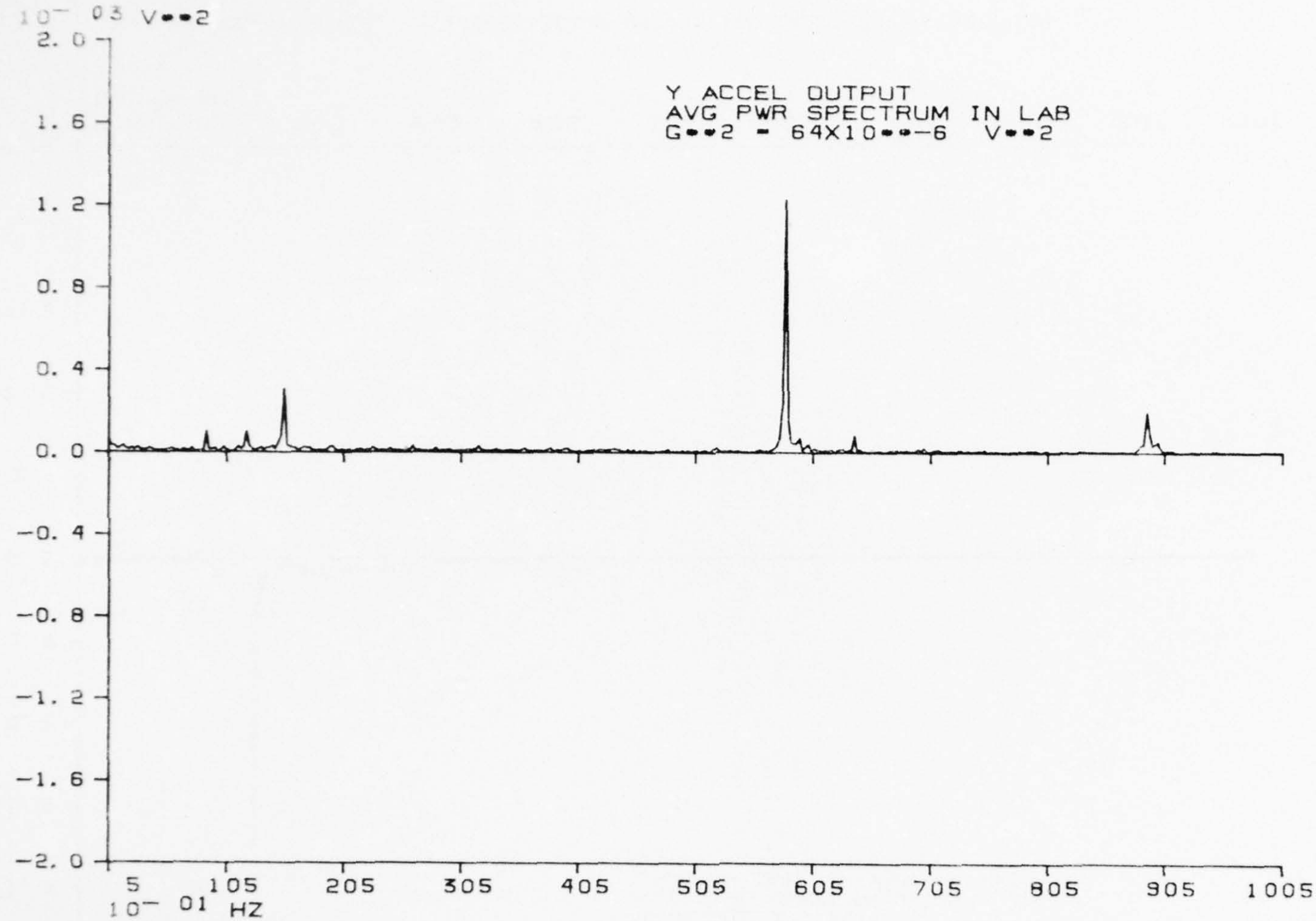

Figure C-28. Y acceleration output for laboratory operation.

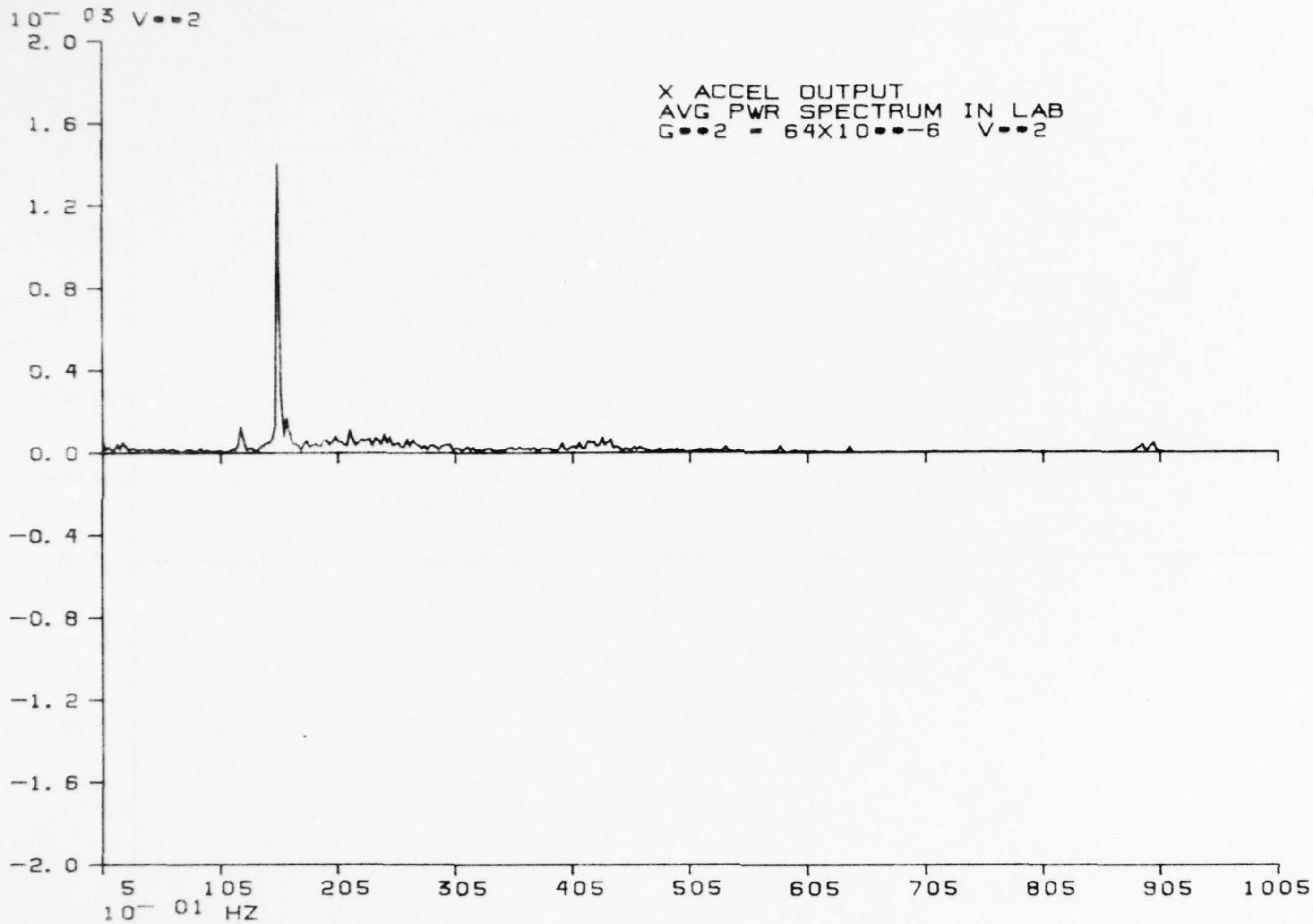

Figure C-29. X acceleration output for laboratory operation.

Appendix D. SUMMARY OF TEST RESULTS

Tables D-1 through D-8 contain a summary of gyrocompass test results at each of eight azimuth headings. Gyrocompass error for each individual run is contained in the column labeled ϵ_o (arc sec). The root mean square (RMS), average (AVG), and standard deviation (σ) of the eight error values are shown at the bottom of this column, Other pertinent data are given including IMU channel drifts, azimuth resolver readings, environmental conditions, and power turn-on/turn-off operations.

The original data taken at 225° on 13 December 1976, as shown in Table D-6, was noted to yield the largest errors. The system was re-emplaced at 225° on 14 December 1976 and five additional test runs were made to gain assurance that potential errors in the test setup and operations were not contributing to the large gyrocompass errors. Data obtained from the five test reruns are presented in Table D-9.

Table D-10 presents a summary of pretest, field-test and post-test errors on an RMS, AVG, and σ basis versus azimuth heading. Also shown are composite statistics for pretest, field-test, and post-test errors based on the total of 64 runs for each of the 3 test conditions.

The error data contained in Table D-10 are plotted in Figures D-1 through D-3 to provide a visual comparison of pretest, field-test and post-test gyrocompass performance.

Pretest and post-test calibration results are presented in Tables D-11 and D-12.

TABLE D-1. PII IMU MISSILE-MOUNTED GYROCOMPASS FIELD TEST

IMU S/N: 001

Date: 2 Dec 1976

Heading: 0°

Weather: Sunny

Remarks Legend: (1) Temperature (°F) Range
(2) Wind Speed (mph); and Direction (deg) Range
(3) Other

Run No.	α (arc sec) (deg, min, sec)	α_o (arc sec) (deg, min, sec)	ϵ_o (arc sec)	DN (°/hr)	DW (°/hr)	RSV (deg, min, sec)	Remarks
1	358 17 08	358 18 43	-95	0.1045	0.0166	359 59 26	(1) 35-40 (2) 3-5, 310-340 CW (3) 9 min IMU warmup; Veh traffic
2	358 18 36	358 18 50	-14	0.1015	0.0130	359 59 24	(1) 42-44 (2) 3-5, 350-50 CW (3) Veh traffic
3	358 19 36	358 19 30	6	0.0992	0.0140	359 59 04	(1) 45-47 (2) 2-5, 340-70 CW (3) 28 VDC pwr off/on; veh idling beside EL
4	358 19 19	358 19 21	-2	0.0992	0.0126	359 59 24	(1) 48-49 (2) 2-4, 270-80 CW (3) veh traffic
5	358 19 15	358 18 50	25	0.0971	0.0139	359 59 24	(1) 50-50 (2) 2-4 270-10 CW (3) 28 VDC pwr off/on; veh idling beside EL
6	358 19 16	358 19 28	-12	0.0970	0.0145	359 59 24	(1) 51-51 (2) 1-5, 240-10 CW (3) no veh traffic
7	358 20 43	358 21 17	-34	0.0952	0.0094	359 59 28	(1) 52-52 (2) 2-5, 260-350 CW (3) all IMU pwr off/on; 9 min warmup; veh traffic
8	358 21 22	358 20 33	49	0.0971	0.0080	359 59 24	(1) 53-53 (2) 2-4, 240-10 CW (3) veh traffic
		RMS	41				
		Avg	-10				
		σ	43				

Lat = 034° 38' 33"; should be 034° 37' 52"
EL Jacks not extended

TABLE D-2. PII IMU MISSILE-MOUNTED GYROCOMPASS FIELD TEST

IMU S/N: 001

Date: 9 Dec 1976

Heading: 40°

Weather: Sunny

Remarks Legend: (1) Temperature (°F) Range
(2) Wind Speed (mph); and Direction (deg) Range
(3) Other

Run No.	α (arc sec) (deg, min, sec)	α_o (arc sec) (deg, min, sec)	ϵ_o (arc sec)	DN (°/hr)	DW (°/hr)	RSV (deg, min, sec)	Remarks
1	038 35 20	038 36 13	-53	0.0776	0.0844	359 59 26	(1) 31-34 (2) 2-4, 150-180 CW (3) 1 hr IMU warmup veh idling beside EL
2	038 34 47	038 35 15	-28	0.0787	0.0840	358 54 30	(1) 34-37 (2) 3-7, 150-180 CW (3) veh traffic
3	038 34 35	038 35 31	-56	0.0740	0.0866	359 59 23	(1) 39-41 (2) 2-5, 80-150 CW (3) 28 VDC pwr off/on; veh traffic
4	038 34 23	038 34 54	-31	0.0741	0.0865	359 59 26	(1) 40-42 (2) 3-5, 70-170 CW (3) veh idling beside EL
5	038 34 27	038 35 39	-72	0.0735	0.0856	359 59 31	(1) 43-44 (2) 3-5, 100-180 CW (3) 28 VDC pwr off/on; veh traffic
6	038 34 20	038 35 45	-85	0.0753	0.0809	359 59 23	(1) 46-47 (2) 3-6, 90-160 CW (3) veh idling beside EL
7	038 33 25	038 35 01	-96	0.0786	0.0838	359 59 28	(1) 48-49 (2) 3-6, 60-150 CW (3) 28 VDC pwr off/on; vehicle idling beside EL
8	038 53 40	038 33 25	15	0.0762	0.0802	000 00 23	(1) 49-51 (2) 2-5, 80-150 CW (3) no veh traffic
		RMS	61				
		Avg	-51				
		σ	36				

TABLE D-3. PII IMU MISSILE-MOUNTED GYROCOMPASS FIELD TEST

IMU S/N: 001

Date: 7 Dec 1976

Heading: 70°

Weather: Cloudy

Remarks Legend: (1) Temperature (°F) Range
(2) Wind Speed (mph); and Direction (deg) Range
(3) Other

Run No.	α (arc sec) (deg, min, sec)	α_o (arc sec) (deg, min, sec)	ϵ_o (arc sec)	DN (°/hr)	DW (°/hr)	RSV (deg, min, sec)	Remarks
1	069 30 16	069 31 00	-44	0.0137	0.1066	359 59 28	(1) 42-43 (2) 2-5, 300-340 CW (3) 9 min IMU warmup; veh traffic
2	069 29 50	069 29 55	-5	0.0165	0.1063	359 59 31	(1) 42-43 (2) 2-5, 300-400 CW (3) veh idling beside EL
3	069 30 05	069 29 57	8	0.0321	0.1073	359 59 39	(1) 42-42 (2) 3-7, 310-330 CW (3) 28 VDC pwr off/on; veh idling beside EL
4	069 30 14	069 30 07	7	0.0321	0.1088	359 59 39	(1) 42-43 (2) 4-7, 300-330 CW (3) veh idling beside EL
5	069 29 42	069 30 15	-33	0.0198	0.0979	359 59 26	(1) 29-31 (2) no wind data, sensors frozen (3) 9 min IMU warmup; no veh traffic
6	069 30 44	069 30 26	18	0.0174	0.0974	359 59 55	(1) 32-34 (2) no wind data, sensors frozen (3) veh traffic
7	069 30 36	069 30 25	11	0.0189	0.1103	359 59 36	(1) 35-36 (2) no wind data, sensors frozen (3) 28 VDC off/on; veh idling beside EL
8	069 30 51	069 30 33	18	0.0210	0.1114	359 59 58	(1) 32-38 (2) no wind data, sensors frozen (3) veh idling beside EL
		RMS	22				
		Avg	-2				
		σ	24				

Lat = 034° 38' 33"; should be 034° 37' 52"
EL Jacks not extended

TABLE D-4. PII IMU MISSILE-MOUNTED GYROCOMPASS FIELD TEST

IMU S/N: 001

Date: 6 Dec 1976

Heading: 135°

Weather: Cloudy, light rain

Remarks Legend: (1) Temperature (°F) Range
(2) Wind Speed (mph); and Direction (deg) Range
(3) Other

Run No.	α (arc sec) (deg, min, sec)	α_o (arc sec) (deg, min, sec)	ϵ_o (arc sec)	DN (°/hr)	DW (°/hr)	RSV (deg, min, sec)	Remarks
1	133 51 22	133 49 00	142	-0.0830	0.0669	359 59 21	(1) 52-54 (2) 7-13, 100-120 CW (3) 1 hr IMU warmup; no veh traffic
2	133 50 30	133 49 35	55	-0.0834	0.0677	359 59 26	(1) 53-54 (2) 7-12, 110-140 CW (3) veh traffic
3	133 50 18	133 48 10	128	-0.0880	0.0714	359 59 26	(1) 53-53 (2) 4-8, 100-120 CW (3) 28 VDC pwr off/on; no veh traffic
4	133 50 11	133 49 15	56	-0.0876	0.0719	359 59 23	(1) 54-54 (2) 1-5, 60-110 CW (3) veh traffic
5	133 51 31	133 50 14	77	-0.0873	0.0608	359 59 26	(1) 54-54 (2) 2-7, 100-130 CW (3) 28 VDC pwr off/on, veh idling beside EL
6	133 51 59	133 50 09	110	-0.0863	0.0608	359 59 29	(1) 54-54 (2) 4-9, 100-130 CW (3) no veh traffic
7	133 50 32	133 49 51	41	-0.0847	0.0726	359 59 21	(1) 54-54 (2) 4-8, 110-130 CW (3) 28 VDC pwr off/on; veh idling beside EL
8	133 51 00	133 50 08	52	-0.0849	0.0733	359 59 29	(1) 54-54 (2) 6-13, 100-120 CW (3) veh idling beside EL
		RMS	90				
		Avg	83				
		σ	39				

Lat = 034° 38' 33"; should be 034° 37' 52"
EL Jacks not extended

TABLE D-5. PII IMU MISSILE-MOUNTED GYROCOMPASS FIELD TEST

IMU S/N: 001

Date: 13 Dec 1976

Heading: 180°

Weather: Cloud AM, Sunny PM

Remarks Legend: (1) Temperature (°F) Range
(2) Wind Speed (mph); and Direction (deg) Range
(3) Other

Run No.	α (arc sec) (deg, min, sec)	α_o (arc sec) (deg, min, sec)	ϵ_o (arc sec)	DN (°/hr)	DW (°/hr)	RSV (deg, min, sec)	Remarks
1	225 45 15	225 46 20	-65	-0.0559	-0.0933	359 59 31	(1) 37-41 (2) 4-7, 350-10 CW (3) 9 min IMU warmup; veh traffic
2	225 47 59	225 45 37	142	-0.0656	-0.0880	359 59 24	(1) 41-43 (2) 4-8, 360-20 CW (3) no veh traffic
3	225 48 47	225 46 14	153	-0.0301	-0.0856	359 59 57	(1) 49-50 (2) 3-6, 330-10 CW (3) all pwr off for 45 min, 9 min IMU warmup; veh idling beside EL
4	225 48 00	225 46 30	90	-0.0247	-0.0857	359 59 57	(1) 51-52 (2) 3-7, 330-10 CW (3) veh idling beside EL
5	225 48 36	225 46 25	131	-0.0609	-0.0948	359 59 28	(1) 55-56 (2) 3-5, 350-20 CW (3) all pwr off for 45 min, 9 min IMU warmup; veh traffic
6	225 47 16	225 44 39	157	-0.0625	-0.0951	359 59 28	(1) 56-56 (2) 2-5, 340-20 CW (3) veh traffic
7	225 46 54	225 45 05	109	-0.0736	-0.0859	359 59 57	(1) 56-56 (2) 2-4, 350-20 CW (3) 28 VDC pwr off/on; veh idling beside EL
8	225 47 33	225 44 42	171	-0.0767	-0.0857	359 59 31	(1) 56-56 (2) 2-4, 340-20 CW (3) veh idling beside EL
		RMS	132				
		Avg	111				
		σ	76				

TABLE D-6. PII IMU MISSILE-MOUNTED GYROCOMPASS FIELD TEST

IMU S/N: 001

Date: 14 Dec 1976

Heading: 225°

Weather: Sunny

Remarks Legend: (1) Temperature (°F) Range
(2) Wind Speed (mph); and Direction (deg) Range
(3) Other

Run No.	α (arc sec) (deg, min, sec)	α_o (arc sec) (deg, min, sec)	ϵ_o (arc sec)	DN (°/hr)	DW (°/hr)	RSV (deg, min, sec)	Remarks
1	181 24 28	181 23 22	66	-0.1032	-0.0362	359 59 31	(1) 39-41 (2) 3-5, 90-130 CW (3) 20 min system warmup; veh idling beside EL
2	181 27 16	181 25 41	95	-0.1037	-0.0343	559 59 58	(1) 46-48 (2) 3-9, 100-130 CW (3) veh idling beside EL
3	181 26 25	181 25 28	57	-0.0982	0.0345	000 00 03	(1) 48-52 (2) 4-7, 110-130 CW (3) 28 VDC pwr off/on, veh traffic
4	181 26 01	181 25 23	38	-0.0992	-0.0350	359 59 58	(1) 52-52 (2) 3-7, 90-150 CW (3) veh traffic
5	181 25 10	181 25 20	-10	-0.0982	-0.0199	359 59 28	(1) 53-54 (2) 3-8, 90-130 CW (3) 28 VDC off-on; veh traffic
6	181 26 03	181 25 06	57	-0.0981	-0.0227	359 59 29	(1) 55-55 (2) 3-8, 110, 150 CW (3) veh traffic
7	181 25 27	181 24 29	58	-0.1017	-0.0148	359 59 28	(1) 56-56 (2) 3-7, 100-150 CW (3) 28 VDC pwr off/on; veh idling beside EL
8	181 25 34	181 24 10	84	-0.1026	-0.0167	359 59 22	(1) 56-57 (2) 3-8, 100-150 CW (3) veh traffic
		RMS	63				
		Avg	56				
		σ	32				

TABLE D-7. PII IMU MISSILE-MOUNTED GYROCOMPASS FIELD TEST

IMU S/N: 001

Date: 10 Dec 1976

Heading: 270°

Weather: Cloudy

Remarks Legend: (1) Temperature (°F) Range

(2) Wind Speed (mph); and Direction (deg) Range

(3) Other

Run No.	α (arc sec) (deg, min, sec)	α_o (arc sec) (deg, min, sec)	ϵ_o (arc sec)	DN (°/hr)	DW (°/hr)	RSV (deg, min, sec)	Remarks
1	257 42 30	267 40 54	96	0.0089	-0.1068	359 59 29	(1) 42-44 (2) 2-4, 130-180 CW (3) 9 min system warmup; no veh traffic
2	267 39 27	267 38 27	60	0.076	-0.1065	359 59 24	(1) 44-46 (2) 2-4, 120-170 CW (3) veh traffic
3	267 41 17	267 38 58	139	0.0053	-0.1130	359 59 31	(1) 47-49 (2) 2-4, 110-150 CW (3) 28 VDC pwr off/on; veh traffic
4	267 40 30	267 38 57	93	0.0050	-0.1111	359 59 29	(1) 49-51 (2) 2-4, 120-150 CW (3) veh idling beside EL
5	267 40 38	267 38 34	124	0.0240	-0.1187	359 59 28	(1) 51-51 (2) 2-4, 110-150 CW (3) 28 VDC pwr off/on; veh traffic
6	267 40 41	267 39 25	76	0.0188	-0.1171	359 59 29	(1) 52-52 (2) 2-5, 120-150 CW (3) veh idling beside EL
7	267 41 03	267 39 22	101	0.0126	-0.1089	359 59 26	(1) 52-53 (2) 2-7, 120-170 CW (3) 28 VDC pwr off/on; veh traffic
8	267 39 41	267 38 30	71	0.0132	-0.1096	359 59 31	(1) 53-53 (2) 2-6, 120-150 CW (3) veh idling beside EL
		RMS	98				
		Avg	95				
		σ	27				

AD-A043 921 ARMY MISSILE RESEARCH AND DEVELOPMENT COMMAND REDSTO--ETC F/G 17/7
PERSHING PII INERTIAL MEASUREMENT UNIT FIELD GYROCOMPASS TEST.(U)
JUN 77 H V WHITE

UNCLASSIFIED DRDMI-TG-77-16 NL

2 OF 2
AD A043921

END
DATE FILMED
9-77
DDC

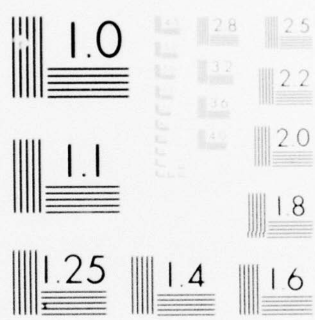

MICROCOPY RESOLUTION TEST CHART
NATIONAL BUREAU OF STANDARDS-1963-A

TABLE D-8. PII IMU MISSILE-MOUNTED GYROCOMPASS FIELD TEST

IMU S/N: 001

Date: 3 Dec 1976

Heading: 315°

Weather: Partly Cloudy

Remarks Legend: (1) Temperature (°F) Range
(2) Wind Speed (mph); and Direction (deg) Range
(3) Other

Run No.	α (arc sec) (deg, min, sec)	α_o (arc sec) (deg, min, sec)	ϵ_o (arc sec)	DN (°/hr)	DW (°/hr)	RSV (deg, min, sec)	Remarks
1	318 22 34	318 22 41	-7	0.0800	-0.0594	359 59 26	(1) 43-45 (2) 2-6, 100-180 CW (3) 1 hr IMU warmup; veh traffic
2	318 24 14	318 24 02	12	0.0792	-0.0580	359 59 28	(1) 48-50 (2) 3-4, 80-130 CW (3) veh traffic
3	318 24 30	318 23 48	42	0.0804		359 59 28	(1) 52-55 (2) 2-4, 30-210 CW (3) 28 VDC pwr off/on; veh traffic
4	318 27 49	318 26 16	93	0.0805	-0.0612	359 59 26	(1) 57-58 (2) 2-3, 0-290 CW (3) veh traffic
5	318 26 36	318 25 43	53	0.0814	-0.697	359 59 24	(1) 64-66 (2) 2-4, 70-0 CW (3) all pwr off for 1 hr, 9 min IMU warmup; veh traffic
6	318 25 14	318 24 42	32	0.0830	-0.0720	359 59 28	(1) 67-68 (2) 2-5, 150-250 CW (3) veh traffic
7	318 24 52	318 24 15	37	0.0760	-0.0545	359 59 26	(1) 68-70 (2) 2-8, 170-230 CW (3) 28 VDC pwr off/on; no veh traffic
8	318 25 16	318 24 45	31	0.0779	-0.0545	359 59 28	(1) 67-67 (2) 3-7, 180-220 CW (3) veh traffic
		RMS	46				
		Avg	37				
		σ	29				

Lat = 034° 38" 33"; should be 034° 37' 52"3
EL Jacks not extended

TABLE D-9. PII IMU MISSILE-MOUNTED GYROCOMPASS FIELD TEST

IMU S/N: 001

Date: 14 Dec 1976

Heading: 225° (Rerun)

Weather: Partly Cloudy

Remarks Legend: (1) Temperature (°F) Range

(2) Wind Speed (mph); and Direction (deg) Range

(3) Other

Run No.	α (arc sec) (deg, min, sec)	α_o (arc sec) (deg, min, sec)	ϵ_o (arc sec)	DN (°/hr)	DW (°/hr)	RSV (deg, min, sec)	Remarks
1	222 20 09	222 18 19	110	-0.0597	-0.0962	359 59 28	(1) 60-60 (2) 3-5, 90-130 CW (3) veh traffic
2	222 20 34	222 18 21	133	-0.0615	-0.0962	359 59 29	(1) 60-60 (2) 3-9, 110-130 CW (3) veh idling beside EL
3	222 19 02	222 17 50	72	-0.0676	-0.0896	359 59 24	(1) 59-60 (2) 4-6, 110-130 CW (3) 28 VDC pwr off/on; no veh traffic
4	222 18 09	222 16 20	109	-0.0613	-0.0929	359 59 31	(1) 59-60 (2) 3-7, 90-150 CW (3) veh traffic
5	222 20 53	222 18 32	141	-0.0651	-0.1039	359 59 28	(1) 58-59 (2) 2-8, 90-130 CW (3) 28 VDC pwr off/on; veh idling beside EL
6							
7							
8							
		RMS	116				
		Avg	113				
		σ	27				

TABLE D-10. PII IMU GYROCOMPASS FIELD TEST RESULTS IMU S/N: 001: COMPILATION OF PRETEST, FIELD AND POST-TEST DATA

Heading (deg)	Statistics for 8 Runs	Pretest Error (arc sec)	Field Test Error (arc sec)	Post-Test Error (arc sec)
0	RMS	31	(2 Dec) 41*	78
	Avg	-19	-10	-57
	σ	27	43	58
45	RMS	45	(9 Dec) 61	64
	Avg	-40	(40°) -51	-63
	σ	22	36	12
90	RMS	40	(7-8 Dec) 22*	55
	Avg	5	(70°) -2	-52
	σ	43	24	20
135	RMS	25	(6 Dec) 90*	41
	Avg	9	83	36
	σ	25	39	21
180	RMS	44	(14 Dec) 63	38
	Avg	32	56	23
	σ	31	32	32
225	RMS	48	(13 Dec) 132	20
	Avg	42	111	14
	σ	24	76	15
270	RMS	32	(10 Dec) 98	32
	Avg	7	95	20
	σ	34	27	27
315	RMS	40	(3 Dec) 46*	60
	Avg	25	37	38
	σ	33	29	50
Composite Statistics for 64 Runs for Each Test Condition	RMS	39	77	52
	Avg	8	40	-5
	σ	38	66	52

*Lat = 034° 38' 33"; should be 034° 37' 52"
EL Jacks not extended

TABLE D-11. PRETEST CALIBRATION DATA, 40-FOOT CABLES, 2 NOVEMBER 1976

Entries are Deviations from Acceptance Test Values			
DFZ E	0.00777695 deg/hr	DIX E	0.06210616 deg/hr/G
DSZ E	0.00777695 deg/hr		
		DIY E	0.06210616 deg/hr/G
DIZ E	0.16653737 deg/hr/G	DELTYX	0.00005547 rad
		DELTZY	-0.00001263 rad
KIY E	-156.24057007 μG/G		
KIYHE	-113.91108704 μG/G		
		KOZ E	-97.67112732 μG
KIX E	-179.68435669 μG/G		
		KSZ E	-81.70867920 μG
KIXHE	-154.54333496 μG/G		
		KOZHE	-85.04553223 μG
		KSZHE	-90.18788147 μG
DOZ E	0.01000393 deg/hr/G		
		KOX E	26.49459839 μG
DFX E	0.08050755 deg/hr		
		KSX E	21.72198868 μG
		KOXHE	-5.78488159 μG
KIZ E	50.74204254 μG/G		
		KSXHE	-27.40397263 μG
KIZHE	43.49652863 μG/G		
DFY E	0.02019069 deg/hr		
		DELTZX	-0.00000712 rad
DSX E	0.00466868 deg/hr		
DSY E	-0.00466868 deg/hr		
		KOY E	2.69024658 μG
KTXE	-0.00050398 deg/hr/deg/hr	KSY E	11.00490761 μG
KTYE	-0.00039612 deg/hr/deg/hr	KOYHE	-52.97576904 μG
KTZE	0.00032379 deg/hr/deg/hr	KSYHE	-50.74983978 μG

TABLE D-12. POST TEST CALIBRATION DATA, 40-FOOT CABLES, 16 DECEMBER 1976

Entries are Deviations from Acceptance Test Values

DFZ E	-0.04159076 deg/hr
	-0.01083504 deg/hr/G
DIZ E	0.10650995 deg/hr/G
KIY E	-93.79339600 μG/G
KIYHE	-47.91403198 μG/G
KIX E	-106.87594604 μG/G
KIXHE	-53.13750458 μG/G
DOZ E	-0.01711116 deg/hr/G
DFX E	0.07787050 deg/hr
KIX E	57.22663116 G/G
KIZHE	20.30768967 G/G
DFY E	0.03096781 deg/hr
DSX E	-0.00273511 deg/hr
DSY E	0.00273511 deg/hr
KTXE	-0.00054308 deg/hr/deg/hr
ICTYE	-0.0003451 deg/hr/deg/hr
ICTZE	-0.00009416 deg/hr/deg/hr

DIX E	0.00174049 deg/hr/G
DIY E	0.00174049 deg/hr/G
DELTYX	0.00003333 rad
DELTZY	-0.00002276 rad
KOZ E	-160.22668457 μG
KSZ E	-111.99859619 μG
KOZHE	-99.77009583 μG
KSZHE	-71.48503113 μG
KOX E	44.75085449 μG
KSX E	48.16700745 μG
KOXHE	-12.49636841 μG
KSXHE	-21.57628632 μG
DELTZX	0.00002585 rad
KOY E	39.71406555 μG
KSY E	44.71518707 μG
KOYHE	-17.06207275 μG
KSYHE	-20.80200958 μG

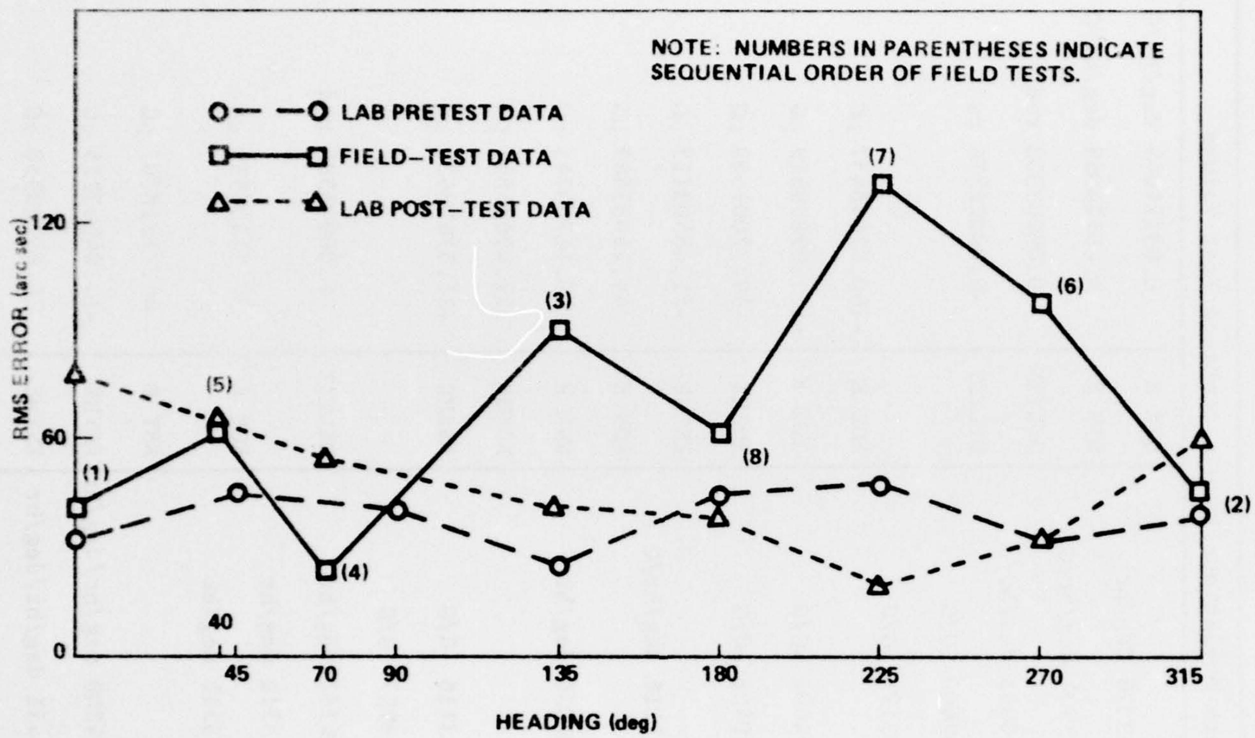

Figure D-1. PII IMU S/N 001 gyrocompass RMS error.

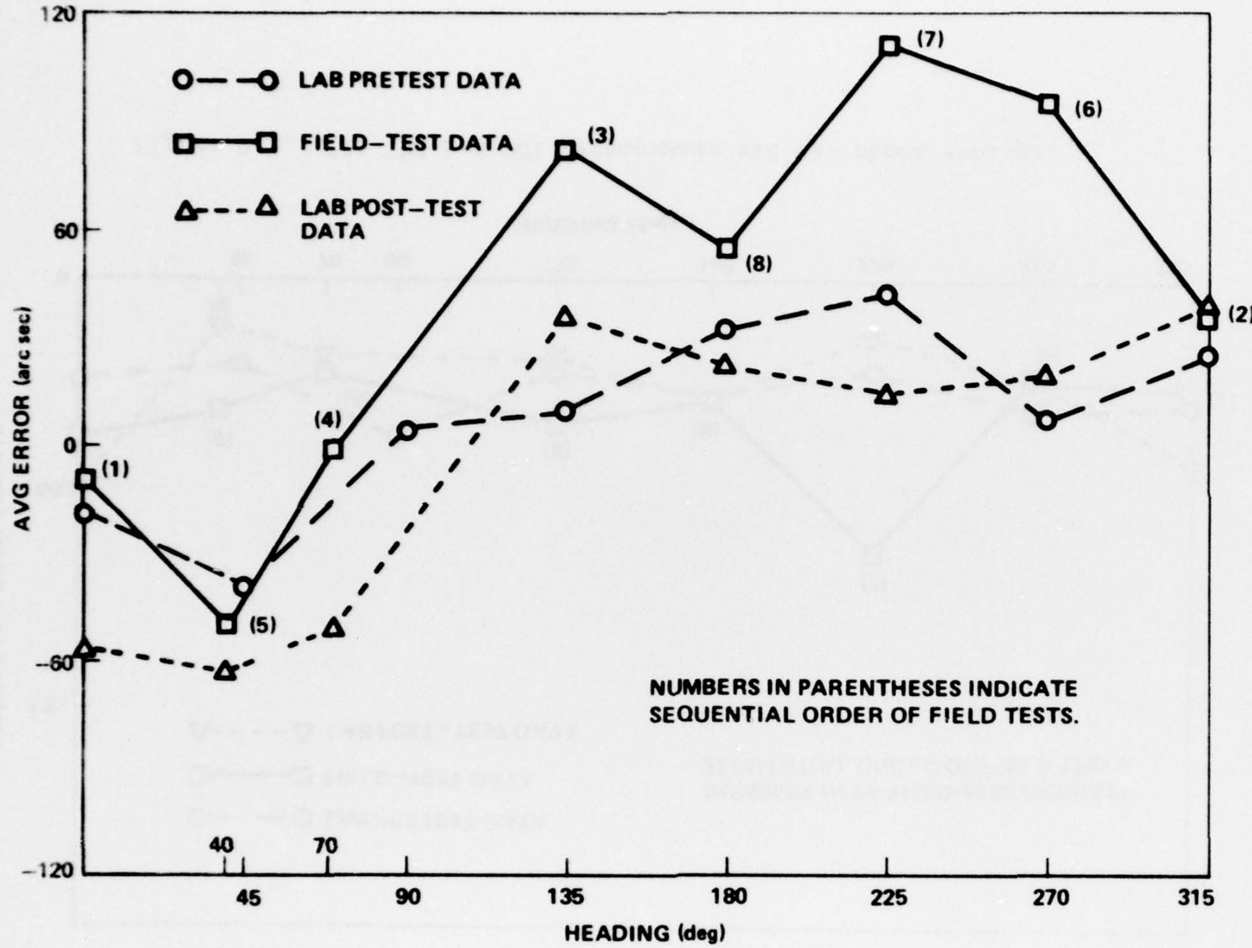

Figure D-2. PII IMU S/N 001 gyrocompass average error.

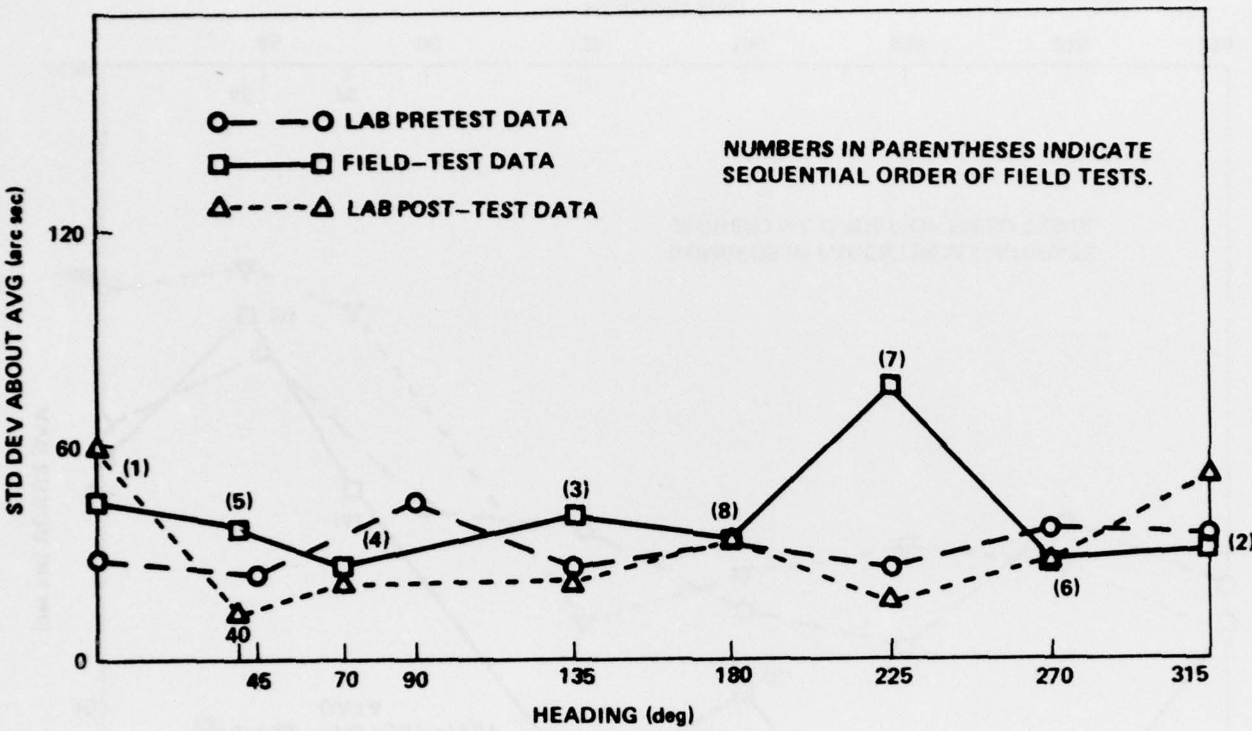

Figure D-3. PII IMU S/N 001 gyrocompass std dev about average.

DISTRIBUTION

	No. of Copies
Defense Documentation Center Cameron Station Alexandria, Virginia 23144	12
Commander US Army Materiel Development and Readiness Command	
Attn: DRCRD	1
DRCDL	1
5001 Eisenhower Avenue Alexandria, Virginia 22333	
The University of Tennessee Department of Electrical Engineering Attn: Dr. J. C. Hung Knoxville, Tennessee 37916	1
NASA Johnson Space Center EG5 Attn: Mr. Malcolm Jones Houston, Texas 77058	1
DRCPM-PE-E, Mr. Pettitt	1
-PE-EA, Mr. Wagner	1
Mr. Gregory	1
DRSMI-L, Mr. Voigt	1
DRDMI-X, Dr. McDaniel	1
-T, Dr. Kobler	1
-TG	1
-TGL, Mr. White	5
-TGG, Mr. Ciliax	1
-TGN, Mr. McLean	1
-ESL, Mr. Graham	1
-TBD	3
-TI (Record Set)	1
(Reference Copy)	1